C9. Seismic Isolation and Energy Dissipation (Systematic Rehabilitation)

C9.1 Introduction

Seismic isolation and energy dissipation systems are viable design strategies for seismic rehabilitation of buildings. Other special seismic systems—including active control, hybrid combinations of active and passive energy devices, tuned mass and liquid dampers—are being developed and may provide practical solutions in the near future. These systems include devices that enhance building performance primarily by modifying building response characteristics.

Conceptually, isolation reduces response of the superstructure by "decoupling" the building from the ground. Typical isolation systems reduce forces transmitted to the superstructure by lengthening the period of the building and adding some amount of damping. Added damping is an inherent property of most isolators, but may also be provided by supplemental energy dissipation devices installed across the isolation interface. Under favorable conditions, the isolation system reduces drift in the superstructure by a factor of at least two—and sometimes by as much as factor of five—from that which would occur if the building were not isolated. Accelerations are also reduced in the structure, although the amount of reduction depends on the force-deflection characteristics of the isolators and may not be as significant as the reduction of drift. Reduction of drift in the superstructure protects structural components and elements, as well as nonstructural components sensitive to drift-induced damage. Reduction of acceleration protects nonstructural components that are sensitive to acceleration-induced damage.

Passive energy dissipation devices add damping (and sometimes stiffness) to the building's structure. A wide variety of passive energy dissipation devices are available, including fluid viscous dampers, viscoelastic materials, and hysteretic devices. Ideally, energy dissipation devices dampen earthquake excitation of the structure that would otherwise cause higher levels of response, and damage to components and elements of the building. Under favorable conditions, energy dissipation devices reduce drift of the structure by a factor of about two to three, if no stiffness is added, and by larger factors if the devices also add stiffness to the structure. Energy dissipation devices will also reduce force in the structure—provided the structure is responding elastically—but would not be expected to reduce force in structures that are responding beyond yield.

Active control systems sense and resist building motion, either by applying external force or by modifying structural properties of active elements (e.g., so-called "smart" braces). Tuned mass or liquid dampers modify properties and add damping to key building modes of vibration. There are other types of special seismic systems, and additional concepts will be undoubtedly be developed in the future.

Consideration of special seismic systems, such as isolation or energy dissipation systems, should be made early in the design process and be based on the Rehabilitation Objectives established for the building (Chapter 2). Whether a special seismic system is found to be the "correct" design strategy for building rehabilitation will depend primarily on the performance required at the specified level of earthquake demand. In general, special seismic systems will be found to be more attractive as a rehabilitation strategy for buildings that have more stringent Rehabilitation Objectives (i.e., higher levels of performance and more severe levels of earthquake demand). Table C9-1 provides some simple guidance on the Performance Levels for which isolation and energy dissipation systems should be considered as possible design strategies for building rehabilitation.

Table C9-1 Applicability of Isolation and Energy Dissipation Systems

Performance Level	Performance Range	Isolation	Energy Dissipation
Operational	Damage Control	Very Likely	Limited
Immediate Occupancy		Likely	Likely
Life Safety	Limited Safety	Limited	Likely
Collapse Prevention		Not Practical	Limited

Table C9-1 suggests that isolation systems should be considered for achieving the Immediate Occupancy Structural Performance Level and the Operational Nonstructural Performance Level. Conversely, isolation will likely not be an appropriate design strategy for achieving the Collapse Prevention Performance Level. In general, isolation systems provide significant protection to the building structure, nonstructural components, and contents, but at a cost that precludes practical application when the budget and Rehabilitation Objectives are modest.

Energy dissipation systems should be considered in a somewhat broader context than isolation systems. For the taller buildings (where isolation systems may not be feasible), energy dissipation systems should be considered as a design strategy when performance goals include the Damage Control Performance Range. Conversely, certain energy dissipation devices are quite economical and might be practical for performance goals that address only Limited Safety. In general, however, energy dissipation systems are more likely to be an appropriate design strategy when the desired Performance Level is Life Safety, or perhaps Immediate Occupancy. Other objectives may also influence the decision to use energy dissipation devices, since these devices can also be useful for control of building response due to small earthquakes, wind, or mechanical loads.

C9.2 Seismic Isolation Systems

Section C9.2.1 of this *Commentary* provides background on seismic isolation concepts and the development, approach, and philosophy of pertinent design codes including the seismic isolation provisions of the 1994 *NEHRP Recommended Provisions for Seismic Regulations for New Buildings* (BSSC, 1995). Section 2.6 (Provisions for Seismically Isolated Structures) of the 1994 *NEHRP Provisions* (plus changes proposed for the 1997 edition of these provisions) is the primary basis and reference for the isolation system design criteria of Section 9.2 of these *Guidelines*.

Section C9.2.1 also provides background on projects in the United States that have utilized isolation as a design strategy for seismic rehabilitation. Motivating factors for selecting isolation are discussed, and guidance is provided for establishing objectives and design criteria appropriate for the desired Performance Level.

Section C9.2.2 describes in detail the mechanical properties and modeling theory for various types of isolation devices. This information is intended as reference material for *Guidelines* users who are interested in better understanding the characteristics and behavior of isolators, or who need to develop detailed mathematical models of isolation system components.

Section C9.2.3 provides comment on the selection of design criteria for seismic isolation, in particular the selection of an appropriate linear or nonlinear procedure. Sections C9.2.4 and C9.2.5 discuss linear and nonlinear procedures, respectively, focusing on methods that are unique to isolation.

Commentary is not provided for Sections 9.2.6 (Nonstructural Components), 9.2.7 (Detailed System Requirements), 9.2.8 (Design and Construction Review), and 9.2.9 (Isolation System Testing and Design Properties) of the *Guidelines.* These sections are similar in content to corresponding sections of the 1994 *NEHRP Provisions* and the 1996 edition of *Recommended Lateral Force Requirements and Commentary*—commonly referred to as the *Blue Book*—produced by the Structural Engineers Association of California (SEAOC, 1996). The reader is directed to the commentaries of these references for discussion of topics not covered in this *Commentary.*

C9.2.1 Background

C9.2.1.1 Development of Isolation Provisions for New Buildings

Until the early 1980s, the design concept of seismic isolation had not been utilized in the United States. As isolation system products matured and became commercially available, research projects led to practice, and isolation began to be seriously considered, particularly for those projects seeking improved seismic performance. This activity identified a need to supplement existing codes with design requirements developed specifically for isolated structures. This need was shared by the public and its agents (i.e., building officials), who required assurance that this new technology was being implemented properly, as well as by the engineering profession, which required a minimum standard for design and construction.

Early efforts directed at creating design provisions for isolated structures began with the Northern Section of SEAOC in the mid-1980s. In 1986, this section of SEAOC published *Tentative Seismic Isolation Design*

Requirements (SEAOC, 1986), the first collection of design provisions for base-isolated structures. These provisions were based on the same seismic criteria required for design of fixed-base buildings, and used similar design concepts, such as the prescription of minimum design force and displacement by formula.

Recognizing the need for a document that would better represent a consensus opinion of all sections of SEAOC, the SEAOC Seismology Committee developed design provisions, "General Requirements for the Design and Construction of Seismic-Isolated Structures," that were published as Appendix 1L of the *1990 SEAOC Blue Book* (SEAOC, 1990). These provisions were also adopted (with minor editorial changes) by the International Conference of Building Officials (ICBO) and published as a nonmandatory appendix to Chapter 23 of the 1991 *Uniform Building Code* (UBC) (ICBO, 1991). The Seismology Committee of SEAOC and ICBO have revised their respective design provisions periodically, and current versions of isolation system criteria may be found in the 1996 *SEAOC Blue Book* (SEAOC, 1996) or the 1994 *UBC* (ICBO, 1994).

In 1992, Technical Subcommittee 12 (TS-12) of the 1994 Provisions Update Committee was formed by the Building Seismic Safety Council to incorporate design requirements for base isolation and energy dissipation systems into the 1994 *NEHRP Recommended Provisions*. TS-12 based its recommendations directly on the isolation provisions of the 1994 *UBC*, modified to conform to the strength-design approach and nomenclature of the *Provisions*. In general, the design provisions for isolated buildings found in Section 2.5 of the *Provisions* conform to those of the *UBC*. Differences between the *Provisions* and the *UBC* will be resolved in the 1997 editions of these documents, when both sets of provisions are based on strength design.

The 1994 *NEHRP Recommended Provisions* and the changes proposed by TS-12 for the 1997 *NEHRP Recommended Provisions* for new buildings were used as resource documents for the development of the *Guidelines* for seismic isolation rehabilitation of existing buildings. The following section of the *Commentary* discusses the philosophy and criteria underlying the NEHRP/UBC/SEAOC provisions for seismic isolation of new buildings (Kircher and Bachman, 1991).

C9.2.1.2 Design Philosophy for Isolation Provisions for New Buildings

The underlying philosophy guiding the development of the NEHRP/UBC/SEAOC provisions for isolation of new buildings may be characterized as a combination of the primary performance objective for fixed-base buildings—which is the protection of life safety for a major earthquake—and the additional performance objective of damage reduction, an inherent benefit of seismic isolation. The design criteria of the NEHRP/UBC/SEAOC provisions are based on a combination of life safety and damage reduction goals. These criteria are summarized in the following statements.

1. The NEHRP/UBC/SEAOC provisions specify two levels of earthquake: the BSE-1 (referred to as the Design Basis Earthquake in SEAOC/UBC provisions) and the Maximum Capable Earthquake.

   The BSE-1 is the same earthquake level of ground shaking as that required by the NEHRP/UBC/SEAOC provisions for design of fixed-base structures: a level of ground motion that has a 10% probability of being exceeded in a 50-year time period (BSE-1 earthquake).

   In this Chapter 9, the design earthquake filling this role for the rehabilitation of existing buildings is user-specified.

   The Maximum Capable Earthquake is an additional, higher level of earthquake ground motion defined as the maximum level of ground shaking that may be expected at the building site within the known geological framework. The 1994 editions of the NEHRP/UBC/SEAOC provisions permit this level to be taken as the level of earthquake ground motion that has a 10% probability of being exceeded in a 100-year time period (10%/100 year earthquake).

   In this Chapter 9, the Maximum Considered Earthquake fills this role for the rehabilitation of existing buildings.

2. The NEHRP/UBC/SEAOC provisions for new buildings require the isolation system to be capable of sustaining loads corresponding to the Maximum Capable Earthquake without failure (e.g., the isolation system is to be designed and tested for Maximum Capable Earthquake displacement). Likewise, the provisions require building separations and utilities that cross the isolation

interface to be designed to accommodate Maximum Capable Earthquake displacement.

3. The NEHRP/UBC/SEAOC provisions require the structure (above the isolation system) to remain "essentially elastic" for the design earthquake, which may be specified as the BSE-1 (e.g., inelastic response of the lateral-load-resisting superstructure system is limited to about one-third of that permitted by the NEHRP/UBC/SEAOC provisions for design of a comparable, fixed-base building).

Design provisions for fixed-base buildings provide reasonable protection against major structural failure and loss of life, but are not intended "to limit damage, maintain functions, or provide for easy repair" (SEAOC, 1996). Based on this philosophy, the lateral forces required for strength design of fixed-base structures are as little as one-eighth of the force level that would occur in buildings responding elastically during a major earthquake, if the structure remained fully elastic. Life safety is provided by design provisions that require the structural system to have sufficient ductility and stability to displace significantly beyond the elastic limit without gross failure or collapse. However, damage to structural elements, nonstructural components, and/or contents of a fixed-base building can occur during an earthquake and would be likely for a major event.

The NEHRP/UBC/SEAOC provisions for fixed-base buildings are based on earthquake forces corresponding to the BSE-1 (reduced for design of elements, as discussed above). Survival for response beyond the BSE-1 level is implicitly addressed by special ductility and detailing requirements. In contrast, the NEHRP/UBC/SEAOC provisions for isolated buildings explicitly consider response beyond the design earthquake or the BSE-1 by requiring the isolation system to be designed for displacements corresponding to the Maximum Capable Earthquake, an event that represents "worst-case" earthquake demands on the isolation system. The intent of requiring the isolation system to be explicitly designed (and verified) for Maximum Capable Earthquake displacement is to provide reasonable assurance that the isolation system will be at least as "safe" as a fixed-base structure. Explicit design (and testing) of the isolation system for "worst-case" earthquake displacement is necessary at this time because a sufficient base of experience does not exist that would justify less conservative criteria.

Ideally, lateral displacement of an isolated structure occurs in the isolation system, rather than in the superstructure above. The lateral-load-resisting system of the superstructure should be designed to have sufficient stiffness and strength to avoid large inelastic displacements. For this reason, the NEHRP/UBC/SEAOC provisions contain criteria that limit the inelastic response of the superstructure to a fraction of that permitted for a fixed-based building. Although damage control for the design earthquake or the BSE-1 is not an explicit objective of the NEHRP/UBC/SEAOC provisions, an isolated structure designed for limited inelastic response of the superstructure will also reduce the level of damage that would otherwise occur during an earthquake. Isolated structures designed in conformance with the NEHRP/UBC/SEAOC provisions should, in general, be able to:

1. Resist minor and moderate levels of earthquake ground motion without damage to structural elements, nonstructural components, or building contents

2. Resist major levels of earthquake ground motion without any of the following occurring: (a) failure of the isolation system, (b) significant damage to structural elements, (c) extensive damage to nonstructural components, or (d) major disruption to facility function

The performance objectives for isolated structures, stated above, considerably exceed the performance anticipated for fixed-base structures during moderate and major earthquakes. Table C9-2 provides a tabular comparison of the performance expected for isolated and fixed-base structures designed in accordance with NEHRP/UBC/SEAOC provisions. Loss of function is not included in this table. For certain (fixed-base) facilities, loss of function would not be expected to occur until there is significant structural damage causing closure of, or restricted access to the building. In other cases, the facility could have only limited or no structural damage, but would not be functional as a result of damage to vital nonstructural components and contents. Isolation would be expected to mitigate structural and nonstructural damage, and to protect the facility against loss of function.

C9.2.1.3 Overview of Seismic Isolation Rehabilitation Projects

A number of buildings have been (or are in the process of being) rehabilitated using seismic isolation. These

Table C9-2 Protection Intended for New Buildings

Risk Category	Earthquake Ground Motion Level		
	Minor	Moderate	Major
Life Safety[1]	F/I	F/I	F/I
Structural Damage[2]	F/I	F/I	I
Nonstructural Damage[3] (Contents Damage)	F/I	I	I

1. Loss of life is not expected for fixed-base (F) or isolated (I) buildings.
2. Significant structural damage is not expected for fixed-base (F) or isolated (I) buildings.
3. Significant nonstructural (contents) damage is not expected for fixed-base (F) or isolated (I) buildings

buildings include the Salt Lake City and County Building in Salt Lake City, Utah (Mayes, 1988), the Rockwell Building in Seal Beach, California (Hart et al., 1990), the Hawley Apartments in San Francisco, California (Zayas and Low, 1991), the Mackay School of Mines in Reno, Nevada (Way and Howard, 1990), the U.S. Court of Appeals, San Francisco, California (Amin et al., 1993), Oakland City Hall in Oakland, California (Honeck et al., 1993), and San Francisco City Hall (Naaseh, 1995). A summary of these projects is provided in Table C9-3.

The rehabilitation projects summarized in Table C9-3 range in size from a 20,000-square-foot building to buildings of up to 500,000 square feet. The original structural systems of these buildings include wood bearing walls, nonductile reinforced concrete moment frames, and steel moment frames with unreinforced masonry (URM) infill and URM bearing walls. Most of the buildings are owned by a local, state, or federal government agency and often have historical significance. The collective size of the buildings in Table C9-3 is over 3 million square feet, and their combined value is close to $1 billion.

The types of isolators used to date in the United States to rehabilitate buildings include lead-rubber bearing (LRB) isolators, rubber-bearing (RB) isolators, friction-pendulum system (FPS) isolators, high-damping rubber bearing (HDR) isolators, and sliding polytetrafluoroethylene (PTFE) isolators. These five types of isolators are representative of the range of products currently available in the US. The projects listed in Table C9-3 have required as few as 31 isolators for the Hawley Apartments, a four-story, 20,000-square-foot residential building, and as many as 591 isolators for San Francisco City Hall, a five-story, 500,000-square-foot historical structure. The extent of new structure added above the isolation system also varies greatly from one project to another. In some cases, such as the Mackay School of Mines, only minimal strengthening of the original structure was required. In other cases, such as the Rockwell Building, the superstructure was substantially strengthened by the addition of new framing at the building perimeter.

C9.2.1.4 Seismic Isolation Rehabilitation Goals

The philosophy or purpose for seismic rehabilitation using isolation is directly dependent on the owner's motivation to upgrade the building, and expectations of upgraded building performance during and following an earthquake. For this reason, Rehabilitation Objectives may vary greatly from project to project.

To date, there are five primary considerations, listed and described below, that have motivated owners to choose isolation for rehabilitation of existing buildings. With each consideration, one or more project(s) are identified that selected seismic isolation for building rehabilitation based on that consideration as well as others.

1. **Functionality**. The facility should remain open and operational during and after an earthquake or be able to resume operation within a short period of time (e.g., Rockwell Building, computer/financial center operation).

2. **Contents Protection**. Important contents must be protected against damage due to earthquake shaking (e.g., San Francisco Asian Art Museum, $3 billion of art contents).

3. **Investment Protection**. Long-term economic loss due to earthquake damage should be mitigated (e.g., State of California Justice Building; Pyle et al., 1993).

4. **Historical Building Preservation**. Seismic rehabilitation modification or demolition of historical building features must be minimized (e.g., Salt Lake City and County Building, Oakland City Hall, U.S. Court of Appeals, and San Francisco City Hall).

Table C9-3 Summary of US Seismic Isolation Rehabilitation Projects

Building/Project Information			*Structural Information*		
Name (Location)	**Status**	**Size in Sq. Ft.**	**Isolation System**	**Original Structure**	**New Structure**
Salt Lake City and County Building (Salt Lake City, UT)	Complete (1988)	170,000	447 Isolators (208 LRB + 239 RB + PTFE)	1894 5-story URM bearing wall w/clock tower (240' total height)	Steel braced frame (clock tower only)
Rockwell Building (Seal Beach, CA)	Complete (1991)	300,000	78+ Isolators (52 LRB + 26 RB + PTFE)	1967 8-story RC moment frame	RC moment frame at perimeter, floors 1–6
Hawley Apartments (San Francisco, CA)	Complete (1991)	20,000	31 Isolators (FPS)	1920 4-story wood bearing wall	Steel moment frame at first floor
Mackay School of Mines (Reno, NV)	Complete (1993)	50,000	106 Isolators (64 HDR + 42 PTFE)	1908 3-story URM bearing wall	Floor ties/wall anchors (new basement)
Campbell Hall, Western Oregon State College (Monmouth, OR)	Complete (1994)		42+ Isolators (26 LRB + 16 RB + PTFE)	1872–1898 3-story URM bearing wall	
Oakland City Hall (Oakland, CA)	Complete (1995)	153,000	126 Isolators (42 LRB + 69 RB + 15 PTFE)	1914 18-story steel frame/ URM in-fill w/clock tower (324' total height)	RC shear walls at cores, steel braced frame at clock tower
U.S. Court of Appeals (San Francisco, CA)	Complete (1995)	350,000	256 Isolators (FPS)	1905 4-story steel frame/URM in-fill with 1933 addition	RC shear walls
Long Beach Veterans Admin. Hospital (Long Beach, CA)	Complete (1995)	350,000	156 Isolators (110 LRB + 18 RB + 30 PTFE)	1967 12-story RC perforated shear wall	Basement columns strengthened
Building S-12 Hughes (El Segundo, CA)	Complete (1995)	240,000	45+ Isolators (24 LRB + 21 RB + PTFE)	1960s 12-story RC shear wall/frame building	First floor and substructure strengthened
Kerckhoff Hall, Univ. of California, Los Angeles (Westwood, CA)	Complete (1996)	92,000	126+ Isolators (33 LRB + 93 RB + PTFE)	6-story RC and brick wall structure	First floor and substructure strengthened
San Francisco City Hall (San Francisco, CA)	Complete (1997)	500,000	591 Isolators (530 LRB + 61 PTFE)	1912 5-story steel frame/URM in-fill with dome (~300' total height)	Steel braced frame in dome and RC shear walls at lower floors

LRB: Lead-rubber bearing isolators

RB: Rubber bearing isolators

PTFE: Sliding polytetra fluoroethylene isolators

FPS: Friction pendulum system isolators

HDR: High damping rubber bearing isolators

5. **Construction Economy**. The building is of a size and/or complexity that makes seismic isolation the most economical construction alternative (e.g., Oakland and San Francisco City Halls).

Each rehabilitation project will have a different set of motivating factors and related performance objectives, and therefore will likely require different design criteria. The first essential step in developing design criteria is to identify and rank the owner's seismic risk goals in terms of facility function, damage and investment protection, historical preservation, and construction economy. These goals will guide the engineer's selection of performance objectives and design criteria appropriate for the building. Owners who place a high priority on functionality or protection of contents or investment will require more stringent design criteria, such as those in the *Guidelines* for Immediate Occupancy. Owners more intent on historical preservation or construction economy will require less stringent design criteria, such as those in the *Guidelines* for Life Safety. Owners that are only interested in Collapse Prevention should probably consider other, more economical design strategies than seismic isolation.

C9.2.2 Mechanical Properties and Modeling of Seismic Isolation Systems

C9.2.2.1 General

The three basic properties of an isolation system are: (1) horizontal flexibility to increase structural period and reduce spectral demands (except for very soft soil sites), (2) energy dissipation (also known as damping) to reduce displacements, and (3) sufficient stiffness at small displacements to provide adequate rigidity for service-level environmental loadings. The horizontal flexibility common to all practical isolation systems serves to uncouple the building from the effects of high-frequency earthquake shaking typical of rock or firm soil sites—thus serving to deflect the earthquake energy and significantly reduce the magnitude of the resulting inertia forces in the building. Energy dissipation in an isolation system, in the form of either hysteretic or viscous damping, serves to reduce the displacement response of an isolation system (Skinner et al., 1993; Kelly, 1993; Soong and Constantinou, 1994), generally resulting in more compact isolators.

The reduction of bearing displacements in highly damped isolation systems typically results in reduction of the shear force in the isolation system. This is demonstrated in Figures C9-1 and C9-2. The results are from nonlinear time history analyses of an eight-story isolated building supported by 45 isolators (Winters and Constantinou, 1993; Soong and Constantinou, 1994). Each isolator has bilinear hysteretic properties that characterize a wide range of elastomeric and sliding isolation systems. A total of twelve isolation systems, having an isolated period (T_I) in the range of 1.5 to 3 seconds and effective damping (β_{eff}) in the range of 0.06 to 0.37, were analyzed. The seismic input was representative of Seismic Zone 4, Soil Profile Type S_2, of the 1991 *UBC* (ICBO, 1991). This input consisted of nine pairs of earthquakes, with each pair applied along the principal directions of the structure.

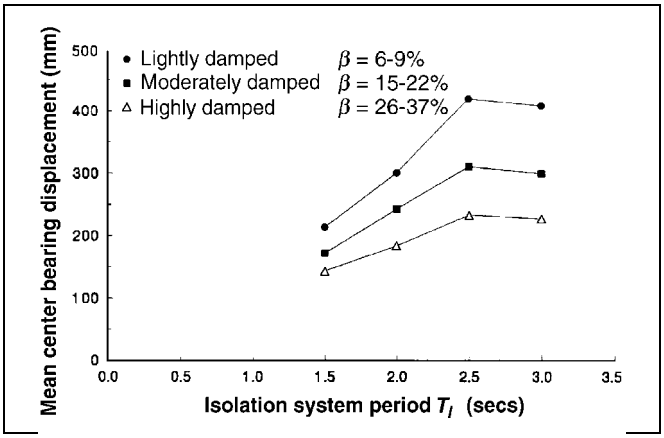

Figure C9-1 ***Center Bearing Displacement (Mean of Nine Analyses) in Eight-Story Building with Hysteretic Isolation System***

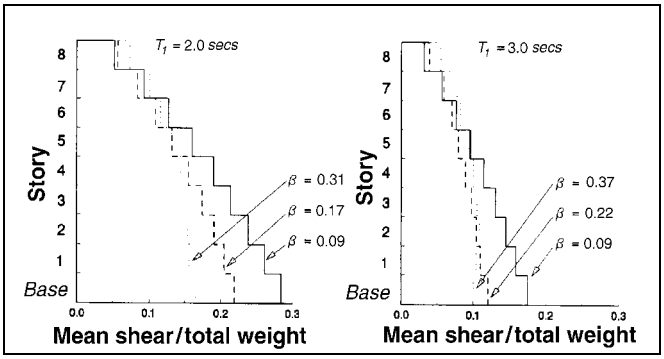

Figure C9-2 ***Distribution of Shear Force (Mean of Nine Analyses) with Height in Eight-Story Building with Hysteretic Isolation System***

Figure C9-1 demonstrates the increase of bearing displacement with (1) increasing period, and (2) decreasing effective damping. Figure C9-2 demonstrates the reduction of shear force in the isolation system (termed "base" in the figure) with increasing effective damping. Note in this figure that for highly damped isolation systems, the shear force distribution is nearly constant over the height of the structure, whereas for lightly damped systems this distribution is approximately triangular. The latter is indicative of response in the fundamental mode of vibration, whereas the former is indicative of higher mode response, which is typically accompanied by higher accelerations in upper floors. Nevertheless, the benefits offered by highly damped systems are evident. For example, in the system with an isolated period equal to 2.0 seconds, an effective damping of 0.31 results in a 40% reduction in bearing displacements and lower structural shear forces in the bottom two-thirds of the structure, all in comparison with the response of a lightly damped (β_{eff} = 0.09) system. However, the accelerations in the top floor of the building with the highly damped isolators are 40% higher than those in the lightly damped building. Thus, highly damped systems offer advantages when the primary intent of seismic isolation is to protect the structural system. Lightly damped systems may be preferable when the intent of seismic isolation is to protect secondary systems, such as sensitive equipment (Kelly, 1993; Skinner et al., 1993). Typical seismic isolation systems are horizontally flexible and vertically stiff. Vertical ground motions are likely to be amplified in most isolation systems. If protection of secondary systems is of primary importance, due consideration of vertical ground motion is necessary; vertical isolation of either the building or individual secondary systems may also be appropriate.

The benefits of reduced bearing displacements, shear forces, and accelerations may be realized with linear seismic isolation systems. For example, Figure C9-3 compares the distribution of shear force over the height of an eight-story building for highly damped isolation systems that have either bilinear hysteretic behavior, or linearly elastic and linearly viscous behavior. A system consisting of low-damping elastomeric bearings and linear fluid viscous devices has substantially linear behavior and offers the benefits of reduced bearing displacements, shear forces, and floor accelerations. Skinner et al. (1993) provide several examples that demonstrate many of these features of seismic isolation for a wide range of isolation system properties.

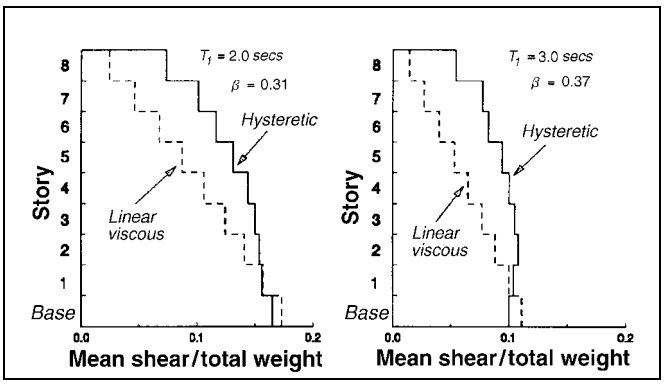

Figure C9-3 ***Comparison of Distribution of Shear Force with Height in Eight-Story Building with Hysteretic and Linear Viscous Isolation System***

C9.2.2.2 Mechanical Properties of Seismic Isolators

A. Elastomeric Isolators

Elastomeric bearings represent a common means for introducing flexibility into an isolated structure. They consist of thin layers of natural rubber that are vulcanized and bonded to steel plates. Natural rubber exhibits a complex mechanical behavior, which can be described simply as a combination of viscoelastic and hysteretic behavior. Low-damping natural rubber bearings exhibit essentially linearly elastic and linearly viscous behavior at large shear strains. The effective damping is typically less than or 0.07 for shear strains in the range of 0 to 2.0.

Lead-rubber bearings are generally constructed of low-damping natural rubber with a preformed central hole, into which a lead core is press-fitted. Under lateral deformation, the lead core deforms in almost pure shear, yields at low level of stress (approximately 8 to 10 MPa in shear at normal temperature), and produces hysteretic behavior that is stable over many cycles. Unlike mild steel, lead recrystallizes at normal temperature (about 20°C), so that repeated yielding does not cause fatigue failure. Lead-rubber bearings generally exhibit characteristic strength that ensures rigidity under service loads. Figure C9-4 shows an idealized force-displacement relation of a lead-rubber bearing. The characteristic strength, Q, is related to the lead plug area, A_p, and the shear yield stress of lead, σ_{YL}:

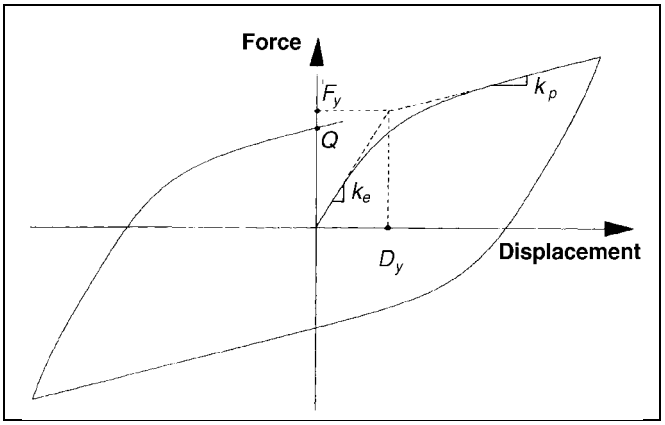

Figure C9-4 ***Idealized Hysteretic Force-Displacement Relation of Elastomeric Bearing***

$$Q = A_p \sigma_{YL} \tag{C9-1}$$

The post-yield stiffness, k_p, is typically higher than the shear stiffness of the bearing without the lead core:

$$k_p = \frac{A_r G f_L}{\Sigma t} \tag{C9-2}$$

where A_r is the bonded rubber area, Σt is the total rubber thickness, G is the shear modulus of rubber (typically computed at shear strain of 0.5), and f_L is a factor larger than unity. Typically, f_L is 1.15, and the elastic stiffness ranges between 6.5 to 10 times the post-yield stiffness.

The behavior of lead-rubber bearings may be represented by a bilinear hysteretic model. Computer programs *3D-BASIS* (Nagarajaiah et al., 1991; Reinhorn et al., 1994; Tsopelas et al., 1994) and *ETABS, Version 6* (CSI, 1994) have the capability of modeling hysteretic behavior for isolators. These models typically require definition of three parameters, namely, the post-yield stiffness k_p, the yield force F_y, and the yield displacement D_y. For lead-rubber bearings in which the elastic stiffness is approximately equal to 6.5 k_p, the yield displacement can be estimated as:

$$D_y = \frac{Q}{5.5 k_p} \tag{C9-3}$$

The yield force is then given by

$$F_y = Q + k_p D_y \tag{C9-4}$$

High-damping rubber bearings are made of specially compounded rubber that exhibits effective damping between 0.10 and 0.20 of critical. The increase in effective damping of high-damping rubber is achieved by the addition of chemical compounds that may also affect other mechanical properties of rubber. Figure C9-5 shows representative force-displacement loops of a high-damping rubber bearing under scragged conditions.

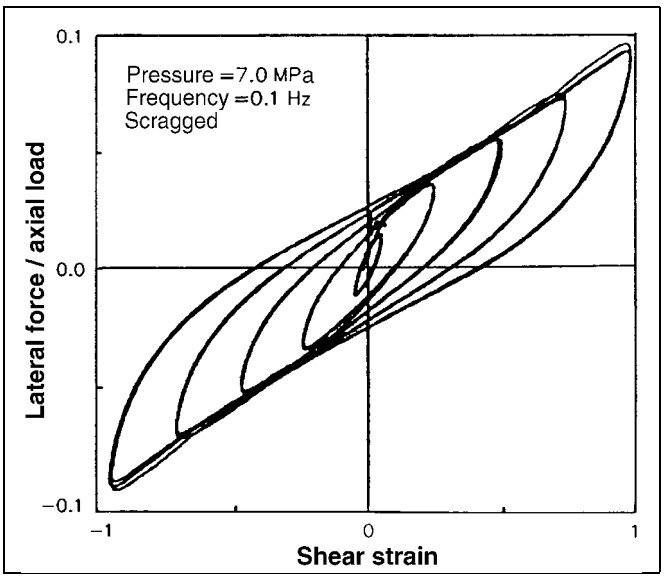

Figure C9-5 ***Force-Displacement Loops of a High-Damping Rubber Bearing***

Scragging is the process of subjecting an elastomeric bearing to one or more cycles of large amplitude displacement. The scragging process modifies the molecular structure of the elastomer and results in more stable hysteresis at strain levels lower than that to which the elastomer was scragged. Although it is usually assumed that the scragged properties of an elastomer remain unchanged with time, recent studies (Cho and Retamal, 1993; Murota et al., 1994) suggest that partial recovery of unscragged properties is likely. The extent of this recovery is dependent on the elastomer compound.

Mathematical models capable of describing the transition between virgin and scragged properties of

high-damping rubber bearings are not yet available. It is appropriate in this case to perform multiple analyses with stable hysteretic models and obtain bounds on the dynamic response. A smooth bilinear hysteretic model that is capable of modeling the behavior depicted in Figure C9-4 is appropriate for such analyses, as long as the peak shear strain is below the stiffening limit of approximately 1.5 to 2.0, depending on the rubber compound. Beyond this strain limit many elastomers exhibit stiffening behavior, with tangent stiffness approximately equal to twice the tangent stiffness prior to initiation of stiffening. For additional information, refer to Tsopelas et al. (1994).

To illustrate the calculations of parameters from prototype bearings test data, Figure C9-6 shows experimentally determined properties of the high-damping rubber bearings, for which loops are shown in Figure C9-5. The properties identified are the tangent shear modulus, *G*, and the effective damping ratio, β_{eff} (described by Equation C9-18, which is now defined for a single bearing rather than the entire isolation system) under scragged conditions. With reference to Figure C9-4, *G* is related to the post-yielding stiffness k_p.

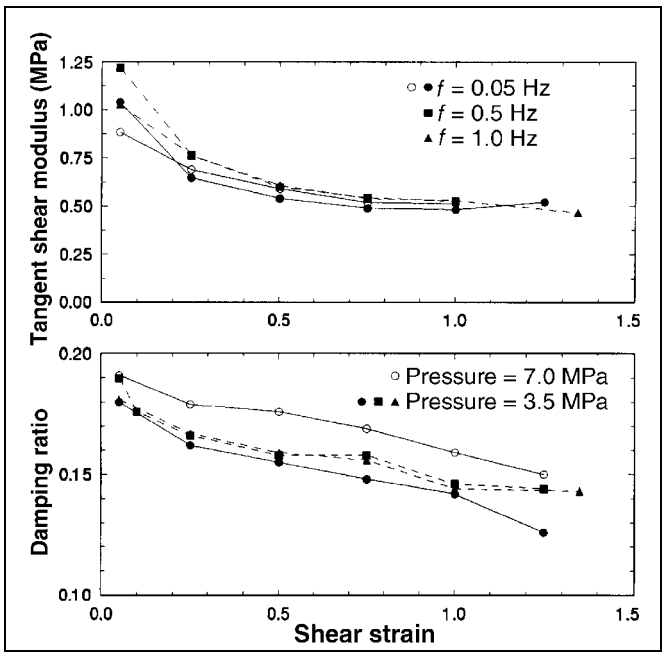

Figure C9-6 ***Tangent Shear Modulus and Effective Damping Ratio of High-Damping Rubber Bearing***

$$k_p = \frac{GA}{\Sigma t} \qquad \text{(C9-5)}$$

where *A* is the bonded rubber area. The results of Figure C9-6 demonstrate that the tangent shear modulus and equivalent damping ratio are only marginally affected by the frequency of loading and the bearing pressure, within the indicated range for the tested elastomer. Different conclusions may be drawn from testing of other high-damping rubber compounds.

The parameters of the bilinear hysteretic model may be determined by use of the mechanical properties *G* and β_{eff} at a specific shear strain, such as the strain corresponding to the design displacement *D*. The post-yield stiffness k_p is determined from Equation C9-5, whereas the characteristic strength, *Q*, can be determined as:

$$Q = \frac{\pi\beta_{eff}k_pD^2}{(2-\pi\beta_{eff})D - 2D_y} \qquad \text{(C9-6)}$$

where D_y is the yield displacement. The yield displacement is generally not known a priori. However, experimental data suggest that D_y is approximately equal to 0.05 to 0.1 times the total rubber thickness, Σt. With the yield displacement approximately determined, the model can be completely defined by determining the yield force (Equation C9-4). It should be noted that the characteristic strength may be alternatively determined from the effective stiffness, k_{eff} (Equation C9-17), of the bearing, as follows:

$$Q = \frac{\pi\beta_{eff}k_{eff}D^2}{2(D-D_y)} \qquad \text{(C9-7)}$$

The effective stiffness is a more readily determined property than the post-yielding stiffness. The effective stiffness is commonly used to obtain the effective shear modulus, G_{eff}, defined as:

$$G_{eff} = \frac{k_{eff}\Sigma t}{A} \qquad \text{(C9-8)}$$

The behavior of the bearing for which the force-displacement loops are shown in Figure C9-5 is now analytically constructed using the mechanical properties at a shear strain of 1.0 and a bearing pressure of 7.0 MPa. These properties are G_{eff} = 0.50 MPa and β_{eff} = 0.16. With the bonded area and total thickness of rubber known, and assuming $D_y = 0.1\Sigma t$, a bilinear hysteretic model was defined and implemented in the program *3D-BASIS*. The simulated loops are shown in Figure C9-7, where it may be observed that the calculated hysteresis loop at shear strain of 1.0 agrees well with the corresponding experimental hysteresis loop. However, at lower peak shear strain the analytical loops have a constant characteristic strength, whereas the experimental loops have a characteristic strength dependent on the shear strain amplitude. Nevertheless, the analytical model will likely produce acceptable results when the design parameters are based on the mechanical properties at a strain corresponding to the design displacement.

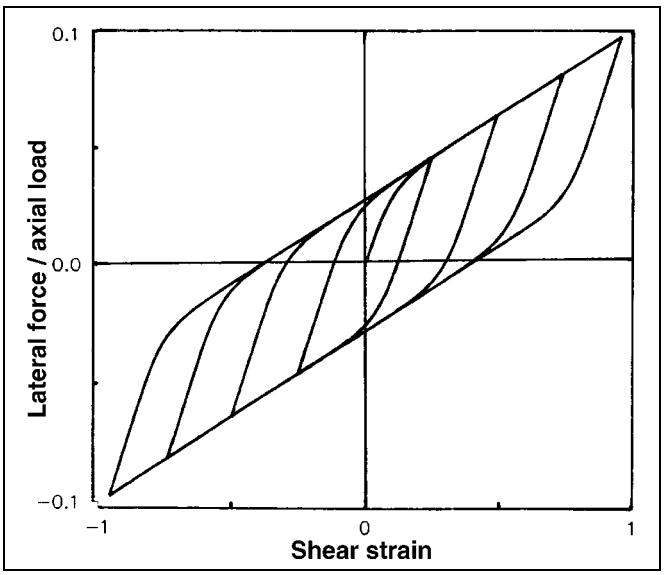

Figure C9-7 Analytical Force-Displacement Loops of High-Damping Rubber Bearing

Elastomeric bearings have finite vertical stiffness that affects the vertical response of the isolated structure. The vertical stiffness of an elastomeric bearing may be obtained from

$$k_v = \frac{E_c A}{\Sigma t} \qquad \text{(C9-9)}$$

where E_c is the compression modulus. Although a number of approximate empirical relations have been proposed for the calculation of the compression modulus, the correct expression for circular bearings is

$$E_c = \left(\frac{1}{6G_{eff}S^2} + \frac{4}{3K} \right)^{-1} \qquad \text{(C9-10)}$$

(Kelly, 1993) where *K* is the bulk modulus (typically assumed to have a value of 2000 MPa) and *S* is the shape factor, which is defined as the ratio of the loaded area to the bonded perimeter of a single rubber layer. For a circular bearing of bonded diameter ϕ and rubber layer thickness *t*, the shape factor is given by

$$S = \frac{\phi}{4t} \qquad \text{(C9-11)}$$

Seismic elastomeric bearings are generally designed with large shape factor, typically 12 to 20. Considering an elastomeric bearing design with *S* = 15, G_{eff} = 1 MPa, and *K* = 2000 MPa, the ratio of vertical stiffness (Equation C9-9) to effective horizontal stiffness (Equation C9-8) is approximately equal to 700. Thus, the vertical period of vibration of a structure on elastomeric isolation bearings will be about 26 times (i.e., $\sqrt{700}$) less than the horizontal period; on the order of 0.1 second. This value of vertical period provides potential for amplification of the vertical ground acceleration by the isolation system. The primary effect of this amplification is to change the vertical load on the bearings, which may need to be considered for certain design applications.

Another consideration in the design of seismically isolated structures with elastomeric bearings is reduction in height of a bearing with increasing lateral deformation (Kelly, 1993). While this reduction of height is typically small, it may be of importance when elastomeric bearings are combined with other isolation elements that are vertically rigid (such as sliding bearings). In addition, incompatibilities in vertical displacements may lead to a redistribution of loads.

B. Sliding Isolators

Sliding bearings will tend to limit the transmission of force to an isolated structure to a predetermined level. While this is desirable, the lack of significant restoring force can result in significant variations in the peak displacement response, and can result in permanent offset displacements. To avoid these undesirable features, sliding bearings are typically used in combination with a restoring force mechanism.

The lateral force developed in a sliding bearing can be defined as:

$$F = \frac{N}{R}U + \mu_s N \text{ sgn } (\dot{U}) \qquad \text{(C9-12)}$$

where

U = Displacement
$\dot{U}$ = Sliding velocity
R = Radius of curvature of sliding surface
μ_s = Coefficient of sliding friction
N = Normal load on bearing

The normal load consists of the gravity load, W, the effect of vertical ground acceleration, $\ddot{U}_v$, and the additional seismic load due to overturning moment, P_s:

$$N = W\left(1 + \frac{\ddot{U}_v}{g} + \frac{P_s}{W}\right) \qquad \text{(C9-13)}$$

The first term in Equation C9-12 denotes the restoring force component, and the second term describes the friction force. For flat sliding bearings the radius of curvature is infinite, so that the restoring force term in Equation C9-12 vanishes. For a spherical sliding surface (Zayas et al., 1987) the radius of curvature is constant, so that the bearing exhibits a linear restoring force; that is, under constant gravity load the stiffness is equal to W/R_o, where R_o is the radius of the spherical sliding surface. When the sliding surface takes a conical shape, the restoring force is constant. Figure C9-8 shows idealized force-displacement loops of sliding bearings with flat, spherical, and conical surfaces.

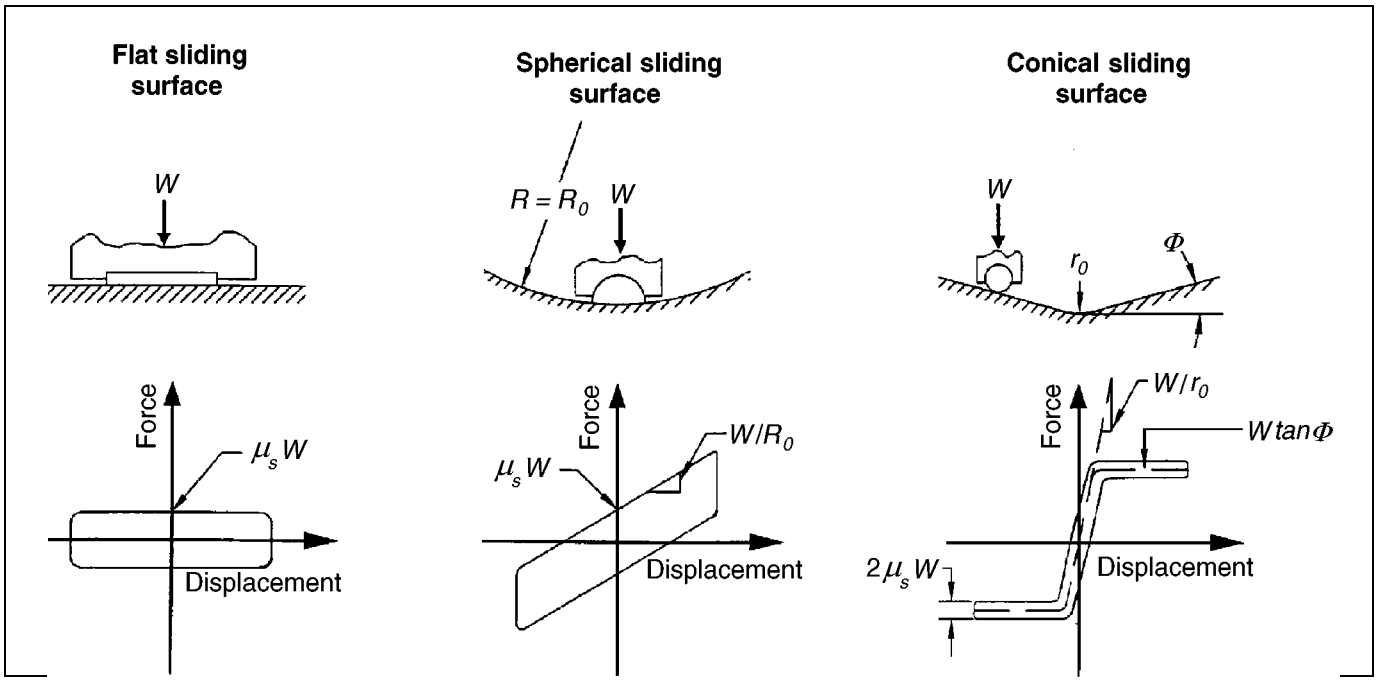

Figure C9-8 Idealized Force-Displacement Loops of Sliding Bearings

Sliding bearings with either a flat or single curvature spherical sliding surface are typically made of PTFE or PTFE-based composites in contact with polished stainless steel. The shape of the sliding surface allows large contact areas that, depending on the materials used, are loaded to average bearing pressures in the range of 7 to 70 MPa. For interfaces with shapes other than flat or spherical, the load needs to be transferred through a bearing as illustrated in Figure C9-8 for the conical sliding surface. Such an arrangement typically results in a very low coefficient of friction.

For bearings with large contact area, and in the absence of liquid lubricants, the coefficient of friction depends on a number of parameters, of which the three most important are the composition of the sliding interface, bearing pressure, and velocity of sliding. For interfaces composed of polished stainless steel in contact with PTFE or PTFE-based composites, the coefficient of sliding friction may be described by

$$\mu_s = f_{max} - (f_{max} - f_{min}) \exp(-a|\dot{U}|) \qquad \text{(C9-14)}$$

where parameters f_{min} and f_{max} describe the coefficient of friction at small and large velocities of sliding and under constant pressure, respectively, all as depicted in Figure C9-9. Parameters f_{max}, f_{min}, and a depend on the bearing pressure, although only the dependency of f_{max} on pressure is of practical significance. A good approximation to the experimental data (Constantinou et al., 1993b) is

$$f_{max} = f_{maxo} - (f_{maxo} - f_{maxp}) \tanh \varepsilon p \qquad \text{(C9-15)}$$

where the physical significance of parameters f_{maxo} and f_{maxp} is as illustrated in Figure C9-9. The term p is the instantaneous bearing pressure, which is equal to the normal load N (Equation C9-13) divided by the contact area; and ε is a parameter that controls the variation of f_{max} with pressure.

Figure C9-9 illustrates another feature of sliding bearings. On initiation of motion, the coefficient of friction exhibits a static or breakaway value, μ_B, which is typically higher than the minimum value f_{min}. To demonstrate frictional properties, Figure C9-10 shows the relation between bearing pressure and the friction coefficients f_{max}, μ_B, and f_{min} of a PTFE-based composite material in contact with polished stainless steel at normal temperature. These data were compiled from testing of bearings in four different testing programs (Soong and Constantinou, 1994).

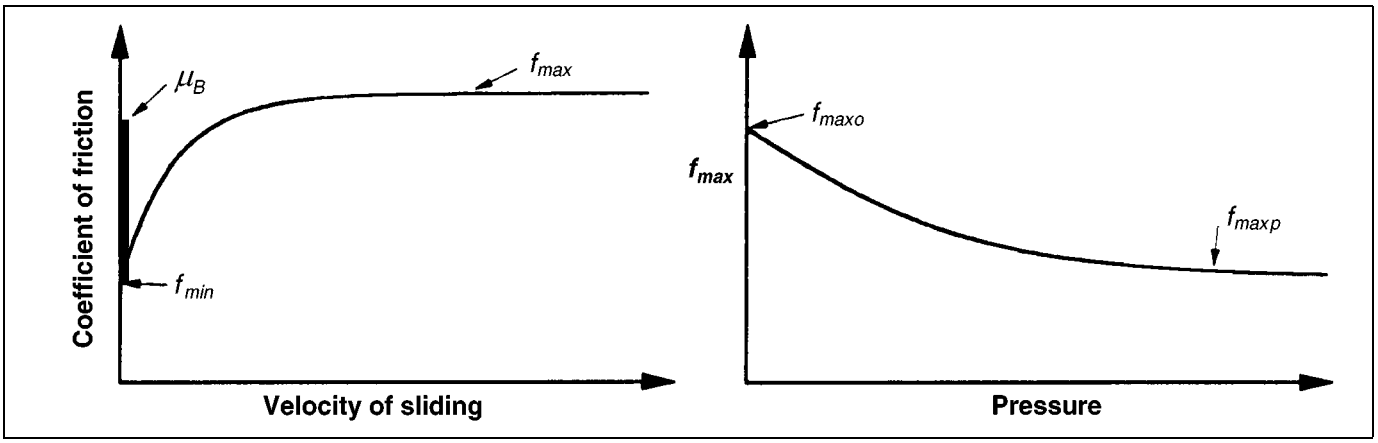

Figure C9-9 Parameters in Model of Friction of Sliding Bearings

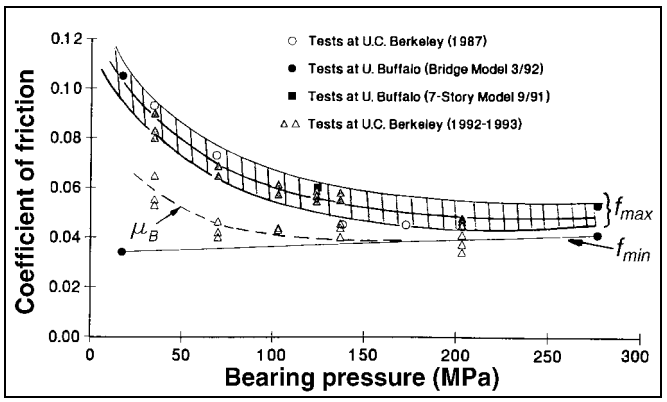

Figure C9-10 Coefficient of Friction of PTFE-based Composite in Contact with Polished Stainless Steel at Normal Temperature

C. Hybrid Isolators

Combined elastomeric-sliding isolation systems have been used in buildings in the United States. Japanese engineers have also used elastomeric bearings in combination with mild steel elements that are designed to yield in strong earthquakes and enhance the energy dissipation capability of the isolation system (Kelly, 1988). These mild steel elements exhibit either elasto-plastic behavior or bilinear hysteretic behavior with low post-yielding stiffness. Moreover, fluid viscous energy dissipation devices have been used in combination with elastomeric bearings. The behavior of fluid viscous devices is described in Section C9.3.3.2C.

Hybrid seismic isolation systems—composed of elastomeric and sliding bearings—should be modeled taking into account the likely significant differences in the relationships between vertical displacement as a function of horizontal displacement. The use of elastomeric and sliding isolators in close proximity to one another under vertically stiff structural framing elements (e.g., reinforced concrete shear walls) may be problematic and could result in significant redistributions of gravity loads.

C9.2.2.3 Modeling of Isolators

A. General

No commentary is provided for this section.

B. Linear Models

For linear procedures (see Section C9.2.3), the seismic isolation system can be represented by an equivalent linearly elastic model. The force in a seismic isolation device is calculated as:

$$F = k_{eff} D \qquad \text{(C9-16)}$$

where all terms are as defined in Section 9.2.2.3B of the *Guidelines*. The effective stiffness of the seismic isolation device may be calculated from test data as follows:

$$k_{eff} = \frac{|F^+| + |F^-|}{|\Delta^+| + |\Delta^-|} \qquad \text{(C9-17)}$$

Figure C9-11 illustrates the physical significance of the effective stiffness.

Analysis by a linear method requires that either each seismic isolator or groups of seismic isolators be represented by linear springs of either stiffness k_{eff} or the combined effective stiffness of each group. The energy dissipation capability of an isolation system is generally represented by effective damping. Effective damping is amplitude-dependent and calculated at design displacement, D, as follows:

$$\beta_{eff} = \frac{1}{2\pi}\left[\frac{\Sigma E_D}{K_{eff} D^2}\right] \qquad \text{(C9-18)}$$

where ΣE_D is the sum of the areas of the hysteresis loops of all isolators, and K_{eff} is the sum of the effective stiffnesses of all seismic isolation devices. Both the area of the hysteresis loops and the effective stiffness are determined at the design displacement, D.

The application of Equations C9-16 through C9-18 to the design of isolation systems is complicated if the effective stiffness and loop area depend on axial load. Multiple analyses are then required to establish bounds on the properties and response of the isolators. For example, sliding isolation systems exhibit such dependencies as described in Section C9.2.2.2B. To account for these effects, the following procedure is proposed.

1. In sliding isolation systems, the relation between horizontal force and vertical load is substantially linear (see Equation C9-12). Accordingly, the net effect of overturning moment on the mechanical

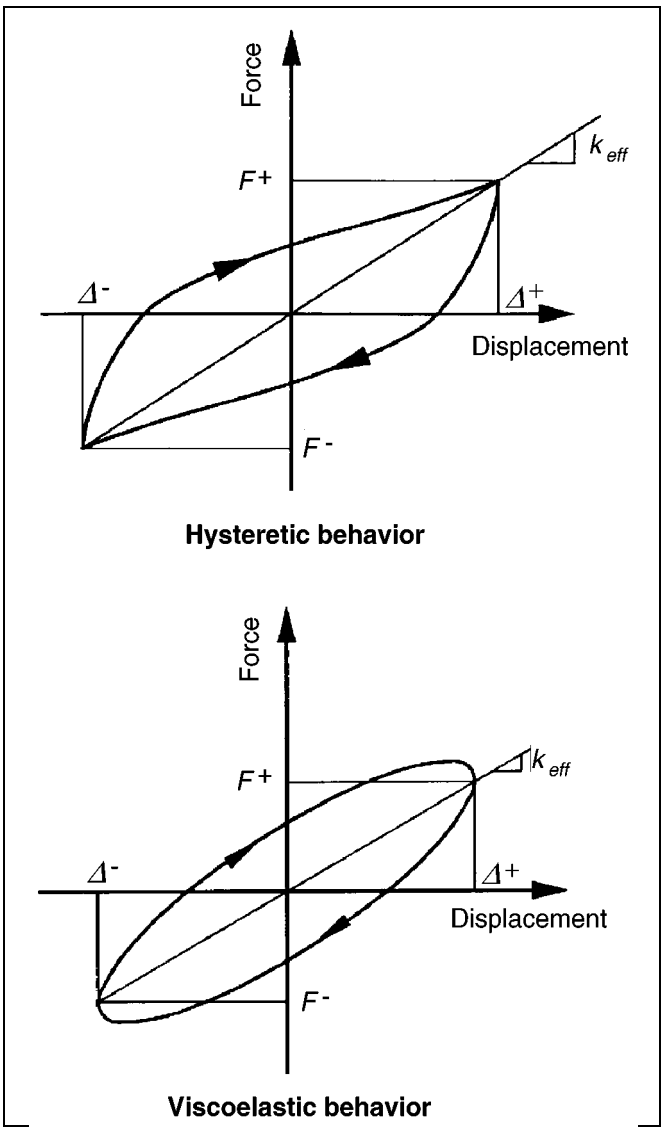

Figure C9-11 Definition of Effective Stiffness of Seismic Isolation Devices

behavior of a group of bearings is small and can be neglected. Al-Hussaini et al. (1994) provided experimental results that demonstrate this behavior up to the point of imminent bearing uplift. Similar results are likely for elastomeric bearings.

2. The effect of vertical ground acceleration is to modify the load on the isolators. If it is assumed that the building is rigid in the vertical direction, and axial forces due to overturning moments are absent, the axial loads can vary between $W(1 - \ddot{U}/g)$ and $W(1 + \ddot{U}/g)$, where $\ddot{U}$ is the peak vertical ground acceleration. However, recognizing that horizontal and vertical ground motion components are likely not correlated unless in the near field, it is appropriate to use a combination rule that uses only a fraction of the peak vertical ground acceleration. Based on the use of 50% of the peak vertical ground acceleration, maximum and minimum axial loads on a given isolator may be defined as:

$$N_c = W(1 \pm 0.20S_{DS}) \qquad \text{(C9-19)}$$

where the plus sign gives the maximum value and the minus sign gives the minimum value. Equation C9-19 is based on the assumption that the short-period spectral response parameter, S_{DS}, is 2.5 times the peak value of the vertical ground acceleration. For analysis for the Maximum Considered Earthquake, the axial load should be determined from

$$N_c = W(1 \pm 0.20S_{MS}) \qquad \text{(C9-20)}$$

Equations C9-19 and C9-20 should be used with caution if the building is located in the near field of a major active fault. In this instance, expert advice should be sought regarding correlation of horizontal and vertical ground motion components.

Load N_c represents a constant load on isolators, which can be used for determining the effective stiffness and area of the hysteresis loop. To obtain these properties, the characteristic strength Q (see Figure C9-11) is needed. For sliding isolators, Q can be taken as equal to $f_{max}N_c$, where f_{max} is determined at the bearing pressure corresponding to load N_c. For example, for a sliding bearing with spherical sliding surface of radius R_o (see Figure C9-8), the effective stiffness and area of the loop at the design displacement D are:

$$k_{eff} = \left(\frac{1}{R_o} + \frac{f_{max}}{D}\right)N_c \qquad \text{(C9-21)}$$

$$\text{Loop Area} = 4f_{max}N_cD \qquad \text{(C9-22)}$$

C. Nonlinear Models

For dynamic nonlinear time-history analysis, the seismic isolation elements should be explicitly

modeled. Sections C9.2.2.2 through C9.2.2.4 present relevant information. When uncertainties exist, and when aspects of behavior cannot be modeled, multiple analyses should be performed in order to establish bounds on the dynamic response.

For simplified nonlinear analysis, each seismic isolation element can be modeled by an appropriate rate-independent hysteretic model. Elastomeric bearings may be modeled as bilinear hysteretic elements as described in Section C9.2.2.2. Sliding bearings may also be modeled as bilinear hysteretic elements with characteristic strength (see Figure C9-4) given by

$$Q = f_{max} N_c \qquad \text{(C9-23)}$$

where N_c is determined by either Equation C9-19 or Equation C9-20, and f_{max} is the coefficient of sliding friction at the appropriate sliding velocity. The post-yield stiffness can then be determined as:

$$k_p = \frac{N_c}{R} \qquad \text{(C9-24)}$$

where R is as defined in Section C9.2.2.2B. The yield displacement D_y in a bilinear hysteretic model of a sliding bearing should be very small, perhaps on the order of 2 mm. Alternatively, a bilinear hysteretic model for sliding bearings may be defined to have an elastic stiffness that is at least 100 times larger than the post-yield stiffness k_p.

Isolation devices that exhibit viscoelastic behavior as shown in Figure C9-11 should be modeled as linearly elastic elements with effective stiffness k_{eff} as determined by Equation C9-17.

C9.2.2.4 Isolation System and Superstructure Modeling

A. General

The model (or models) of the isolation system and superstructure serves two primary functions:

1. **Calculation of the BSE-2 displacement of the isolation system.** BSE-2 displacement is used for designing the isolation system, testing isolator prototypes, establishing required clearances, and specifying displacement demand on nonstructural components that cross the isolation interface.

2. **Calculation of the design earthquake response of the structure.** The design earthquake response is used for design of superstructure components and elements, isolation system connections, foundation and other structural components, and elements below the isolation system.

Several approaches can be used for modeling the isolation system and superstructure, ranging from simplified stick models to detailed, three-dimensional finite element models of the entire building. The extent of the modeling will vary depending on the structural configuration, the type of isolation system, and the degree of linearity (or nonlinearity) expected in the superstructure. In general, flexible, irregular, and/or nonlinear superstructures will require more complex modeling.

B. Isolation System Model

The isolation system should be modeled with sufficient detail to accurately determine the maximum displacement of isolators, including the effects of torsion, and to accurately determine forces acting on adjacent structural elements.

The properties of the isolation system (e.g., effective stiffness) may vary due to changes in vertical load, direction of applied load, and the rate of loading. For some systems, properties may change with the number of cycles of load, or otherwise have some significant degree of variability (e.g., as measured during prototype testing). The model of the isolation system will need to explicitly account for the range of isolation system properties, if properties vary significantly (e.g., effective stiffness changes by more than 15% during prototype testing). Typically, two models will need to be used to bound the range of isolation system stiffness. The stiffer isolation system model would be used to calculate superstructure force; the softer isolation system model would be used to calculate isolation system displacement.

Isolation systems can be susceptible to uplift of isolators due to earthquake overturning load. The model of the isolation system should permit uplift of the superstructure to occur, unless the isolators are shown to be capable of resisting uplift force. Uplift is a nonlinear phenomenon and requires either explicit modeling (i.e., vertical gap element) or a linear model

that releases vertical load in isolators when the uplift force exceeds the isolator's capacity. It is important that the model permit uplift at isolators, so that the forces in the superstructure redistribute accordingly and the maximum uplift displacement is established for design of the isolation system connections and for testing of isolator prototypes.

Special care must be taken to calculate *P*-Δ effects because standard analysis procedures typically ignore the effects of the *P*-Δ moment across isolators. The displacement of the isolation system can create large *P*-Δ moment on the isolators, the substructure and foundation below, and the superstructure above. Depending on the type of isolator, the P-Δ moment will be at least $(P \text{ times } \Delta)/2$ and may be as great as $P \text{ times } \Delta$, where P is the axial load in the isolator and Δ is the horizontal isolator displacement. This moment is applied to both the top and the bottom of the isolator interfaces and is in addition to the moment due to shear across the isolator.

C. Superstructure Model

In general, the superstructure should be modeled with as much detail as would be required for a conventional building.

Special care must be taken in modeling the strength and stiffness of the superstructure. The structural system should have the required strength to respond essentially as a linear elastic system, if the superstructure is modeled with elastic elements. The building will not receive the benefit of the isolation system if the superstructure, rather than the isolation system, yields and displaces.

The lateral-force-resisting system of the superstructure may be considered to be essentially linearly elastic, if at each floor the primary elements and components of the lateral-force-resisting system experience limited inelastic demand (i.e., $m \leq 1.5$). Limited inelastic demand would not preclude a few elements or components from reaching the limits established for the material, provided the effective stiffness of the lateral-force-resisting system of the superstructure did not, as a whole, change appreciably.

C9.2.3 General Criteria for Seismic Isolation Design

C9.2.3.1 General

The basis for design should be established using the procedures of Chapter 2 and the building's Rehabilitation Objective(s).

The criteria for design, analysis, and testing of the isolation system are based primarily on requirements for isolation systems of new buildings. This approach acknowledges that the basic requirements for such things as stability of isolators, prototype testing and, quality control, are just as valid for rehabilitation projects as for new construction. A case might be made for less conservative limits on clearances around the isolated building, provided life safety is not compromised. Again, such an argument would not be appropriate for projects with goals dominated by special damage protection or functionality objectives.

Peer review of the isolation system should be performed for all rehabilitation projects, as required by design provisions for new construction. However, the extent of the review should be gauged to the size and importance of the project. Large, important projects require full design and construction review by a panel of seismic isolation, structural, and geotechnical experts, while small projects may be adequately checked by building authorities with only limited oversight by an outside consultant.

Rather than addressing a specific method of base isolation, the *Guidelines* include general design requirements applicable to a wide range of possible seismic isolation systems. In remaining general, the design provisions rely on mandatory testing of isolation system hardware to confirm the engineering properties used in the design and to verify the overall adequacy of the isolation system. Some systems may not be capable of demonstrating acceptability by test, and consequently should not be used. In general, acceptable isolation systems will:

1. Remain stable for the required design displacement
2. Provide increasing resistance with increasing displacement (although some acceptable systems may not fully comply with this provision)
3. Not degrade under repeated cyclic load

4. Have well-defined engineering properties (e.g., established and repeatable force-deflection characteristics)

C9.2.3.2 Ground Shaking Criteria

No commentary is provided for this section.

C9.2.3.3 Selection of Analysis Procedure

The *Guidelines* require either linear or nonlinear procedures for analysis of isolated buildings.

Linear procedures include prescriptive formulas and Response Spectrum Analysis. Linear procedures based on formulas (similar to the seismic-coefficient equation required for design of fixed-base buildings) prescribe peak lateral displacement of the isolation system, and define "minimum" design criteria that may be used for design of a very limited class of isolated structures (without confirmatory dynamic analyses). These simple formulas are useful for preliminary design and provide a means of expeditious review of more complex calculations.

Response Spectrum Analysis is recommended for design of isolated structures that have either (1) a tall or otherwise flexible superstructure, or (2) an irregular superstructure. For most buildings, Response Spectrum Analysis will not predict significantly different displacements of the isolation system than those calculated by prescriptive formulas, provided both calculations are based on the same effective stiffness and damping properties of the isolation system. The real benefit of Response Spectrum Analysis is not in the prediction of isolation system response, but rather in the calculation and distribution of forces in the superstructure. Response Spectrum Analysis permits the use of more detailed models of the superstructure that better estimate forces and deformations of components and elements considering flexibility and irregularity of the structural system.

Nonlinear procedures include the Nonlinear Static Procedure (NSP) and the Nonlinear Dynamic Procedure (NDP). The NSP is a static pushover procedure, and the NDP is based on nonlinear Time-History Analysis. The NSP or the NDP is required for isolated structures that do not have essentially linearly elastic superstructures (during BSE-2 demand). In this case, the superstructure would be modeled with nonlinear elements and components.

Time-History Analysis is required for isolated structures on very soft soil (i.e., Soil Profile Type E when shaking is strong, or Soil Profile Type F) that could shake the building with a large number of cycles of long-period motion, and for buildings with isolation systems that are best characterized by nonlinear models. Such isolation systems include:

1. Systems with more than about 30% effective damping (because high levels of damping can significantly affect higher-mode response of the superstructure)

2. Systems that lack significant restoring force (because these systems may not stay centered during earthquake shaking)

3. Systems that are expected to exceed the sway-space clearance with adjacent structures (because impact with adjacent structures could impose large demands on the superstructure)

4. Systems that are rate- or load-dependent (because their properties will vary during earthquake shaking)

For the types of isolation systems described above, appropriate nonlinear properties must be used to model isolators. Linear properties could be used to model the superstructure, provided the superstructure's response is essentially linearly elastic for BSE-2 demand.

The restrictions placed on the use of linear procedures effectively suggest that nonlinear procedures be used for virtually all isolated buildings. However, lower-bound limits on isolation system design displacement and force are specified by the *Guidelines* as a percentage of the demand prescribed by the linear formulas, even when dynamic analysis is used as the basis for design. These lower-bound limits on key design attributes ensure consistency in the design of isolated structures and serve as a "safety net" against gross underdesign.

C9.2.4 Linear Procedures

C9.2.4.1 General

No commentary is provided for this section.

C9.2.4.2 Deformation Characteristics of the Isolation System

The deformation characteristics of the isolation system should be based on tests of isolator prototypes, as defined in Section 9.2.9. This section not only specifies the type and sequence of prototype testing, but also provides the formulas to be used to develop values of the effective stiffness and effective damping of the isolation system. These formulas acknowledge that effective stiffness and effective damping are, in general, amplitude-dependent and should be evaluated for both design earthquake and BSE-2 levels of response.

The effective stiffness and effective damping of the isolation system are quantities that can (and typically do) vary due to changes in the nature of applied load (e.g., systems that are rate-, amplitude- or duration-dependent). There is also potential for variation between as-designed and as-built values of effective stiffness and damping. Like all products, isolators can only be required to meet design criteria to within certain specified manufacturing tolerances. The intent of the *Guidelines* is to use bounding values of isolation system properties such that the design is conservative for all potential sources of isolation system variability. The *Guidelines* explicitly require design properties to bound measured variations of isolator prototypes, due to the nature of applied load. The *Guidelines* do not explicitly address potential differences between as-designed and as-built properties, placing the responsibility for quality control with the engineer responsible for the structural design (Section 9.2.7.2I).

C9.2.4.3 Minimum Lateral Displacements

A. Design Displacement

Equation 9-2 prescribes design earthquake displacement of the isolation system at the center of mass of the building (pure translation, without contribution from torsion). The equation is based on the effective period (minimum value of effective stiffness) and damping coefficient (minimum value of effective damping) of the isolation system evaluated at the design displacement. The damping coefficient is based on median spectral amplification factors of Table 2 of *Earthquake Spectra and Design* (Newmark and Hall, 1982), as defined in Chapter 2 of the *Guidelines*.

Spectral demand is based on the long-period spectral acceleration coefficient specified in Chapter 2 for the design earthquake (i.e., S_{D1}). Equation 9-2 should be modified for use with site-specific spectral demand by replacing S_{D1}/T_D in this equation with the value of the site-specific design spectrum at the effective period of T_D.

Equation 9-2 effectively calculates push-over displacement of the isolated building, assuming no rotation of the building and a rigid superstructure. The assumption of a rigid superstructure is conservative for estimating isolation system displacement, because any flexibility and displacement of the superstructure would tend to decrease displacement in the isolation system.

B. Effective Period at the Design Displacement

Equation 9-3 prescribes the effective period at the design displacement. The effective period is an estimate of isolated building period based on the secant stiffness of the isolation system at the design displacement. This estimate is conservatively based on the minimum value of effective stiffness, which yields the maximum value of effective period (and hence the largest estimate of building displacement).

C. Maximum Displacement

Equation 9-4 prescribes the BSE-2 displacement of the isolation system. Equation 9-4 is the same as Equation 9-2, except all terms are based on BSE-2 demand and response, rather than design earthquake demand and response.

D. Effective Period at the Maximum Displacement

Equation 9-5 prescribes the effective period of the isolated building at maximum displacement. Equation 9-5 is the same as Equation 9-3, except that effective stiffness is based on BSE-2 displacement, rather than design earthquake displacement.

E. Total Displacement

Isolated systems are required to consider additional displacement due to accidental and actual torsion, similar to the additional loads prescribed for conventional (fixed-base) structures. Equations 9-6 and 9-7 provide a simple estimate of combined translational and torsional displacement based on the gross plan dimensions of the buildings (b and d), the distance from the center of the building to the location of interest, and actual plus accidental eccentricity of the building. Eccentricity is the distance between the center of mass of the superstructure (projected on the plane of the isolation system) and the center of rigidity of the isolation system.

Equations 9-6 and 9-7 are based on the assumption that the stiffness of the isolation system is distributed in a plan proportional to the distribution of supported weight of the superstructure above. This is a reasonable assumption, since most isolator units are designed on the basis of supported weight and tend to be larger (and stiffer) when supporting heavier loads.

Equations 9-6 and 9-7 are evaluated for two bounding cases: (1) a structure that is square in plan, and (2) a structure that is very long in plan in one direction. For these two cases, the additional displacement due to 5% eccentricity is found to be:

1. For structures that are square in plan (i.e., $b = d$):

   D_{TD}/D_D or $D_{TM}/D_M = 1.15$

2. For structures that are long in plan (i.e., $b \gg d$):

   D_{TD}/D_D or $D_{TM}/D_M = 1.30$

The *Guidelines* permit reducing these values if the isolation system is configured to resist torsion (i.e., stiffer isolator units are positioned near the edges and corners of the building), but a minimum value of 10% additional displacement due to torsion is required to provide margin on torsional response.

C9.2.4.4 Minimum Lateral Forces

A. Isolation System and Structural Components and Elements at or below the Isolation System

Equation 9-8 prescribes the lateral force to be used for design of the isolation system, the foundation, and other structural components and elements below the isolation system. Lateral force is conservatively based on the maximum value of effective stiffness of the isolation system evaluated at the design displacement.

B. Structural Components and Elements above the Isolation System

The lateral force to be used for design of the superstructure, V_s, is specified to be the same as that prescribed by Equation 9-8 for design of the isolation system (and structure below). This value of lateral force is based on a conservative estimate of peak force of the design earthquake and corresponds, in concept, to the pseudo lateral load, *V*, prescribed by Equation 3-6 for linear static analysis of a conventional (fixed-base) building.

C. Limits on V_s

Two lower-bound limits are placed on the design lateral force for the superstructure. The first requirement is intended to keep components and elements of the superstructure elastic for design wind conditions. Design wind loads are not provided with these *Guidelines*, but should be considered as part of the design of an isolated building. Wind will likely not be a factor, unless the design earthquake loads are small.

The second requirement is intended to prevent premature yielding of the superstructure before the isolation system is fully activated. This requirement requires a 1.5 margin between the lateral force to be used for design of the superstructure and the yield level of the isolation system. In the extreme case of a system that has no stiffness after yielding (e.g., flat sliding isolator), the superstructure would be designed for a lateral force that is 50% above the yield level (e.g., 50% above the friction level of the sliding isolator).

D. Vertical Distribution of Force

Equation 9-9 distributes the lateral design force, V_s, over the height of the building on the basis of an inverted triangular force distribution. This distribution has been found to bound response of most isolated buildings conservatively, even when higher modes are excited by hysteretic behavior or large values of effective damping of the isolation system. A less conservative force distribution (e.g., uniform force distribution) would be appropriate for isolation systems that have relatively small values of effective damping, but Time-History Analysis would be required to verify the appropriate distribution of lateral force over the height of the building.

C9.2.4.5 Response Spectrum Analysis

Response Spectrum Analysis should be performed using the procedures described in Section 3.3.2, using effective stiffness and damping properties for the isolation system. The effective stiffness of the isolation system should be the same as that required for use in the linear procedure formulas of Section 9.2.4.3. The effective damping of the fundamental (isolated) mode in each horizontal direction should be the same as that required for use in the linear procedure formulas of Section 9.2.4.3. Damping values for higher modes of response should be consistent with the values specified in Chapter 2 for conventional (fixed-base) buildings.

The Response Spectrum Analysis should produce about the same isolation system displacement and lateral force as those calculated using the linear formulas of Section 9.2.4.3, since the two methods are based on the same effective stiffness and damping properties for the isolation system. Section 9.2.4.5D requires upward scaling of Response Spectrum results, if displacements predicted by Response Spectrum Analysis are less than those of the linear procedure formulas.

C9.2.4.6 Design Forces and Deformations

Components and elements are to be designed using the acceptance criteria of Section 3.4.2.2, except that deformation-controlled components and elements should be designed using a component demand modifier no greater than $m = 1.5$. Response of structural components and elements is limited to $m = 1.5$ to ensure that the structure remains essentially elastic for the design earthquake. Response of structural components and elements beyond $m = 1.5$ is not recommended without explicit modeling and analysis of building nonlinearity.

C9.2.5 Nonlinear Procedures

C9.2.5.1 Nonlinear Static Procedure

The NSP should follow the push-over methods described in Section 3.3.3, except that the target displacement for the design earthquake is specified by Equation 9-10 and the target displacement for the BSE-2 is specified by Equation 9-11. Target displacements are specified for a control node that is located at the center of mass of the first floor above the isolation system.

Equations 9-10 and 9-11 are based on Equations 9-2 and 9-4, respectively, modified to account for the influence of a flexible superstructure. For isolated buildings with short, stiff superstructures, the isolated period at the design displacement will be several times greater than the effective period of the superstructure (on a fixed base), and the displacement of the isolation system—considering superstructure flexibility—will be about the same as the displacement of the isolation system based on rigid superstructure.

The pattern of applied load should be proportional to the distribution of the product of building mass and the deflected shape of the isolated mode. For isolated buildings with a stiff superstructure (i.e., stiff relative to the isolation system), the deflected shape of the isolated mode is dominated by displacement of the isolation system (e.g., nearly uniform deflected shape). For isolated buildings with a flexible superstructure, the deflected shape is a combination of isolation system and superstructure displacements (e.g., trapezoidal deflected shape).

Isolation systems are typically nonlinear and relatively stiff at low force levels. The deflected shape of such systems is amplitude-dependent and at low levels of ground shaking would be dominated by superstructure displacement. At very low levels of ground shaking, before activation of the isolation system, the deflected shape would appear similar to that of the building on a fixed base (e.g., inverted triangle deflected shape).

C9.2.5.2 Nonlinear Dynamic Procedure

The NDP should follow the time history methods described in Section 3.3.4, except that Section 9.2.5.2B requires upward scaling of time history results, if displacements predicted by Time-History Analysis are less than those of the NSP.

C9.2.5.3 Design Forces and Deformations

No commentary is provided for this section.

C9.2.6 Nonstructural Components

To accommodate the differential movement between the isolated building and the ground, provision for flexible connections should be made. In addition, rigid structures crossing the interface (i.e., stairs, elevator shafts, and walls) should have details that accommodate differential motion at the isolator level without sustaining damage inconsistent with the building's Rehabilitation Objectives.

C9.2.7 Detailed System Requirements

C9.2.7.1 General

No commentary is provided for this section.

C9.2.7.2 Isolation System

No commentary is provided for subsections A through H.

I. Manufacturing Quality Control

A test and inspection program is necessary for both fabrication and installation of the isolation system. Because base isolation is a developing technology, it

may be difficult to reference standards for testing and inspection. Reference can be made to standards for some material such as elastomeric bearings (ASTM D4014). Similar standards are required for other isolation systems. Special inspection procedures and load testing to verify manufacturing quality control should be developed for each project. The requirements will vary with the type of isolation system used.

C9.2.8 Design and Construction Review

Design review of both the design and analysis of the isolation system and design review of the isolator testing program are mandated by the *Guidelines* for two key reasons:

1. The consequences of isolator failure could be catastrophic.

2. Isolator design and fabrication is evolving rapidly, and may be based on technologies unfamiliar to many design professionals.

The *Guidelines* require review to be performed by a team of registered design professionals who are independent of the design team and other project contractors. The review team should include individuals with special expertise in one or more aspects of the design, analysis, and implementation of seismic isolation systems.

The review team should be formed prior to the finalization of design criteria (including site-specific ground shaking criteria) and isolation system design options. Further, the review team should have full access to all pertinent information and the cooperation of the design team and authorities having jurisdiction involved with the project.

C9.2.9 Isolation System Testing and Design Properties

C9.2.9.1 General

The isolation system testing procedures of the *Guidelines* represent minimum testing requirements. Other, more extensive testing procedures may be available in the future that would also be suitable for isolation system testing. For example, a standard for testing seismic isolation systems, units, and components is currently being developed by a committee of the American Society of Civil Engineers.

C9.2.9.2 Prototype Tests

All isolator tests should be witnessed and reported by a qualified, independent inspector.

For each cycle of test the force-deflection behavior of the prototype test specimen must be recorded so that data can be used to determine whether the isolation system complies with both the *Guidelines* and specifications prepared by the engineer responsible for design of the structural system. Both the engineer responsible for design and members of the design review team should review all raw data from prototype tests.

Prototype tests are not required if the isolator unit is of similar dimensional characteristics, of the same type and material, and fabricated using the same process as a prototype isolator unit that has been previously tested using the specified sequence of tests. The independent design review team should determine whether the results of previously tested units are suitable, sufficient, and acceptable.

C9.2.9.3 Determination of Force-Deflection Characteristics

No commentary is provided for this section.

C9.2.9.4 System Adequacy

No commentary is provided for this section.

C9.2.9.5 Design Properties of the Isolation System

No commentary is provided for this section.

C9.3 Passive Energy Dissipation Systems

C9.3.1 General Requirements

The *Guidelines* provide systematic procedures for the implementation of energy dissipation devices in seismic rehabilitation. Although these procedures are seminal and mutable, they constitute the first comprehensive suite of such procedures ever published. The procedures set forth in the *Guidelines* will likely change as more information becomes available. The reader is urged to stay abreast of new developments in the field of energy dissipation systems (EDS).

The *Guidelines* provide procedures to calculate member actions and deformations in building frames incorporating energy dissipation devices, and requirements for testing energy dissipation hardware. Component checking for actions and deformations so calculated shall conform with the procedures set forth in Chapter 3 and the strength and deformation limits presented in the materials chapters.

Issues Besides Seismic and Wind Effects

The properties of some energy dissipation devices may change substantially due to wind effects, aging, operating temperature, and high-cycle fatigue. Although these important issues are not addressed in the *Guidelines*, with the exception of typical wind effects, adequate treatment of these issues in the design phase of a project is of paramount importance to ensure reliable performance of the energy dissipation devices. The engineer of record must consider these issues in designing with energy dissipation devices.

New definitions are presented in the *Guidelines* for components associated with energy dissipation devices, namely, support framing for energy dissipation devices, and points of attachment. These components are illustrated in Figure C9-12.

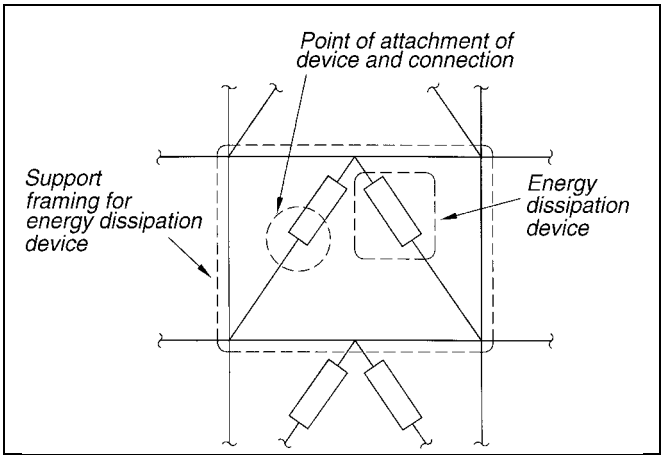

Figure C9-12 Energy Dissipation Nomenclature

The primary reason for introducing energy dissipation devices into a building frame is to reduce the displacements and damage in the frame. Displacement reduction is achieved by adding either stiffness and/or energy dissipation (generally termed *damping*) to the building frame. Metallic-yielding, friction, and viscoelastic energy dissipation devices typically introduce both stiffness and damping; viscous dampers will generally only increase the damping in a building frame. Figure C9-13 simplistically illustrates the impact

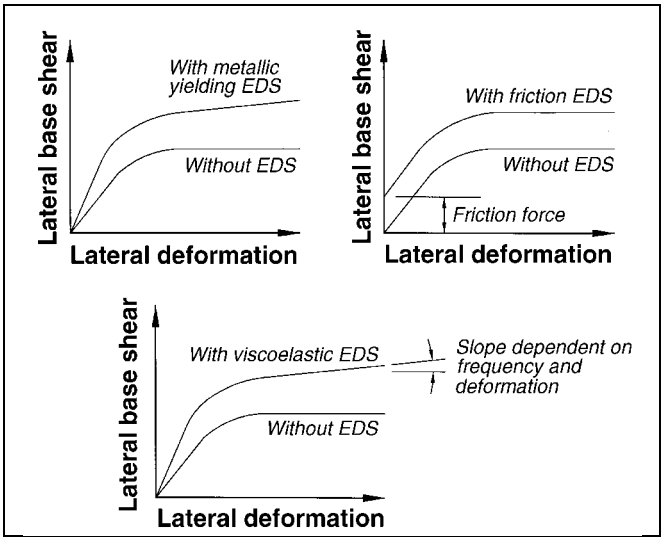

Figure C9-13 Effect of Energy Dissipation on the Force-Displacement Response of a Building

of different types of dampers on the force-displacement response of a building. The addition of viscous dampers will not change the force-displacement relation; that is, the "with viscous EDS" curve will be essentially identical to the "without EDS" curve in Figure C9-13.

As noted above, the force-displacement relation for selected types of energy dissipation devices may be dependent on environmental conditions (e.g., wind, aging, and operating temperature), and excitation frequency, sustained deformations, and bilateral deformations. Such dependence should be investigated by analysis of the mathematical model with limiting values assigned to the properties of the energy dissipation devices.

The Analysis Procedures set forth in the *Guidelines* are approximate only. Roof displacements calculated using the linear and nonlinear procedures are likely to be more accurate than the corresponding estimates of inter-

story drift and relative velocity between adjacent stories. Accordingly, the *Guidelines* require that energy dissipation devices be capable of sustaining larger displacements (and velocities for velocity-dependent devices) than the maxima calculated by analysis in the BSE-2. Recognizing that the response of a building frame incorporating four or more devices in each principal direction in each story will be more reliable than a frame with fewer devices in each principal direction, the increase in displacement (and velocity) capacity is dependent on the level of redundancy in the supplemental damping system. The increased force shall be used to design the framing that supports the energy dissipation devices—reflecting the objective of keeping the device support framing elastic in the BSE-2. The increases in force and displacement capacity listed in the *Guidelines* (= 130% for four or more devices and 200% for fewer than four devices) are based on the judgment of the authors at the time of this writing.

The *Guidelines* require that the stiffness characteristics of the energy dissipation devices and the device support framing be included in the mathematical model of the building. If the stiffness of the support framing is ignored, the lateral stiffness of the building may be substantially underestimated (and the target displacements significantly overestimated). Conversely, if flexible support framing is assumed to be rigid, the effectiveness of the dampers may be overestimated, leading to nonconservative results. The reader is referred to Constantinou et al. (1996) for additional information.

C9.3.2 Implementation of Energy Dissipation Devices

Restrictions on the use of linear procedures are established in Chapter 2. These restrictions also apply to the implementation of energy dissipation devices using linear procedures.

At the time of this writing, the use of linear procedures for implementing energy dissipation devices is limited to buildings in which all components and elements, exclusive of the energy dissipation devices, remain in the linearly elastic range for the BSE-2. Calculation of component actions should reflect the benefits of the added damping. There are no limits on the use of nonlinear procedures except for the restrictions set forth in Chapter 2.

It must be emphasized that linear procedures are only appropriate for linearly elastic buildings incorporating viscoelastic or viscous energy dissipation devices. However, if the level of equivalent viscous damping is small (less than 30% of critical), hysteretic energy dissipation devices can be treated as viscous devices. Procedures for implementing both hysteretic (displacement-dependent) devices and viscous and viscoelastic (velocity-dependent) devices are presented in Section 9.3.4.1.

Given the similarity between metallic-yielding devices and shear links in eccentrically braced steel frames, consideration was given to developing linear procedures for implementing metallic-yielding devices in framing systems permitted to undergo inelastic response. However, the authors were unable to develop robust rules linking the minimum yielding strength of the energy dissipation devices to the yielding strength of the existing framing—a key step in limiting the degree of inelastic action in the existing framing. Accordingly, no such linear procedures were included in the *Guidelines.*

C9.3.3 Modeling of Energy Dissipation Devices

The *Guidelines* identify three types of energy dissipation devices: displacement-dependent, velocity-dependent, and “other.” Metallic-yielding and friction dampers are classed as displacement-dependent devices. Figure C9-14 shows sample force-displacement relations for displacement-dependent devices. Shape-memory alloy dampers can be configured to produce hysteretic response similar to that shown in Figure C9-14.

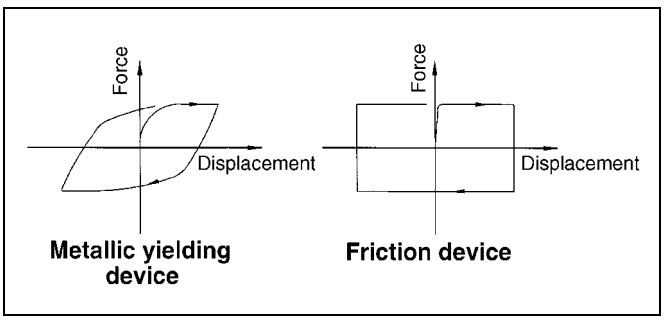

Figure C9-14 ***Idealized Force-Displacement Loops of Displacement-Dependent Energy Dissipation Devices***

Examples of velocity-dependent energy dissipation devices include viscoelastic solid dampers, dampers operating by deformation of viscoelastic fluids (e.g., viscous shear walls), and dampers operating by forcing a fluid through an orifice (e.g., viscous fluid dampers). Figure C9-15 illustrates the typical behavior of these devices.

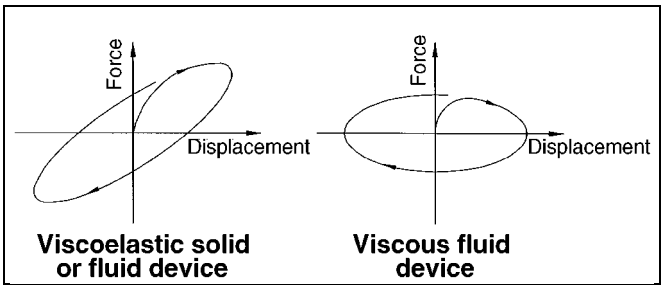

Figure C9-15 ***Idealized Force-Displacement Loops of Velocity-Dependent Energy Dissipation Devices***

Other devices have characteristics that cannot be classified by either of the basic types depicted in Figures C9-14 and C9-15. Examples are devices made of shape-memory alloys, friction-spring assemblies with recentering capability, and fluid restoring force-damping devices. Figure C9-16 presents force-displacement relations for these devices, which dissipate energy while providing recentering capability, and resist motion with a nearly constant force. Shape-memory alloy devices may be designed to exhibit behavior of the type shown in Figure C9-16. The reader is referred to ATC (1993), EERI (1993), and Soong and Constantinou (1994) for more information.

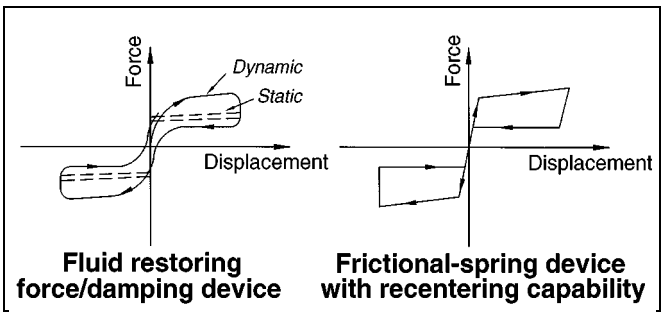

Figure C9-16 ***Idealized Force-Displacement Loops of Energy Dissipation Devices with Recentering Capability***

C9.3.3.1 Displacement-Dependent Devices

Displacement-dependent devices exhibit bilinear or trilinear hysteretic, elasto-plastic or rigid-plastic (frictional) behavior. Details on the behavior and modeling of such devices may be found in Whittaker et al. (1989), Aiken and Kelly (1990), ATC (1993), Soong and Constantinou (1994), Grigorian and Popov (1994), Yang and Popov (1995), and Li and Reinhorn (1995).

C9.3.3.2 Velocity-Dependent Devices

A. Solid Viscoelastic Devices

Solid viscoelastic devices typically consist of constrained layers of viscoelastic polymers. Such devices exhibit viscoelastic solid behavior with mechanical properties dependent on frequency, temperature, and amplitude of motion. A sample force-displacement relation for a viscoelastic solid device under sinusoidal motion of circular frequency, ω, is shown in Figure C9-17. The force may be expressed as:

$$F = k_{eff}D + C\dot{D} \qquad \text{(C9-25)}$$

where all terms are as defined in Section 9.3.3.2 of the *Guidelines*. The effective stiffness of the energy dissipation device is calculated as:

$$k_{eff} = \frac{|F^+| + |F^-|}{|D^+| + |D^-|} \qquad \text{(C9-26)}$$

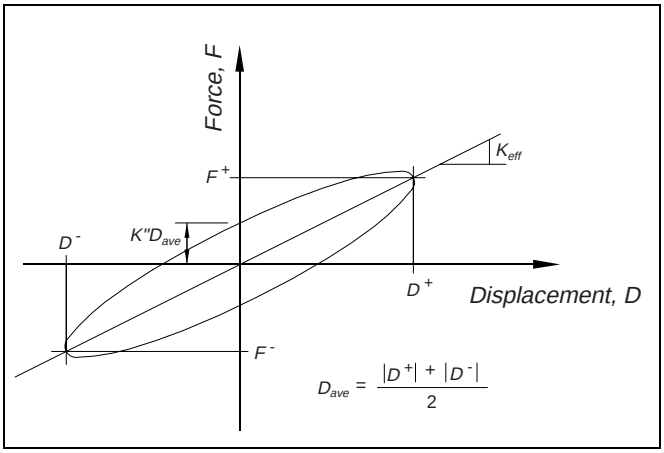

Figure C9-17 ***Idealized Force-Displacement Relation for a Viscoelastic Solid Device***

and the damping coefficient C of the device is calculated as:

$$C = \frac{W_D}{\pi \omega D_{ave}^2} \qquad \text{(C9-27)}$$

where D_{ave} is the average of the absolute values of D^+ and D^-; and W_D is the area enclosed by one complete displacement cycle (D^+ to D^-) of the device.

The effective stiffness is also termed the storage shear stiffness, K' in the literature. The damping coefficient can be described in terms of the loss stiffness, K'':

$$C = \frac{K''}{\omega} \qquad \text{(C9-28)}$$

The effective stiffness and damping coefficient are generally dependent on the frequency, temperature, and amplitude of motion. Figure C9-18 shows normalized values of these parameters from the tests of Chang et al. (1991) of one viscoelastic polymer. Shear strains γ are identified. Note that the frequency and temperature dependence of viscoelastic polymers tend to vary as a function of the composition of the polymer (Bergman and Hanson, 1993). The results presented in Figure C9-18 are not indicative of all viscoelastic solids. The normalized parameters in this figure are the storage shear modulus (G') and loss shear modulus (G'').

Viscoelastic solid behavior can be modeled over a wide range of frequencies using advanced models of viscoelasticity (Kasai et al., 1993). Simpler models are capable of capturing behavior over a limited frequency range—these models will suffice for most rehabilitation projects. For example, the standard linear solid model shown in Figure C9-19 was used to model the behavior of the device of Figure C9-18 at temperature of 21°C. The results presented in Figure C9-20 were obtained using values of $G_1 = 5.18$ MPa, $G_2 = 0.48$ MPa, and $\eta_2 = 0.31$ MPa-sec/rad where

$$G_1 = \frac{K_1 t}{A_b} \qquad G_2 = \frac{K_2 t}{A_b} \qquad \eta_2 = \frac{C_2 t}{A_b} \qquad \text{(C9-29)}$$

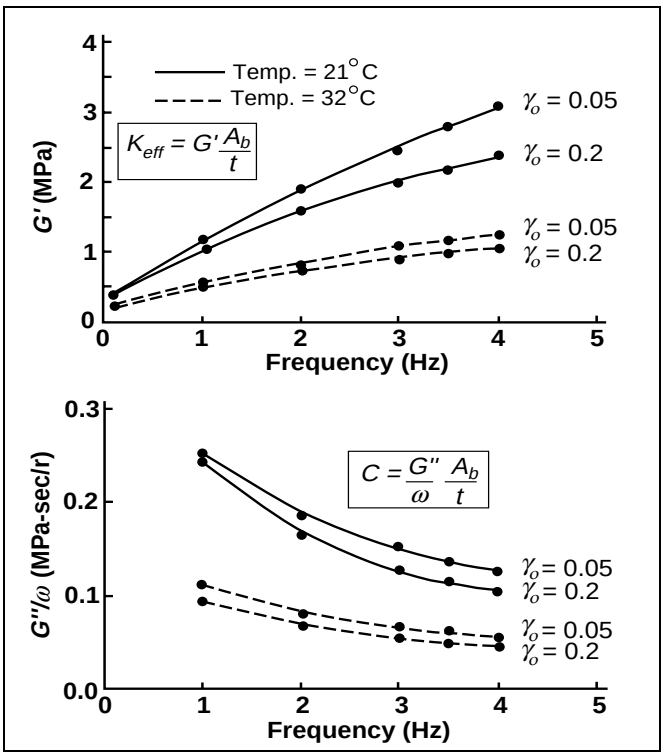

Figure C9-18 ***Normalized Effective Stiffness (G') and Damping Coefficient (G''/ω) of Viscoelastic Solid Device***

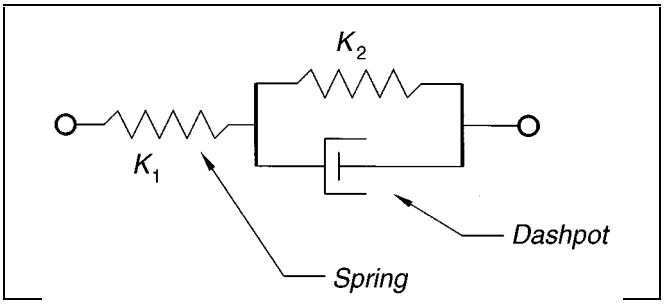

Figure C9-19 ***Model for Viscoelastic Energy Dissipation Device Behavior***

In the above formulae, K_1, K_2, and C_2 are the spring and dashpot constants for the standard linear solid model, A_b is the bonded area of the device, and t is the thickness of viscoelastic material in the device.

B. Fluid Viscoelastic Devices

Fluid viscoelastic devices, which operate by shearing viscoelastic fluids (ATC, 1993), have behaviors that resemble those of solid viscoelastic devices

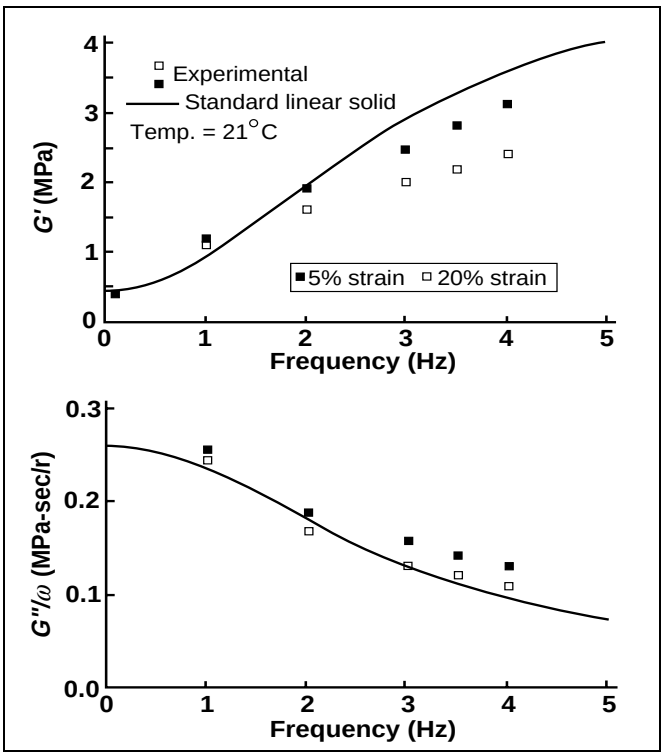

Figure C9-20 ***Properties of Viscoelastic Solid Device Predicted by Standard Linear Solid Model***

(Figure C9-14), except that fluid viscoelastic devices have zero effective stiffness under static loading. Fluid and solid viscoelastic devices are distinguished by the ratio of loss stiffness to effective stiffness as the loading frequency approaches zero: the ratio approaches infinity for fluid viscoelastic devices, and zero for solid viscoelastic devices.

Fluid viscoelastic behavior can be modeled with advanced models of viscoelasticity (Makris et al., 1993). However, fluid viscoelastic devices can be modeled using the Maxwell model of Figure C9-21 in most instances.

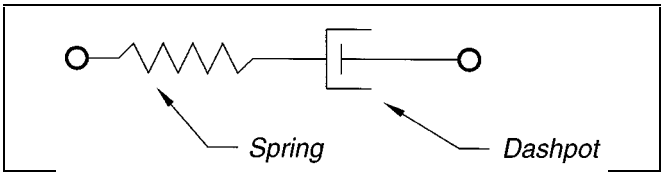

Figure C9-21 ***Maxwell Model for Fluid Viscoelastic Energy Dissipation Devices***

C. Fluid Viscous Devices

Pure viscous behavior can be produced by forcing fluid through an orifice (Constantinou and Symans, 1993; Soong and Constantinou, 1994). Fluid viscous devices may exhibit some stiffness at high frequencies of cyclic loading. Linear fluid viscous dampers exhibiting stiffness in the frequency range $0.5f_1$ to $2.0f_1$ should be modeled as fluid viscoelastic devices, where f_1 is the fundamental frequency of the rehabilitated building.

The frequency range of 0.5 f_1 to 2.0 f_1 is used throughout Section 9.3. The lower limit of 0.5 f_1 corresponds to a fourfold reduction in lateral stiffness; such a reduction is likely an upper bound due to the limited deformation capacity assigned to existing construction. The upper limit of 2.0 f_1 recognizes that building components and elements that are not included in the mathematical model may contribute substantial stiffness, producing a larger value of f_1.

In the absence of stiffness in the frequency range $0.5f_1$ to $2.0f_1$, the force F in a fluid viscous device may be calculated as:

$$F = C_0 |\dot{D}|^{\alpha} \mathrm{sgn}(\dot{D}) \qquad \text{(C9-30)}$$

where the terms are as defined in Section 9.3.3.2 of the *Guidelines*. The simplest form of the fluid viscous damper is the linear fluid damper, for which the exponent α is equal to 1.0. Typical values for α range between 0.5 and 2.0.

C9.3.3.3 Other Types of Devices

Other energy dissipating devices, such as those having hysteresis of the type shown in Figure C9-16, require modeling techniques different from those described above. Tsopelas and Constantinou (1994), Nims et al. (1993), and Pekcan et al. (1995) describe analytical models for some of these devices.

C9.3.4 Linear Procedures

General linear procedures for analysis of rehabilitated buildings incorporating energy dissipation devices have not been developed to the level necessary for inclusion in the *Guidelines*, except for rehabilitated framing systems that are specifically designed to remain linearly elastic for the design earthquake.

The stiffness of the energy dissipation devices and their support framing should be included in the mathematical model to adequately capture the dynamic characteristics of the rehabilitated building. Ignoring the influence of added stiffness of the energy dissipation assembly to the rehabilitated building could lead to: spectral displacement demands being overestimated, spectral force demands being underestimated, and modal damping coefficients being calculated incorrectly. Secant stiffness should be used to linearize the energy dissipation devices; this assumption is conservative, because displacements will be overestimated and the benefits of the damping added by the devices will be underestimated.

The mathematical model of the rehabilitated building should account for both the plan and vertical spatial distribution of the energy dissipation devices to enable explicit evaluation of load paths and design actions in components surrounding the energy dissipation assembly.

Velocity-dependent energy dissipation devices may be dependent on loading frequency, temperature, deformation (or strain), velocity, sustained loads, and bilateral loads. Such dependence should be accounted for in the analysis phase by multiple analyses of the rehabilitated building using bounding values of the dependent properties.

C9.3.4.1 Linear Static Procedure

A. Displacement-Dependent Devices

Two additional restrictions on the use of Linear Static Procedures for implementing displacement-dependent energy dissipation devices are set forth in Section 9.3.4.1. The first restriction:

> "The ratio of the maximum resistance in each story, in the direction under consideration, to the story shear demand calculated using Equations 3-7 and 3-8, shall range between 80% and 120% of the average value of said ratio. The maximum story resistance shall include the contributions from all components, elements, and energy dissipation devices."

is intended to ensure somewhat uniform yielding of the stories in the building frame and to avoid the concentration of damage in any one story. Plastic analysis by story of the building frame (including the energy dissipation devices) is the preferred method of calculating the maximum resistance of each story.

The second restriction:

> "The maximum resistance of all energy dissipation devices in a story, in the direction under consideration, shall not exceed 50% of the resistance of the remainder of the framing where said resistance is calculated at the displacements anticipated in the BSE-2. Aging and environmental effects shall be considered in calculating the maximum resistance of the energy dissipation devices."

is intended to limit the influence of the energy dissipation devices on the response of the rehabilitated building. In short, the second restriction limits the resistance of the energy dissipation devices in any story to one-third of the total resistance of the building frame (including the energy dissipation devices) in that story.

Subject to the limit of 30% total equivalent viscous damping in the rehabilitated building, the added damping afforded by the displacement-dependent devices is used to reduce the pseudo lateral load of Equation 3-6 using the damping modification factor of Table 2-15. The calculation of the damping effect should be estimated as follows:

1. Estimate the modified pseudo lateral load by reducing the pseudo lateral load V of Equation 3-6 by the damping modification factor, B, either B_S or B_1, of Table 2-15 corresponding to the assumed effective damping in the rehabilitated building.

2. Calculate the horizontal forces, F_x, from Equations 3-7 and 3-8 using the modified V in lieu of the V.

3. Calculate the horizontal displacements δ_i at each floor level i by linear analysis of the mathematical model using the horizontal forces F_x.

4. Using the displacements δ_i, estimate the effective damping, β_{eff}, as follows:

$$\beta_{eff} = \beta + \frac{\sum_j W_j}{4\pi W_k} \qquad \text{(C9-31)}$$

where β is the damping in the structural frame and is set equal to 0.05 unless modified in Section 2.6.1.5, W_j is work done by device j in one complete cycle corresponding to floor displacements δ_i, the summation extends over all devices j, and W_k is the maximum strain energy in the frame, determined using Equation 9-27:

$$W_k = \frac{1}{2}\sum_i F_i \delta_i \qquad \text{(C9-32)}$$

where all terms are defined above and the summation extends over all floor levels i.

5. Iterate on steps 1 through 4 until the estimate of the effective damping used to calculate the modified equivalent base (used in step 1) is equal to the effective damping calculated in the subsequent step 4.

B. Velocity-Dependent Devices

One additional restriction on the use of Linear Static Procedures for implementing velocity-dependent energy dissipation devices is set forth in Section 9.3.4.1. The restriction:

> "The maximum resistance of all energy dissipation devices in a story, in the direction under consideration, shall not exceed 50% of the resistance of the remainder of the framing where said resistance is calculated at the displacements anticipated in the BSE-2. Aging and environmental effects shall be considered in calculating the maximum resistance of the energy dissipation devices."

is intended to limit the influence of the energy dissipation devices on the response of the rehabilitated building. In short, the restriction limits the resistance of the energy dissipation devices in any story to one-third of the total resistance of the building frame (including the energy dissipation devices) in that story.

Subject to the limit of 30% total equivalent viscous damping in the rehabilitated building, the added damping afforded by the velocity-dependent devices is used to reduce the pseudo lateral load of Equation 3-6 using the damping modification factor of Table 2-15. The calculation of the damping effect should be estimated as follows:

1. Estimate the modified pseudo lateral load V by reducing V of Equation 3-6 by the damping modification factor, B, either B_s or B_1, of Table 2-15 corresponding to the assumed effective damping in the rehabilitated building.

2. Calculate the horizontal forces, F_x, from Equations 3-7 and 3-8 using the modified V in lieu of V.

3. Calculate the horizontal displacements δ_i at each floor level i by linear analysis of the mathematical model using the horizontal forces F_x.

4. Using the displacements δ_i, estimate the effective damping, β_{eff}, as follows:

$$\beta_{eff} = \beta + \frac{\sum_j W_j}{4\pi W_k} \qquad \text{(C9-33)}$$

where β is the damping in the structural frame and is set equal to 0.05 unless modified in Section 2.6.1.5, W_j is work done by device j in one complete cycle corresponding to floor displacements δ_i, the summation extends over all devices j, and W_k is the maximum strain energy in the frame, determined using Equation C9-34:

$$W_k = \frac{1}{2}\sum_i F_i \delta_i \qquad \text{(C9-34)}$$

where all terms are as defined above. The work done by device j in one complete cycle of loading may be calculated as:

$$W_j = \frac{2\pi^2}{T} C_j \delta_{rj}^2 \qquad \text{(C9-35)}$$

where T is the fundamental period of the rehabilitated building including the stiffness of the velocity-dependent devices, C_j is the damping constant for device j, and δ_{rj} is the relative displacement between the ends of device j along the axis of device j.

5. Iterate on steps 1 through 4 until the estimate of the effective damping used to calculate the modified

equivalent base (used in step 1) is equal to the effective damping calculated in the subsequent step 4.

The calculation of actions in components of a rehabilitated building with velocity-dependent energy dissipation devices is complicated because the viscous components of force are not directly accounted for. Section 9.3.4.1 describes three possible stages of deformation that may result in the maximum member actions: (1) the stage of maximum drift at which the viscous forces are zero, (2) the stage of maximum velocity at which drifts are zero, and (3) the stage of maximum acceleration.

Viscous forces are maximized at the time of maximum velocity. The horizontal components of these viscous forces are balanced by inertia forces such that the resultant lateral displacements are zero. The viscous forces will introduce axial forces into columns supporting the viscous dampers. The magnitude of these axial forces will be dependent on (a) the amount of damping added by the viscous devices, and (b) the number of dampers used to achieve the target level of additional damping.

The time of maximum acceleration is determined assuming that the building undergoes harmonic motion at frequency f_1 and amplitude corresponding to the maximum drift. Under this condition, the maximum acceleration is equal to the acceleration at maximum drift times ($CF_1 + 2\ \beta_{eff} CF_2$). Constantinou et al. (1996) demonstrate that this assumption produces results of acceptable accuracy. Note that the use of $CF_1 = CF_2 = 1$ will result in conservative estimates of component action.

C9.3.4.2 Linear Dynamic Procedure

The primary effect of the added damping and stiffness provided by the energy dissipation devices is a reduction in displacements due to (1) a reduction in the fundamental period, and (2) smaller spectral demands due to additional damping.

The lower-bound limit on the actions and displacements calculated using the linear Response Spectrum Method (= 80% of those actions and deformations estimated using the Linear Static Procedure) is included to guard against inappropriate or incorrect use of dynamic analysis.

A. Displacement-Dependent Devices

Equation 9-26 may be modified to calculate modal damping ratios using modal estimates of the work done by the devices and estimates of the modal strain energy. Recognizing that the displacement of a rehabilitated building will be dominated by first mode response, one strategy worthy of consideration is that which modifies the first mode damping ratio to reflect the additional energy dissipation provided by the dampers, and ignores the benefits of the energy dissipators in reducing response in the higher modes.

B. Velocity-Dependent Devices

Equations 9-33 through 9-35 may be used to calculate modal damping ratios that will account for the additional damping afforded by the energy dissipation devices. The spectral demands should be estimated using the revised estimates of modal damping. Given that the displacement of a rehabilitated building will be dominated by first mode response, one strategy worthy of consideration is that which modifies the first mode damping ratio to reflect the additional energy dissipation provided by the dampers, and ignores the benefits of the energy dissipators in reducing response in the higher modes.

C9.3.5 Nonlinear Procedures

C9.3.5.1 Nonlinear Static Procedure

Section 3.3.3 of the *Guidelines* presents one procedure for nonlinear static analysis. The commentary to this section denotes this procedure as Method 1. An alternative procedure, termed Method 2, is described in Section C3.3.3.3.

Procedures for implementing energy dissipation devices using both Methods 1 and 2 are presented below. The key difference between the methods is the procedure used to calculate the target displacement. Method 1 calculates the target displacement using a series of coefficients and an estimate of the elastic first mode displacement of the building. Method 2 is an iterative procedure that calculates the target displacement as the intersection of a "spectral capacity curve" (conceptually similar to the pushover curve) and a "design demand curve." The design demand curve is derived from the elastic response spectrum using a level of viscous damping consistent with the energy dissipated by the building in one cycle of loading to the assumed target displacement. There is no preferred method for the implementation of energy dissipation devices. There is

no difference between the methods once the target displacement is calculated.

Method 1

A. Displacement-Dependent Devices

The benefit of adding displacement-dependent energy dissipation devices is evidenced by the increase in building stiffness afforded by such devices, and the reduction in target displacement associated with the reduction in T_e. No direct account is taken of the added damping provided by the energy dissipation devices.

The calculation of the target displacement is based on a statistical relationship between the displacement of an elastic single-degree-of-freedom (SDOF) oscillator and the displacement of the corresponding inelastic oscillator—recognizing that the hysteretic energy dissipated by the inelastic oscillator reduces the displacement to that of the elastic oscillator. As such, the hysteretic energy dissipated by a displacement-dependent damper is conceptually identical to that dissipated by a shear link in an eccentrically braced frame. For the latter system, no direct account is taken of the energy dissipated by the shear link for the calculation of the target displacement. Rather, the increase in stiffness and reduction in period due to the addition of the braced framing results in substantially smaller displacement demands. The same rationale applies to displacement-dependent energy dissipation devices.

B. Velocity-Dependent Devices

The target displacement should be reduced to account for the damping added by the velocity-dependent energy dissipation devices. The calculation of the damping effect may be estimated as follows:

1. Estimate the effective damping in the rehabilitated building, including the damping provided by the energy dissipation devices.

2. Calculate the modified target displacement using Equation 3-11 and the damping modification factor from Table 2-15 corresponding to the effective damping calculated in step 1.

3. Impose lateral forces on the mathematical model of the rehabilitated building until the target displacement is reached. Tabulate the horizontal loads (= F_i at floor level i) and horizontal displacements (= δ_i at floor level i) at each floor level at the target displacement. Tabulate the relative axial displacements between the ends of each energy dissipation device (= δ_{rj} for device j)

4. Using the displacements δ_i, estimate the effective damping (β_{eff}) as follows:

$$\beta_{eff} = \beta + \frac{\sum_j W_j \cos^2 \theta_j}{4\pi W_k} \qquad \text{(C9-36)}$$

where β is the damping in the structural frame and is set equal to 0.05 unless modified in Section 2.6.1.5, W_j is work done by device j in one complete cycle corresponding to floor displacements δ_i, θ_j is the angle of inclination of device j to the horizontal, and W_k is the maximum strain energy in the frame, determined using Equation C9-37:

$$W_k = \frac{1}{2}\sum_i F_i \delta_i \qquad \text{(C9-37)}$$

where all terms are as defined above. The work done by device j in one complete cycle of loading may be calculated as:

$$W_j = \frac{2\pi^2}{T_s} C_j \delta_{rj}^2 \qquad \text{(C9-38)}$$

where T_s is the secant fundamental period of the rehabilitated building including the stiffness of the velocity-dependent devices (if any), calculated using Equation 3-10 but replacing the effective stiffness K_e with the secant stiffness K_s at the target displacement (see Figure 9-1); C_j is the damping constant for device j, and δ_{rj} is the relative displacement between the ends of device j along the axis of device j at a roof displacement corresponding to the target displacement. Procedures to calculate the work done by a nonlinear viscous damper in one cycle of loading are given in the following discussion on Method 2. (Note that the Method 2 discussion uses global frame displacements, Δ, and not the local component displacements, δ, used above.)

5. Iterate on steps 1 through 4 until the estimate of the effective damping (β_{eff}) used to calculate the modified target displacement (used in step 2) is equal to the effective damping calculated in the subsequent step 4.

The maximum actions in the building frame should be calculated at three stages: maximum drift, maximum velocity, and maximum acceleration. Calculation of component actions and deformations at the time of maximum drift is routine. Similar calculations of component actions and deformations at the times of maximum velocity and maximum acceleration are more complicated and will generally require additional modal analysis. One such procedure is illustrated by example in Section C9.3.9.5, Figure C9-31; the steps in the procedure are enumerated below. This procedure can be used with both Methods 1 and 2.

1. Estimate the secant stiffness of each component and element in the building frame at the target displacement. Replace the elastic stiffness of each component and element with the calculated secant stiffness. Perform eigenvalue analysis of the building frame and identify modal frequencies and shapes. (The first mode period should be similar to the secant period.) Using the design response spectrum, perform Response Spectrum Analysis using these frequencies and shapes, and calculate the maximum roof displacement using a modal combination rule (e.g., SRSS). Scale the modal displacements by the ratio of the target displacement to the maximum roof displacement to update the modal displacements. These modal data would correspond to the floor displacements listed in lines 4 through 6 of Table C9-10.

2. Calculate the modal actions in each component and element at the time of maximum drift. Combine these actions using a modal combination rule. This modal information would correspond to the first-story column actions listed in lines 16 and 17 of Table C9-10.

3. Calculate the modal viscous forces in each velocity-dependent energy dissipation device using modal relative displacements and modal frequencies.

4. For each mode of response, apply the calculated modal viscous forces to the mathematical model of the building at the points of attachment of the devices and in directions consistent with the corresponding mode shape of the building.

5. For each mode of response, apply the horizontal inertia forces at each floor level of the building to the mathematical model concurrently with the modal viscous forces so that the horizontal displacement at each floor level is zero.

6. Calculate the modal component actions resulting from the application of the modal viscous and inertia forces. Combine these actions using a modal combination rule. This modal information would correspond to the first-story column actions listed in line 18 of Table C9-10.

7. Calculate modal component actions for checking at the time of maximum acceleration as the linear combination of component actions due to displacement (step 2) multiplied by factor CF_1 and component actions due to viscous effects (step 6) multiplied by factor CF_2. For each mode of response, factors CF_1 and CF_2 should be calculated using (a) the effective modal damping ratio, and (b) Equations 9-31 and 9-32. The resulting modal component actions should be combined by an appropriate rule to calculate component actions for design. Component actions for design shall equal or exceed the component actions due to displacement. This modal information would correspond to the first-story column actions listed in lines 19 and 20 of Table C9-10.

8. Calculate the component actions for design as the maximum value of the component actions estimated at the times of maximum drift, maximum velocity, and maximum acceleration.

The acceptance criteria of Section 3.4.3 apply to buildings incorporating energy dissipation devices. Checking for displacement-controlled actions shall use deformations corresponding to the target displacement and maximum component forces. Checking for force-controlled actions shall use maximum component actions determined in step 8 above. Evaluation of the energy dissipation devices should be based on experimental data.

The commentary to Section 3.3.3 provides information on two Nonlinear Static Procedures. The procedures described above are intended for use with the nonlinear procedure presented in Section 3.3.3 and are described

as Method 1 in the commentary to Section 3.3.3. The second procedure, termed Method 2 in the commentary to Section 3.3.3, may also be used to implement energy dissipation devices. The reader is referred to the following commentary for information on how to use Method 2 to implement passive energy dissipation devices.

Method 2

The target displacement of the rehabilitated building is obtained in Method 2 by the spectral capacity curve (a property of the rehabilitated building) on the design demand curve. The spectral capacity curve is developed using the base shear-roof displacement relation of the rehabilitated building. The design demand curve is established from the 5%-damped pseudo-acceleration response spectrum after adjustment for the effective damping of the rehabilitated building due to inelastic action in the seismic framing system exclusive of the energy dissipation devices, and the added damping provided by the energy dissipation devices.

Design Demand Curve. The 5%-damped response spectrum (spectra) should be developed using the procedures set forth in Chapter 2.

To apply Method 2 to rehabilitated buildings with energy dissipation devices, the 5%-damped spectrum is modified to account for the damping in the rehabilitated building. The spectrum is modified by multiplying the 5%-damped spectral acceleration ordinates by the damping modification factors B_s or B_1, which vary with period range and damping level from Table 2-15. Figure C9-22 illustrates the construction of such a response spectrum from the corresponding 5%-damped spectrum. The modified design demand curve is prepared by constructing the spectral acceleration versus spectral displacement relation for the rehabilitated building at the damping level corresponding to the effective damping of the rehabilitated building.

Given that this simplified method of nonlinear analysis is based in part on modal analysis, a brief review of modal analysis theory is provided below. The reader is referred to Chopra (1995) for additional information.

Modal Analysis Theory. Consider a building represented by reactive weights W_i lumped at N degrees-of-freedom (DOF). The key dynamic

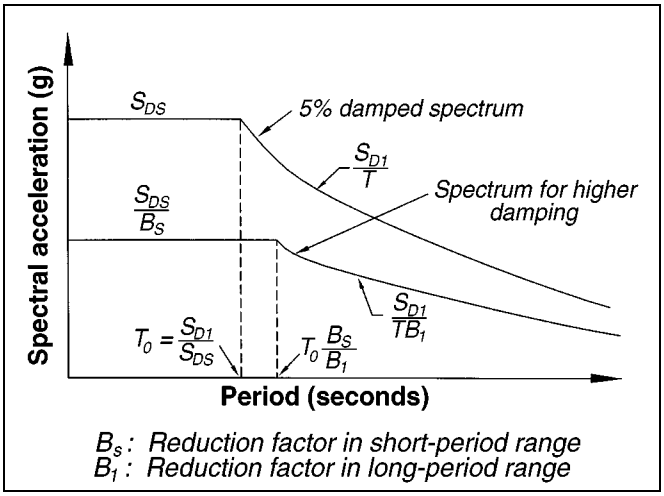

Figure C9-22 Construction of Response Spectrum for Damping Higher than 5%

characteristics of the building are the natural periods and the mode shapes. For this discussion, the amplitude of the m-th mode shape at DOF i is designated as ϕ_{im}. The building can be represented by a single DOF system with weight equal to:

$$W_{sm} = \frac{\left(\sum_{i=1}^{N} W_i \phi_{im} \right)}{\sum_{i=1}^{N} W_i \phi_{im}^2} \qquad \text{(C9-39)}$$

Note that the m-th modal weight is less than the total weight of the building and the sum of all the modal weights equals the total weight of the building.

If the spectral acceleration and displacement responses of this single DOF system are denoted as S_{am} and S_{dm}, respectively, the contribution of the m-th mode to the peak response of the building is:

Base shear:

$$V_m = \frac{W_{sm} S_{am}}{g} \qquad \text{(C9-40)}$$

Displacement at DOF i:

$$\delta_{im} = \phi_{im} \Gamma_m S_{dm} \qquad \text{(C9-41)}$$

where Γ_m is the *m*th modal participation factor:

$$\Gamma_m = \frac{\sum_{i=1}^{N} W_i \phi_{im} S_i}{\sum_{i=1}^{N} W_i \phi_{im}^2} \quad \text{(C9-42)}$$

The term S_i in Equation C9-42 is the horizontal displacement at DOF *i* corresponding to a unit horizontal ground displacement. For a two-dimensional mathematical model, S_i is equal to 1.0.

Spectral Capacity Curve. The force-displacement relation from the NSP is manipulated to produce the push-over curve for the building. The push-over curve is typically presented in terms of base shear (ordinate) and roof displacement (abscissa).

To determine whether the design of a rehabilitated building is acceptable, the spectral capacity curve is overlain on the design demand spectrum. The spectral capacity curve is typically presented as spectral acceleration (S_a) versus spectral displacement (S_d).

The spectral capacity curve can be derived from the push-over curve of the rehabilitated building by the following procedure.

1. At selected increments of displacement in the push-over analysis, the fundamental mode shape of the rehabilitated building is determined. This mode shape can be evaluated by either: (a) performing an eigenvalue analysis of the building using the secant stiffness of the framing members at the selected level of displacement, or (b) selecting a mode shape with ordinates equal to the displacements at the selected level of displacement; that is, at DOF *i*, the modal ordinate ϕ_i is equal to δ_i. Method (b) is often used for the Ritz analysis of complex dynamic systems (Chopra, 1995).

2. The spectral acceleration is computed as:

$$S_a = \frac{V}{W_{sm}} g \quad \text{(C9-43)}$$

where *V* is the base shear computed in the NSP; and W_{sm} is calculated per Equation C9-39 using the assumed mode shaped ordinates.

3. The spectral displacement is computed as:

$$S_d = \frac{\delta_t}{\phi_{rm} \Gamma_m} \quad \text{(C9-44)}$$

where δ_r is the roof displacement computed in the pushover analysis, ϕ_{rm} is the amplitude of the mode shape at the roof, and Γ_m is the modal participation factor calculated for the assumed mode shape per Equation C9-42.

Effective Damping of Rehabilitated Building. The effective damping of the rehabilitated building must be calculated in order to construct the design demand curve. In general, the effective damping will be dependent on the level of deformation in the framing system.

The effective damping is defined as:

$$\beta_{eff} = \frac{W_D}{4\pi W_k} \quad \text{(C9-45)}$$

where W_D is the energy dissipated by the rehabilitated building (including the energy dissipation devices) in one complete cycle of motion. The term W_k is the strain energy stored in the rehabilitated building at displacements equal to those used to estimate W_D.

In the push-over analysis, lateral loads F_i (typically a function of a selected displacement quantity) are applied at each reactive weight (W_i), resulting in corresponding displacements δ_i. The strain energy can be estimated as:

$$W_k = \frac{1}{2}\sum_{i=1}^{N} F_i \delta_i \qquad \text{(C9-46)}$$

The dissipated energy should be calculated for a complete cycle of motion at displacements equal to those used to calculate the strain energy, as follows:

$$W_D = W_{DS} + W_{DE} \qquad \text{(C9-47)}$$

where W_{DS} is the energy dissipated by the framing system exclusive of the energy dissipation system (typically assumed to be hysteretic), and W_{DE} is the energy dissipated by the energy dissipation devices, which may be either displacement-dependent or velocity-dependent. For velocity-dependent energy dissipation devices, the dissipated energy should be calculated for one cycle of motion of roof displacement amplitude δ_r, at the frequency corresponding to the secant period of the rehabilitated building. This secant period may be calculated by equating the maximum kinetic and strain energies in the building as follows:

$$T_s = 2\pi \sqrt{\frac{\sum_{i=1}^{N} W_i \delta_i^2}{g \sum_{i=1}^{N} F_i \delta_i}} \qquad \text{(C9-48)}$$

For an SDOF system, Equation C9-48 simplifies to:

$$T_s = 2\pi \sqrt{\frac{Dm}{V}} \qquad \text{(C9-49)}$$

where D is the displacement of the mass m, and V is the base shear corresponding to displacement D.

Analysis of Buildings Incorporating Displacement-Dependent Devices. Displacement-dependent energy dissipation devices should be explicitly represented in the mathematical model by bilinear, elasto-plastic, or rigid-plastic (friction) elements.

The Method 2 procedure for hysteretic energy dissipation devices is demonstrated below by the sample analysis of a one-story building for which friction devices are being considered.

Sample Analysis. For a one-story building, the push-over and spectral capacity curves are identical, namely,

- $N = 1$
- $\phi_{1m} = 1$
- $\delta_1 = \delta_r = D$
- $\Gamma_1 = 1$
- $W_{sm} = W_1$
- $S_a = Vg/W_1$
- $S_d = D$

The computed spectral capacity curves for the sample building (before and after rehabilitation) are shown in Figure C9-23, together with 20%, 30%, and 40% damped design demand curves.

The first step in the analysis procedure is to compute: (1) the force-displacement relation for the building before rehabilitation using push-over analysis, and (2) the effective damping in the building before rehabilitation (using Equation C9-45 and the force-displacement relation). The effective damping can be estimated using the bilinear hysteresis loop as follows.

The area contained within the hysteresis loop for the building is not precisely known, but is assumed to be a percentage of the area of the "perfect" bilinear hysteresis loop used to describe the computed push-over curve. For a bilinear system, where the spectral acceleration at lateral displacement D is defined as A, and the spectral acceleration at the yield displacement D_y is defined as A_y, the effective damping can be calculated as:

$$\beta_b = \frac{2(A_y D - D_y A)}{\pi A D} \qquad \text{(C9-50)}$$

The effective damping of the building is then computed as:

$$\beta_{eff} = q\beta_b \qquad \text{(C9-51)}$$

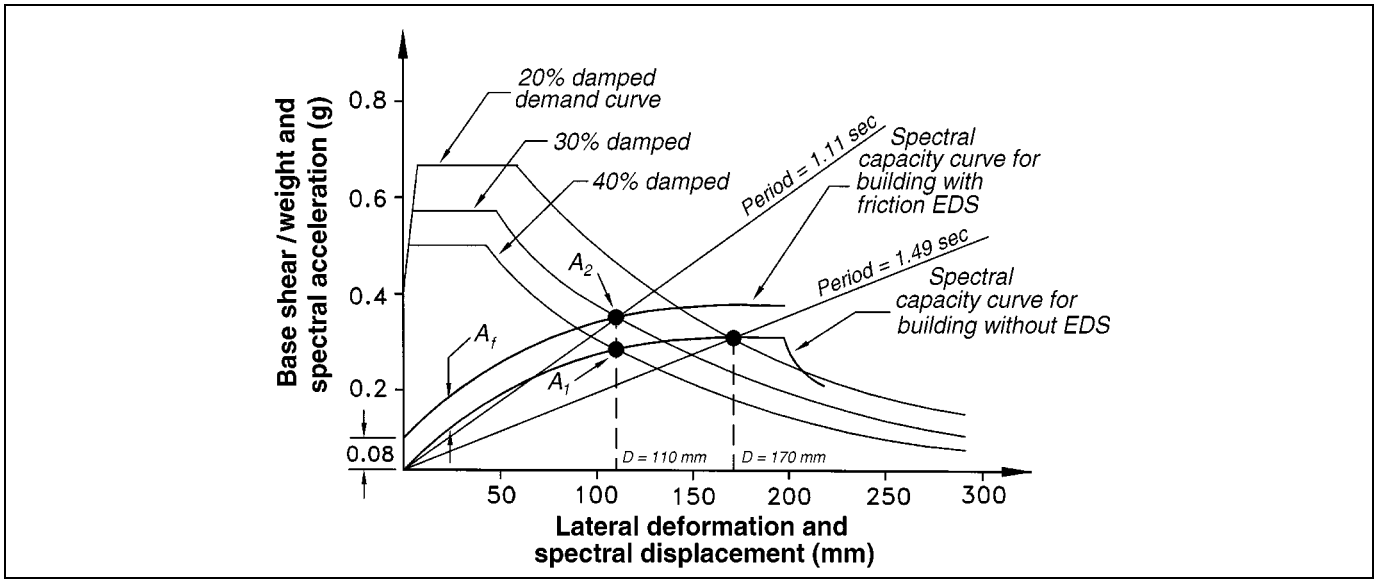

Figure C9-23 Spectral Capacity and Demand Curves for Rehabilitated One-Story Building

where q is a factor, less than one, equal to the ratio of the "actual" area of the hysteresis loop to that of the assumed perfect bilinear oscillator. Figure C9-24 shows the bilinear representation of the push-over curve, and the actual and perfect loop areas. For this example, q is approximately equal to 0.5. The value of factor q will depend on the type of construction and expected level of deformation. For example, a value $q = 0.2$ is inferred from the shake table test data of Li and Reinhorn (1995) for buildings rehabilitated with energy dissipation devices. Accordingly, it is recommended that a value of $q = 0.2$ be used for rehabilitated buildings unless a higher value can be justified.

The third step in the analysis procedure is to evaluate the spectral demand on the building before rehabilitation. The spectral demand is obtained iteratively by: (1) selecting points (displacements) on the spectral capacity curve—typically at the intersection of the spectral curve and the demand curves (e.g., 20%, 30%, and 40% damping); (2) calculating the effective damping of the building, β_{eff}, at the selected displacement points; and (3) comparing the calculated effective damping, β_{eff}, for each selected displacement point, with the demand curve damping value corresponding to the selected displacement point.

Returning to the sample building, consider the intersection point of the spectral capacity curve and the 20%-damped design demand curve at $D = 170$ mm,

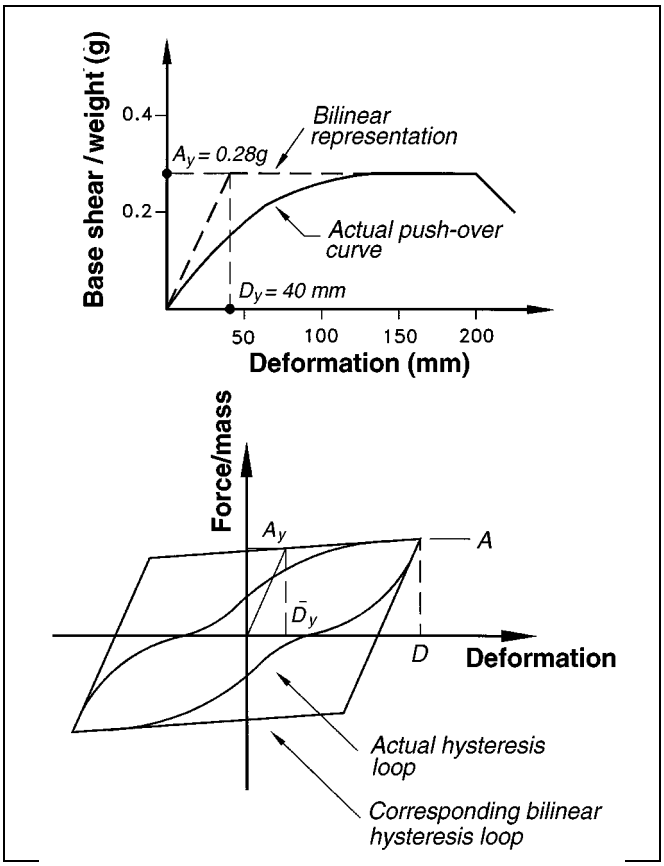

Figure C9-24 Representation of the Push-over Curve and Hysteresis Loops

$A = 0.31g$. Using values of $A_y = 0.28g$, $D_y = 40$ mm, and $q = 0.5$, the secant period T_s equals 1.5 seconds, β_b equals 0.40, and the effective damping of the building β_{eff} equals 0.20—the demand curve damping value associated with the trial displacement of 170 mm. No further iterations are necessary. The roof displacement demand on this one-story building before rehabilitation is therefore 170 mm (see Figure C9-23).

The three steps outlined above are repeated for the analysis of the rehabilitated building, as follows. The addition of friction energy dissipation devices serves to increase the strength of the sample building (as shown in Figure C9-23) by an amount assumed equal to A_f. The effective damping of the rehabilitated building is computed using Equation C9-45 by separating the hysteresis loop area into that area contributed by the energy dissipators (a near rectangular loop, if the energy dissipation device support framing is stiff), and the remainder of the rehabilitated building, as follows:

$$\beta_{eff} = \frac{2A_f D + 2q(A_y D - D_y A)}{\pi A_2 D} \qquad \text{(C9-52)}$$

where the spectral accelerations A_1 and A_2 are as defined in Figure C9-23. Following the procedure presented above, consider the intersection point of the spectral capacity curve for the rehabilitated building and the 30%-damped demand curve ($D = 110$ mm, $A_y = 0.28g$). Using $A_1 = 0.29g$, $A_2 = 0.36g$, $A_f = 0.08g$, $D_y = 40$ mm, and $q = 0.5$, the secant period T_s equals 1.11 seconds, and the effective damping β_{eff} is 0.30—the demand curve damping value associated with the trial displacement of 110 mm. No further iterations are necessary. The roof displacement demand on this one-story rehabilitated building is therefore 110 mm (see Figure C9-23)—65% of the displacement demand on the building before rehabilitation.

C. Analysis of Buildings Incorporating Velocity-Dependent Devices

Viscoelastic Energy Dissipation Devices. Viscoelastic energy dissipation devices exhibit effective stiffness that is generally dependent on frequency, amplitude of motion, and temperature. As such, the mathematical model of a rehabilitated building incorporating viscoelastic devices should account for the stiffness of these devices.

Viscoelastic devices should be modeled using linear or nonlinear springs representing the effective stiffness of the device at a fixed temperature and frequency. This frequency should be the inverse of the secant period of the structure with the added viscoelastic devices. The effect of temperature on the response of the viscoelastic device can be accounted for in the NSP by performing a series of analyses to bound the response of the rehabilitated building.

To demonstrate the analysis process, consider the sample one-story building with the friction devices replaced by viscoelastic devices. The displacement demand can be evaluated by calculating the effective damping:

$$\beta_{eff} = \frac{\frac{W_{DE}}{m} + 4q(A_y D - D_y A)}{2\pi A_2 D} \qquad \text{(C9-53)}$$

where m is the building mass, W_{DE} is the energy dissipated by the viscoelastic energy dissipation devices in one cycle of loading, and the remaining terms are as defined in Figure C9-25.

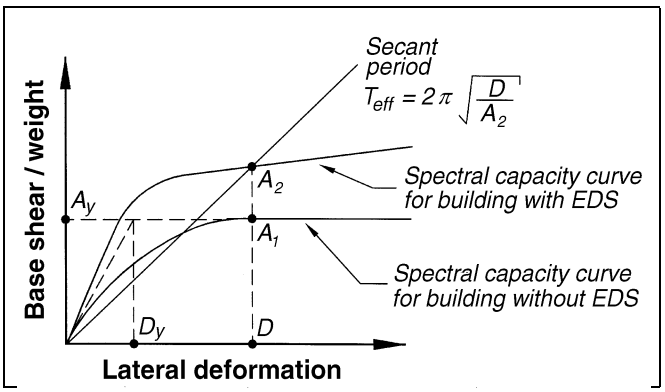

Figure C9-25 ***Definition of Parameters for Simplified Nonlinear Analysis of One-Story Building with Viscoelastic Energy Dissipation System (EDS)***

The energy dissipated by the viscoelastic energy dissipators can be calculated as:

$$W_{DE} = \frac{2\pi^2}{T_s}\sum_i C_j \cos^2\theta_j \Delta_{rj}^2 \qquad \text{(C9-54)}$$

where the summation extends over all energy dissipation devices; C_j is the damping coefficient of device *j* (Equations C9-27 and C9-28); θ_j is the angle of inclination of device *j* to the horizontal; and Δ_{rj} is the relative displacement of the attachment points of the energy dissipation device as shown in Figure C9-26.

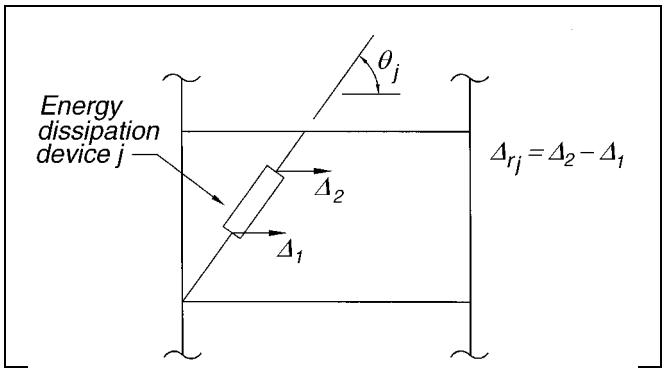

Figure C9-26 ***Definition of Angle and Relative Displacement of Energy Dissipation Device***

The calculation of the capacity-demand intersection point follows the same procedure as that described above for displacement-dependent devices. For displacement-dependent devices, the member actions can be based on the forces and deformations associated with the capacity-demand intersection point. For velocity-dependent energy dissipation devices, one further step is needed to calculate member actions, because the calculated member forces are based solely on nodal displacements and do not include the member forces resulting from nodal velocities (or viscous forces). Separate analysis should be performed to quantify these effects using the peak viscous force along the axis of each viscoelastic energy dissipation device, calculated as follows:

$$F_j = \frac{2\pi}{T_s} C_j \Delta_{rj} \cos\theta_j \qquad \text{(C9-55)}$$

where C_j is the damping coefficient of device *j* at displacement amplitude $\Delta_{rj}\cos\theta_j$, and frequency equal to the inverse of the calculated secant period.

Fluid Viscous Energy Dissipation Devices. Fluid viscous energy dissipation devices do not generally exhibit stiffness. Accordingly, the push-over curve of the rehabilitated building, as determined by the NSP, is identical to that of the building without the energy dissipation system.

For a building with a capacity curve as shown in Figure C9-27, the effective damping is given by

$$\beta_{eff} = \frac{\frac{W_{DE}}{m} + 4q(A_y D - D_y A)}{2\pi AD} \qquad \text{(C9-56)}$$

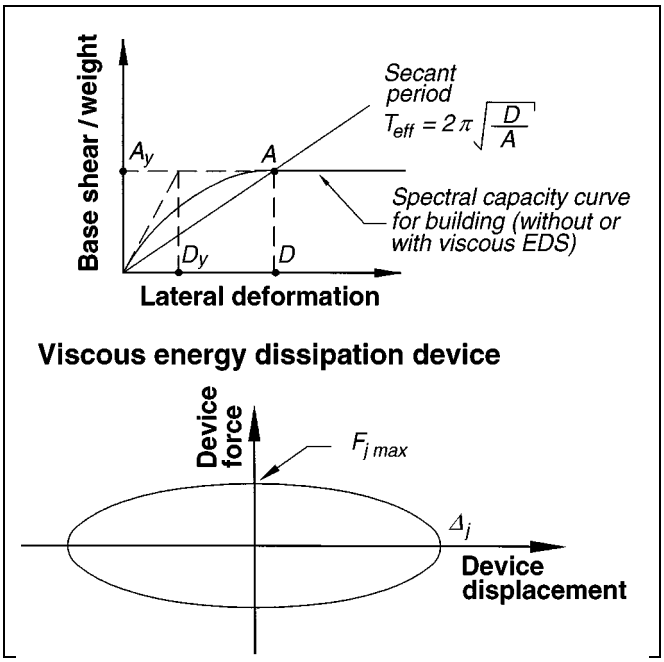

Figure C9-27 ***Definition of Parameters for Simplified Nonlinear Analysis of One-Story Building with Viscous Energy Dissipation System (EDS)***

where W_{DE} is the work done by the viscous energy dissipation devices in one cycle of loading. For the general case of a nonlinear viscous device with force

given by Equation C9-30, the work done (Soong and Constantinou, 1994) is:

$$W_{DE} = \sum_i \lambda F_{j\max} \Delta_j \qquad \text{(C9-57)}$$

where λ is a function of the velocity exponent as given in Table C9-4.

Table C9-4 Values of Parameter λ

Exponent α	Parameter λ
0.25	3.7
0.50	3.5
0.75	3.3
1.00	3.1
1.25	3.0
1.50	2.9
1.75	2.8
2.00	2.7

Alternatively, the work done may be expressed in terms of the relative displacement Δ_{rj} as defined in Figure C9-26:

$$W_{DE} = \left(\frac{2\pi}{T_s}\right)^{\alpha} \sum_i \lambda C_{0j} \left|\Delta_{rj} \cos\theta_j\right|^{1+\alpha} \qquad \text{(C9-58)}$$

where C_{0j} is the damping constant of device j (Equation C9-30). For a linear viscous device, for which the exponent α is equal to 1.0, Equation C9-58 takes the form:

$$W_{DE} = \frac{2\pi}{T_s} \sum_i C_{0j} \cos^2\theta_j \Delta_{rj}^2 \qquad \text{(C9-59)}$$

which is identical to Equation C9-54, except that C_{0j} is a constant in Equation C9-58, whereas C_j in Equation C9-54 is typically dependent on the excitation frequency and amplitude (velocity).

The calculation of the capacity-demand intersection point follows the same procedure as that described above for hysteretic and viscoelastic energy dissipation devices, except that Equations C9-56 through C9-59 are used to evaluate the effective damping of the rehabilitated building. Note that the push-over curve for the rehabilitated building will likely be different from that of the unrehabilitated building, because some existing framing elements are likely to require rehabilitation irrespective of the amount of damping added to the building. For displacement-dependent energy dissipation devices, the member actions can be based on the forces and deformations associated with the capacity-demand intersection point. For velocity-dependent energy dissipation devices, one further step is needed to calculate member actions, because the calculated member forces are based solely on nodal displacements and do not include the member forces resulting from nodal velocities (or viscous forces). Separate analysis should be performed to quantify these effects, using the peak viscous force along the axis of each viscous energy dissipation device calculated as follows:

$$F_j = \left(\frac{2\pi}{T_s}\right)^{\alpha} C_{0j} \left|\Delta_{rj} \cos\theta_j\right|^{\alpha} \qquad \text{(C9-60)}$$

where the secant period T_s is as defined in Figure C9-27.

A procedure to perform such an analysis is outlined in the discussion of Method 1 presented above.

The reader is referred to Section C9.3.9 for additional information on the implementation of energy dissipation devices using Method 2.

C9.3.5.2 Nonlinear Dynamic Procedure

If energy dissipation devices are dependent on loading frequency, operating temperature (including temperature rise due to excitation), deformation (or strain), velocity, sustained loads, and bilateral loads, such dependence should be accounted for in the nonlinear Time-History Analysis. One means by which to account for variations in the force-deformation response of energy dissipation devices is to perform multiple analyses of the rehabilitated building, using the likely bounding response characteristics of the energy dissipation devices. The design of the rehabilitated building, including the energy dissipation devices, should be based on the maximum responses computed from the multiple analyses.

The viscous forces (if any) developed in the seismic framing system should be accounted for in the analysis and design of the seismic framing system. Evaluation of member action histories should be based on nodal displacements (operating on member stiffness matrices) and nodal velocities (operating on member damping matrices).

Key to the acceptable response of a rehabilitated building incorporating energy dissipation devices is the stable response of the energy dissipation devices. The forces and deformations in the energy dissipation devices that develop during the design earthquake should be demonstrated to be adequate by prototype testing per Section 9.3.8 of the *Guidelines*.

C9.3.6 Detailed Systems Requirements

C9.3.6.1 General

No commentary is provided for this section.

C9.3.6.2 Operating Temperature

No commentary is provided for this section.

C9.3.6.3 Environmental Conditions

Energy dissipation devices should be designed with consideration given to environmental conditions, including aging effects, creep, fatigue, ambient temperature, and exposure to moisture and damaging substances. Although such considerations are unusual for conventional construction materials, the key role played by the energy dissipation devices makes it imperative that the environment in which the devices will be installed be considered carefully in the design process.

C9.3.6.4 Wind Forces

Rehabilitated buildings incorporating energy dissipation devices that are subject to failure by low-cycle fatigue (e.g., steel-yielding dampers) should resist the prescribed design wind forces in the elastic range to avoid premature failure.

Other devices that incorporate seals for containing fluids should be investigated for the possibility of seal malfunction and fluid loss, which could result in a substantial reduction of the energy dissipation capability of the device.

Wind-induced displacements in velocity-dependent devices may provide temperature increase in the device that may be of significance and require special considerations in the design of the device.

C9.3.6.5 Inspection and Replacement

Unlike conventional construction materials that are inspected infrequently—or never—some types of energy dissipation hardware will require regular inspection. Further, post-installation testing of certain types of hardware may be prudent, given the limited data available on the aging characteristics of the innovative materials and fluids being proposed for energy dissipation devices. Accordingly, easy access for both routine inspection and testing and scheduled or earthquake-mandated replacement of energy dissipation devices should be provided.

C9.3.6.6 Manufacturing Quality Control

Key to the acceptable response of a building rehabilitated using energy dissipation devices is the reliable response of those devices. Such reliance on the response of the energy dissipation devices makes necessary the implementation of a rigorous production quality control testing program.

C9.3.6.7 Maintenance

Such energy dissipation devices as friction dampers, fluid viscous dampers, viscoelastic dampers, and other mechanical dampers may require periodic maintenance and testing. Devices based on metallic-yielding and the plastic flow of lead likely need no maintenance.

The engineer of record should establish a maintenance and testing schedule for energy dissipation devices to ensure reliable response of said devices over the design life of the damper hardware. The degree of maintenance and testing should reflect the established in-service history of the devices.

C9.3.7 Design and Construction Review

C9.3.7.1 General

Design and construction issues associated with the use of energy dissipation devices are not well understood by many design professionals, due primarily to the limited use of this emerging technology at the time of this writing. Accordingly, all phases of the design and construction of buildings rehabilitated with energy dissipation devices should be reviewed by an independent engineering review panel. This panel should include persons experienced in seismic analysis

and the theory and application of energy dissipation devices.

The peer review should commence during the preliminary design phase of the rehabilitation project and continue through the installation of the energy dissipation devices.

C9.3.8 Required Tests of Energy Dissipation Devices

C9.3.8.1 General

No commentary is provided for this section.

C9.3.8.2 Prototype Tests

A. General

Although reduced-scale prototypes are permitted for certain tests described in Section 9.3.8.1, full-scale tests should be specified wherever possible. Failure characteristics of devices should not be determined by reduced-scale testing.

B. Data Recording

At least one hundred data points per cycle of testing should be recorded to capture the force-displacement response of the device adequately.

C. Sequence and Cycles of Testing

Prototype testing of energy dissipation devices is necessary to confirm the assumptions made in the analysis and design of the rehabilitated building, and to demonstrate that the energy dissipation hardware can sustain multiple cycles of deformation associated with the design wind storm, and the BSE-2.

At least one full-size energy dissipation device of each predominant type and size to be used in the rehabilitated building should be tested. These prototype devices should be fabricated using the identical material and processes proposed for the fabrication of the production devices.

Each prototype energy dissipation device should generally be subjected to a minimum of 2,000 displacement cycles of an amplitude equal to that expected in the design wind storm. The goals of this test are twofold, namely, (1) to demonstrate that the fatigue life of the device will not be exhausted in the design wind storm, and (2) to provide the engineer of record with design properties for the device in the design wind storm. For short-period buildings, the devices may see more than 2,000 significant displacement cycles in the design wind storm; for such buildings, the number of displacement cycles should be increased.

D. Devices Dependent on Velocity and/or Frequency of Excitation

Given the key role played by energy dissipation devices, it is appropriate that these devices be exhaustively tested. The testing program presented in the *Guidelines* is limited in scope and warrants augmentation on a project-by-project basis. As a minimum, each prototype device should be subjected to 20 displacement cycles corresponding to the BSE-2; the frequency of testing should be representative of the frequency characteristics of the building for the BSE-2.

The rules given in the *Guidelines* for evaluating frequency dependence are based on similar rules developed for testing base isolators. The frequency range of 0.5 f_1 to 2.0 f_1 should bound the frequency response of a building. The frequency of 2.0 f_1 corresponds to a stiffer building than that assumed in design (perhaps due to nonstructural components); the frequency of 0.5 f_1 corresponds to a fourfold decrease in building stiffness due to the effects of earthquake shaking—likely an upper bound for a rehabilitated building. Data from these tests should fall within the limiting values assumed by the engineer of record for the design of the building.

E. Devices Dependent on Bilateral Displacement

If the force-displacement properties of an energy dissipation device are influenced by building displacements in the direction perpendicular to the longitudinal axis of the energy dissipation device (termed bilateral displacement), such influence should be investigated by testing. The force-displacement response of the prototype device should be recorded at two levels of bilateral displacement: zero displacement, and the displacement equal to that calculated in the design earthquake. Data from these tests should fall within the limiting values assumed by the engineer of record for the design of the building.

F. Testing Similar Devices

No commentary is provided for this section.

C9.3.8.3 Determination of Force-Displacement Characteristics

The force-deformation characteristics of an energy dissipation device should be assessed using the cyclic test results of Section 9.3.8.2. The equations given for effective stiffness (k_{eff}) and effective damping (β_{eff}) are strictly valid only for viscoelastic devices.

C9.3.8.4 System Adequacy

Given the use of multiple Performance Levels in the *Guidelines*, the engineer of record may choose to augment the prototype testing requirements with tests at displacement levels different from those specified. These additional tests would serve to confirm the assumptions made in the analysis regarding the response of the energy dissipation devices at varying levels of building response.

C9.3.9 Example Applications of Analysis Procedures

C9.3.9.1 Introduction

The purpose of this section is to demonstrate by example some of the procedures presented in Section 9.3 of the *Guidelines*. Specifically, the use of the Linear Static, Linear Dynamic, and Nonlinear Static Procedures are described in Sections C9.3.9.3, C9.3.9.4, and C9.3.9.5, respectively.

The sample building used in this study is composed of a series of three-story, three-bay frames (see Figure C9-28). The effects of torsion are ignored and two-dimensional analysis is used for evaluation. The tributary floor weights are shown in Figure C9-28. For clarity, the frame is modeled as shear-type building with the story shear-story drift relations shown in Figure C9-28. The solution of the eigen problem for this frame results in the modal data presented in Table C9-5.

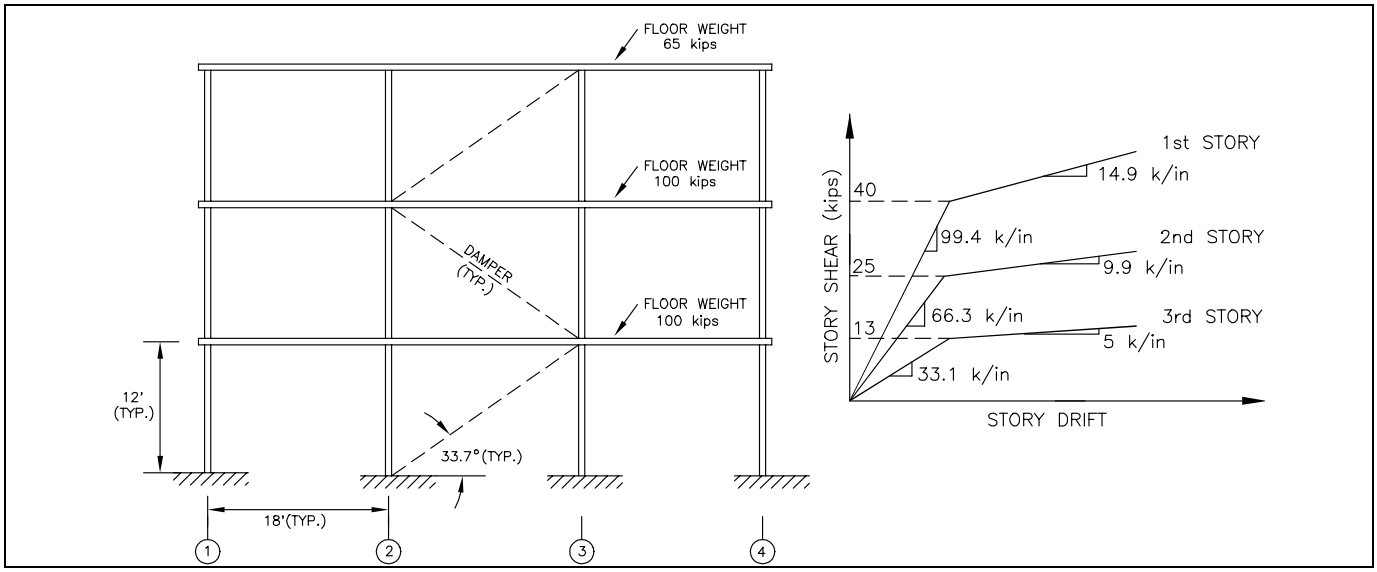

Figure C9-28 Sample Building Information

For the purpose of this study, the energy dissipation devices are assumed to be linear viscous dampers. (No preference for such dampers is inferred by this assumption.) Further, the mechanical characteristics of the sample dampers are assumed to be independent of excitation frequency, bilateral displacement, and ambient and operating temperature. (However, this may not be a reasonable assumption and must be investigated by the engineer as a key part of the design process.) The energy dissipation system consists of three linear fluid viscous dampers located in the central bay of the building as shown in Figure C9-28. It is assumed that all three dampers have identical properties (damping coefficient) and that the properties are to be selected to provide damping for the linear procedure of 20% in the fundamental mode. Assuming 5% damping in the building frame, the effective damping of the building is 25% of critical (see Equation 9-28). The

Table C9-5 Modal Analysis of the Sample Building Using Elastic Properties

	Mode 1	Mode 2	Mode 3	Reference
Period (sec)	0.75	0.34	0.22	
Frequency (rad/s)	8.38	18.45	28.46	
Mode Shapes				
Roof	1	1	1	
2	0.64	–0.73	–3.10	
1	0.29	–0.62	4.67	
Modal Weight (kips)	218.3	31.3	15.3	Equation C9-39
Participation Factor	1.38	0.45	0.07	
Effective Damping	0.25	0.67	0.63	
Coefficient B_S or B_1	2.05	3.0	3.0	Table 2-15
Spectral Accel. (g)	0.49	0.33	0.33	Spectral demand divided by appropriate *B*
Spectral Displ. (in)	2.69	0.38	0.16	
Factor CF_1	0.89	0.60	0.62	Equation 9-31
Factor CF_2	0.45	0.80	0.78	Equation 9-32

braced framing supporting the dampers is initially assumed to be infinitely rigid. This assumption is investigated further later in this section.

The seismic hazard at the site of the sample building is described by the 5%-damped response spectrum of Figure C9-22, with $S_{DS} = 1$, $S_{D1} = 0.6$, and $T_0 = 0.6$ second.

C9.3.9.2 Properties of Energy Dissipation Devices

The damping coefficient for each damper is selected to provide 20% of critical damping in the fundamental mode using elastic component properties. Using the eigen data presented in Table C9-5—β equal to 0.05, β_{eff} equal to 0.25, and θ_j equal to 33.7° at all three levels—the calculated value for C_0 is 4.28 kip-sec/in.

C9.3.9.3 Application of the Linear Static Procedure (LSP)

Analysis of the building using the LSP is permitted, provided the building frame remains elastic, the effective damping in the fundamental mode is less than 30% of critical, and criteria regarding the maximum resistance of the energy dissipation devices are satisfied (see item 1 in Section 9.3.4.1B).

A. Pseudo Lateral Load

The pseudo lateral load for the LSP is calculated using Equation 3-6. For the sample building, $C_1 = C_2 = 1.0$ for a building responding in the elastic range, $C_3 = 1.0$ if second-order effects are ignored, $T = 0.75$ second from the eigen analysis, $W = 265$ kips, $\beta_{eff} = 0.25$, $B_s = 2.05$ (Table 2-15) and $B_1 = 1.6$ (Table 2-15). The cutoff period for the modified spectrum ($= T_0 B_s/B_1$) is 0.77 second. The fundamental period of the building is less than the cutoff period. The spectral acceleration can therefore be calculated as equal to:

$$S_a = \frac{S_{DS}}{B_s} = \frac{1.0}{2.05} = 0.49g \qquad \text{(C9-61)}$$

and the pseudo lateral load is equal to 129 kips.

B. Vertical Distribution of Seismic Force

The vertical distribution of the pseudo lateral load *V* is calculated using Equation 3-8. The exponent *k* is equal to 1.12 for *T* equal to 0.75 second. The vertical distribution factors are equal to:

$$C_{v3} = 0.41$$

$$C_{v2} = 0.40$$

$$C_{v1} = 0.19$$

The lateral loads are calculated as the product of the vertical distribution factors and *V*. These loads represent the inertial forces at the time of maximum displacement.

C. Linear Analysis Results

The member forces at the time of maximum displacement are calculated by routine analysis using the story inertial forces calculated above. The relative axial displacements in the dampers can be calculated as the product of the inter-story drift and the cosine of the angle of inclination of the dampers to the horizontal plane (= 33.7 degrees in this instance for all three stories).

At the time of maximum velocity, the damper relative axial velocities are calculated as the product of the damper relative axial displacement at the time of maximum displacement, the damping coefficient (C_0), and the first modal radial frequency (= 8.38 radians per second).

State combination factors CF_1 and CF_2 are calculated to determine component actions at the time of maximum acceleration. Using Equations 9-31 and 9-32, the state factors are calculated to be equal to 0.89 and 0.45, respectively.

Table C9-6 summarizes key story shear data. Figure C9-29 shows the forces acting on the frame at the three stages identified above. Actions in one first story column are shown. The capacity of the column should be checked for all three sets of actions.

The limit on the use of the LSP set forth in item 1 of Section 9.3.4.1B can be evaluated using the data presented in Table C9-6. The maximum resistance of the frame, exclusive of the energy dissipation devices, is calculated as the resistance at maximum displacement in the BSE-2. Assume that the specified seismic hazard is that associated with the BSE-2. The resistances of each story of the frame at the maximum displacement are listed in the last column in Table C9-6. The maximum resistance of the energy dissipation devices in each story is equal to the horizontal component of the maximum damper axial forces: 40 kips, 39 kips, and 32 kips, in the third, second, and first stories, respectively. The criterion of item 1 is therefore violated and the design must be modified.

As an aside, consider the third column in the third story. The gravity load carried by this column is approximately 22 kips (based on tributary areas). The maximum axial load delivered by the damper is 27 kips—producing a maximum compression load of 49 kips and a maximum tension load of 5 kips.

Table C9-6 Summary of Results of the LSP

Floor or Story	Lateral Load	Floor Displ.	Story Drift	Damper Axial Displ. (in.)	Damper Axial Veloc. (in./s)	Damper Axial Force (kips)	Story Shear at Maximum Drift (kips)
3	53.4	4.504	1.613	1.342	11.243	48.1*	53.4
2	52.0	2.891	1.590	1.323	11.082	47.4	105.4
1	23.9	1.301	1.301	1.082	9.068	38.8	129.3

***** Horizontal component exceeds 50% of story shear at maximum drift.

D. Damper Support Framing

To maximize the effect of the supplemental damping hardware, the damper support should be stiff so as to maximize the relative displacement and velocity between the ends of the damper. Assuming that more than four dampers are installed in the sample building in each principal direction and in each story, and that the dampers are installed in line with the bracing, the braces must be designed for a minimum axial force equal to 130% of the maximum axial force in the damper. For the brace supporting the third story damper, the minimum design axial force is equal to 62.5 kips (= 1.3

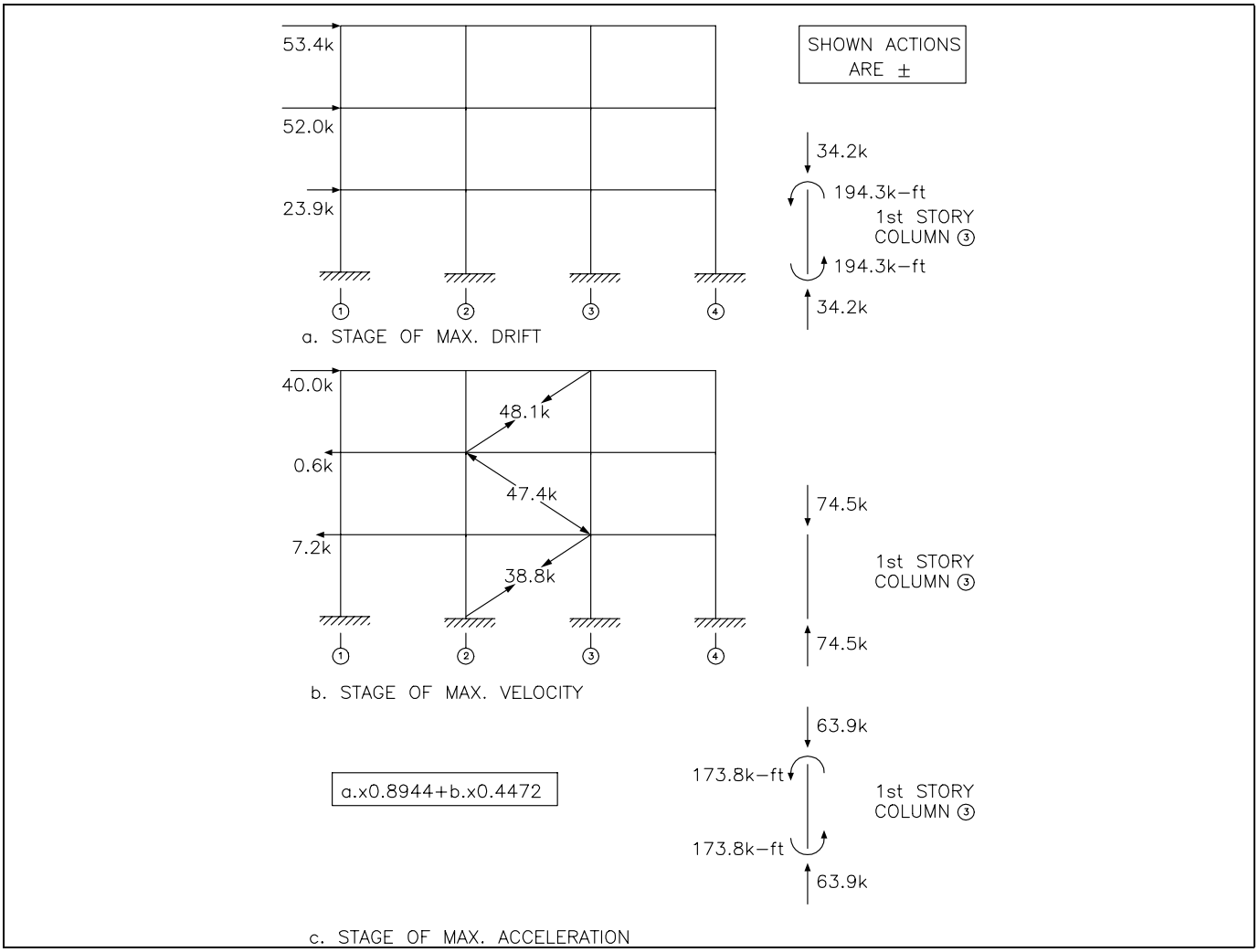

Figure C9-29 Loads on Building and LSP Actions in a Selected Component

x 48.1). Strength design can be used to design the brace without additional load factors. A 6 in. x 6 in. x 0.25 in. tube section (F_y = 46 ksi) is sufficient for this purpose. The stiffness of this brace (K_b) is 625 kips/inch. The brace-damper system can be idealized as a spring-dashpot system (Maxwell model)—see Figure C9-21. This spring-dashpot system has stiffness K' and damping coefficient C given by Constantinou et al. (1996):

$$K' = \frac{C_0 \tau \omega^2}{1 + \tau^2 \omega^2}, \quad C = \frac{C_0}{1 + \tau^2 \omega^2}, \quad \tau = \frac{C_0}{K_b} \quad \text{(C9-62)}$$

where ω is the circular frequency (= 8.38 radians/sec.). Substituting C_0 equal to 4.28 k-sec/inch into Equation C9-62 produces stiffness equal to 2.1 kips/inch and a damping coefficient equal to 4.27 k-sec/inch.

The calculated stiffness K' of 2.1 kips/inch is small by comparison with the minimum story stiffness of 33.1 kips/inch and will not appreciably alter the dynamic characteristics of the frame. Further, the damping coefficient is essentially unchanged. Accordingly, analysis based on the assumption of infinite brace stiffness is most adequate for this example.

C9.3.9.4 Application of the Linear Dynamic Procedure (LDP)

The sample frame and energy dissipation devices studied in Section C9.3.9.3 are analyzed using the response spectrum method. Calculations are performed for each of the three modes. Table C9-5 presents modal properties and Table C9-7 presents calculated modal responses and modal responses combined by the SRSS rule. Figure C9-30 presents the forces in the frame at the times of maximum displacement, velocity, and drift. Actions in a selected first story column are presented at the bottom of Figure C9-30. The capacity of this column should be checked for all three sets of actions and the actions due to the SRSS combination.

C9.3.9.5 Application of the Nonlinear Static Procedure (NSP)

One NSP is presented in the *Guidelines* (Method 1). Two procedures are described in this *Commentary* (Method 1 and Method 2). The two methods differ only in the means by which the roof displacement is determined. In Method 1, the target roof displacement is given by Equation 3-11. In Method 2, the roof displacement is calculated by comparison of the spectral capacity curve and design demand spectrum (see Section C9.3.5.1); Figure C9-31 illustrates the steps in Method 2 that are described in Section C9.3.5.1. The two methods should produce similar results unless the strength ratio R (see Equation 3-12) is greater than 5. For buildings with small strength ratios, the NDP is recommended.

Table C9-7 Summary of Results of the LDP

Response Quantity	Floor/Story	Mode 1	Mode 2	Mode 3	SRSS
Floor Displacement (in.)	3 2 1	3.70 2.38 1.07	0.17 –0.12 –0.11	0.01 –0.03 0.05	3.70 2.39 1.08
Story Drift (in.)	3 2 1	1.32 1.31 1.07	0.29 0.02 0.11	0.04 0.08 0.05	1.34 1.32 1.08
Damper Axial Displacement (in)	3 2 1	1.10 1.09 0.89	0.24 0.02 0.09	0.04 0.07 0.04	1.12 1.09 0.90
Damper Axial Velocity (inches/sec.)	3 2 1	9.194 9.152 7.472	4.484 0.276 1.612	1.065 2.012 1.207	10.284 9.375 7.739
Damper Axial Force (kips)	3 2 1	39.3 39.2 32.0	19.2 1.2 6.9	4.6 8.6 5.2	44.0 40.2 33.1
Story Shear at Maximum Drift (kips)	3 2 1	43.7 87.1 106.6	9.7 1.2 10.4	1.5 5.6 5.1	44.8 87.3 107.2
Inertia Force at Maximum Drift (kips)	3 2 1	43.7 43.4 19.5	9.7 –10.9 –9.2	1.5 –7.1 10.7	

A. Force-Displacement Relations

Evaluation of the relationships between base shear force and roof displacement is key to the NSP. For the sample building, the mathematical model is subjected to two load patterns: (1) loads proportional to floor weights (uniform pattern), and (2) loads proportion to the vertical distribution factors of Equation 3-8 (modal pattern). The force-displacement relations (also termed push-over curves) for these two load patterns are shown in Figure C9-32. The force-displacement relations are evaluated to displacements greater than the target displacement. At a minimum, the relation should be established for control node displacements equal to 150% of the target displacement.

For the sample building, the effective stiffness at 60% of the yield displacement is equal to the initial stiffness

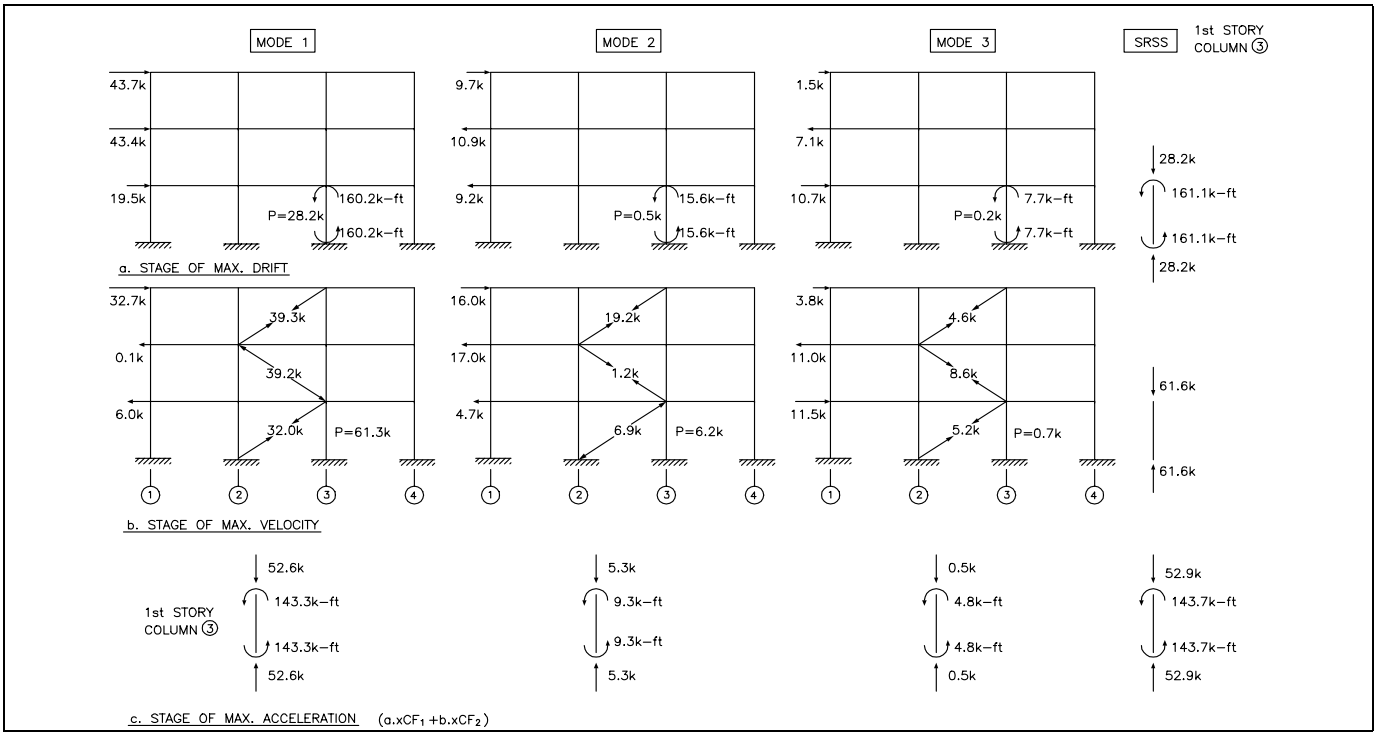

Figure C9-30 Loads on Building and LDP Actions in a Selected Component

and the effective period (T_e) is equal to 0.75 second (see Table C9-5).

Table C9-8 lists the modal properties of the building at different levels of roof displacement calculated using the modal load pattern. For this calculation, member stiffnesses are modified by the ratio of the secant stiffness at the selected displacement level to the effective elastic stiffness. For comparison, the elastic modal properties, appropriate for roof displacements less than 1.1 inches, are given in Table C9-5. Although modal periods increase with increasing roof displacements, the modal shapes and participation factors are somewhat invariant to changes in stiffness.

Table C9-9 presents modal data corresponding to the use of a uniform load pattern. A comparison of the modal data presented in Tables C9-8 and C9-9, at identical levels of roof displacement, demonstrates why multiple load patterns must be considered. Namely, substantially different modal properties may be obtained if different load patterns are used.

B. Fundamental Mode Response Estimates, Method 2, Modal Pattern

The analysis is performed first using the modal pattern of loads. An initial roof displacement of 4.2 inches is assumed. Equations C9-43 and C9-44 are used to convert the force-displacement relation (push-over curve) to the corresponding spectral capacity curve. Modal properties at the roof displacement of 4.2 inches are used for this purpose. A bilinear representation of the spectral capacity curve is shown in Figure C9-33a.

The effective damping is calculated by Equation 9-36. The damping afforded by the building frame, exclusive of the dampers, may either be assumed to be equal to 0.05 or determined using Equation C9-51 as follows. Values for D and A are calculated at the assumed roof displacement of 4.2 inches: D = 3.05 inches and A = 0.24 g; factor q is assumed to be equal to 0.2. The calculated damping in the frame, exclusive of the dampers, is 0.055. The damping ratio provided by the energy dissipators of 0.37 is calculated using Equations 9-36 and 9-37 and the modal properties corresponding to a roof displacement of 4.2 inches (equal to the assumed roof displacement). The effective damping in the rehabilitated building is 0.42 (= 0.05 + 0.37).

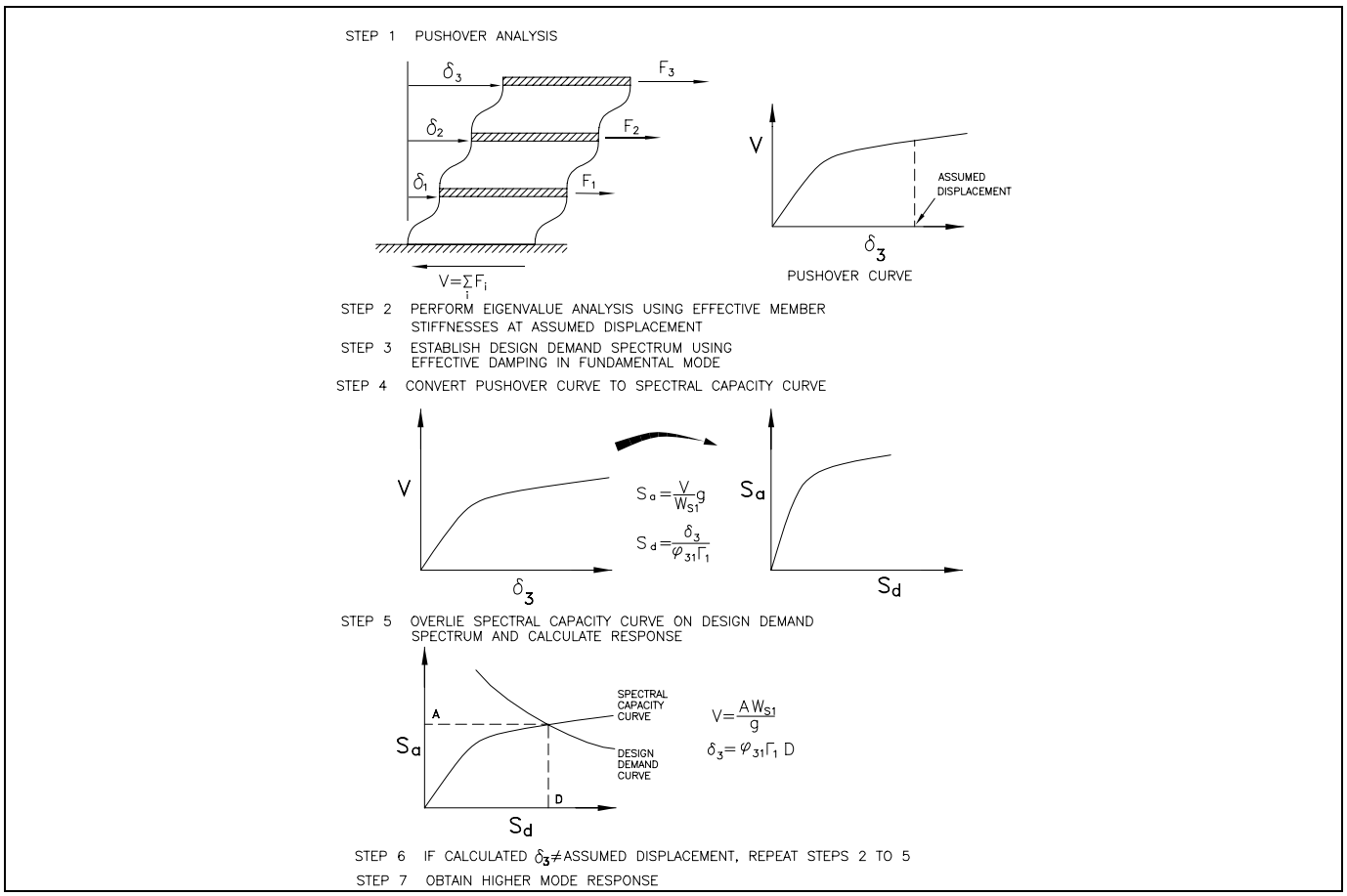

Figure C9-31 NSP Method 2 Schematic

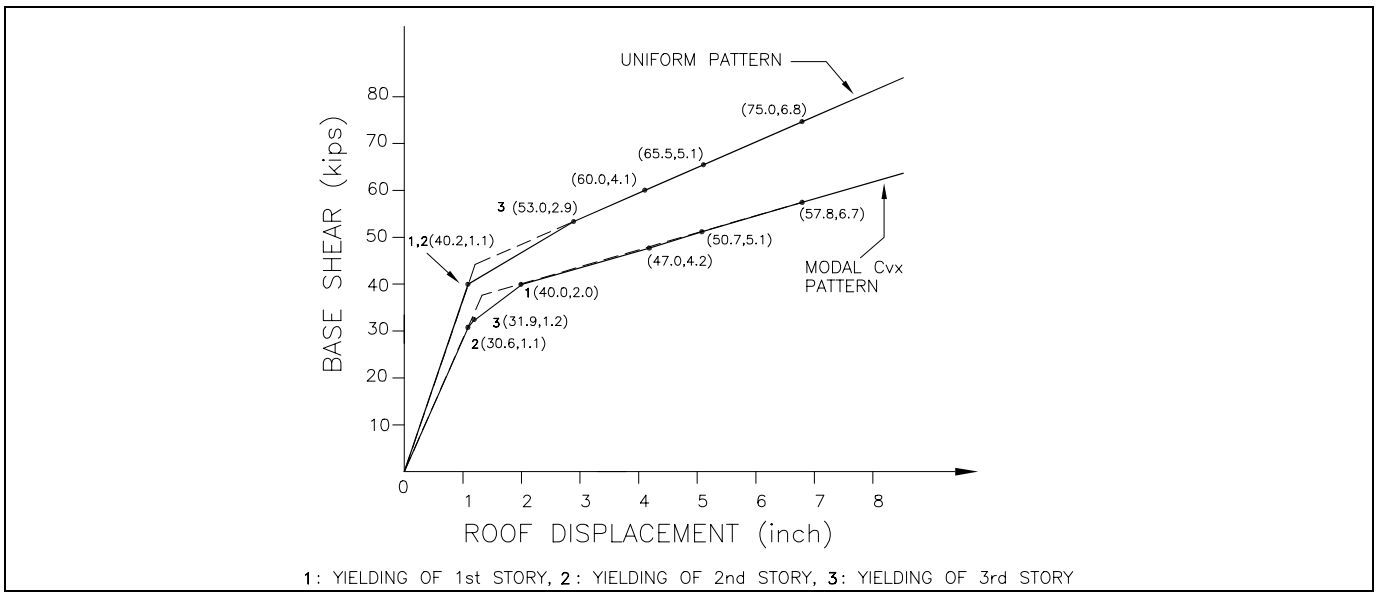

Figure C9-32 Force-Displacement Relations for Sample Building

The design demand curve is established using the 5%-damped spectrum modified to reflect the effective damping in the building. For effective damping equal to 0.42, and a first mode period of 1.19 second, the damping modification factor (for T equal to 1.19 second) is equal to 1.92. The resulting design demand curve is presented in Figure C9-33a. The intersection of the design demand and spectrum capacity curves (D = 3.7 inches, A = 0.26 g) corresponds to the target displacement. This information is converted to base shear and roof displacement using Equations C9-40 and C9-41, resulting in a base shear force equal to 50.7 kips and a roof displacement of 5.1 inches.

Table C9-8 Displacement-Dependent Modal Properties, Modal Load Pattern

Roof Displacement	Parameter	Mode 1	Mode 2	Mode 3
4.2 inches	T_i (sec.)	1.19	0.54	0.35
	ω (rad./sec)	5.28	11.59	18.21
	Mode shape ordinates (θ_i)	1	1	1
		0.60	–0.92	–3.75
		0.19	–0.49	8.29
	W_{si} (kips)	199	34	32
	Γ_i	1.38	0.44	0.06
5.1 inches	T_i (sec.)	1.26	0.57	0.37
	ω (rad./sec)	5.00	10.97	17.07
	Mode shape ordinates (θ_i)	1	1	1
		0.61	–0.89	–3.58
		0.21	–0.52	7.30
	W_{si} (kips)	203	34	28
	Γ_i	1.38	0.44	0.07
6.1 inches	T_i (sec.)	1.32	0.60	0.39
	ω (rad./sec)	4.75	10.44	16.15
	Mode shape ordinates (θ_i)	1	1	1
		0.62	–0.86	–3.45
		0.23	–0.55	6.62
	W_{si} (kips)	205	34	26
	Γ_i	1.38	0.45	0.07

The calculated roof displacement of 5.1 inches is not equal to the assumed displacement of 4.2 inches. The procedure outlined above is repeated using an assumed roof displacement of 5.1 inches and modal properties corresponding to this displacement (see Table C9-8). The updated spectral capacity curve is shown in Figure C9-33b. The revised effective damping is equal to 0.44 (= 0.05 + 0.39); the damping modification factor corresponding to the revised effective damping ratio is equal to 1.94.

The updated design demand curve is shown in Figure C9-33b. The intersection point of the design demand and spectrum capacity curves is (D = 3.7 inches, A = 0.25 g). The corresponding roof displacement and base shear force are 5.1 inches and 50.6 kips, respectively. The calculated and assumed roof displacements are equal and no further iterations are required.

The floor displacements and story drifts in the first mode are those calculated at the roof displacement of

Table C9-9 Displacement-Dependent Modal Properties, Uniform Load Pattern

Roof Displacement	Parameter	Mode 1	Mode 2	Mode 3
4.2 inches	T_i (sec.)	1.22	0.48	0.36
	ω (rad./sec)	5.14	13.15	17.50
	Mode shape ordinates (θ_i)	1	1	1
		0.78	–0.46	–1.58
		0.35	–0.83	1.64
	W_{si} (kips)	230	26	9
	Γ_i	1.29	0.41	0.12
5.1 inches	T_i (sec.)	1.30	0.53	0.39
	ω (rad./sec)	4.82	11.93	16.30
	Mode shape ordinates (θ_i)	1	1	1
		0.75	–0.52	–1.84
		0.34	–0.75	2.16
	W_{si} (kips)	228	26	11
	Γ_i	1.31	0.42	0.11
6.1 inches	T_i (sec.)	1.39	0.57	0.41
	ω (rad./sec)	4.52	11.06	15.39
	Mode shape ordinates (θ_i)	1	1	1
		0.75	–0.52	–1.94
		0.36	–0.74	2.24
	W_{si} (kips)	230	25	10
	Γ_i	1.31	0.41	0.10

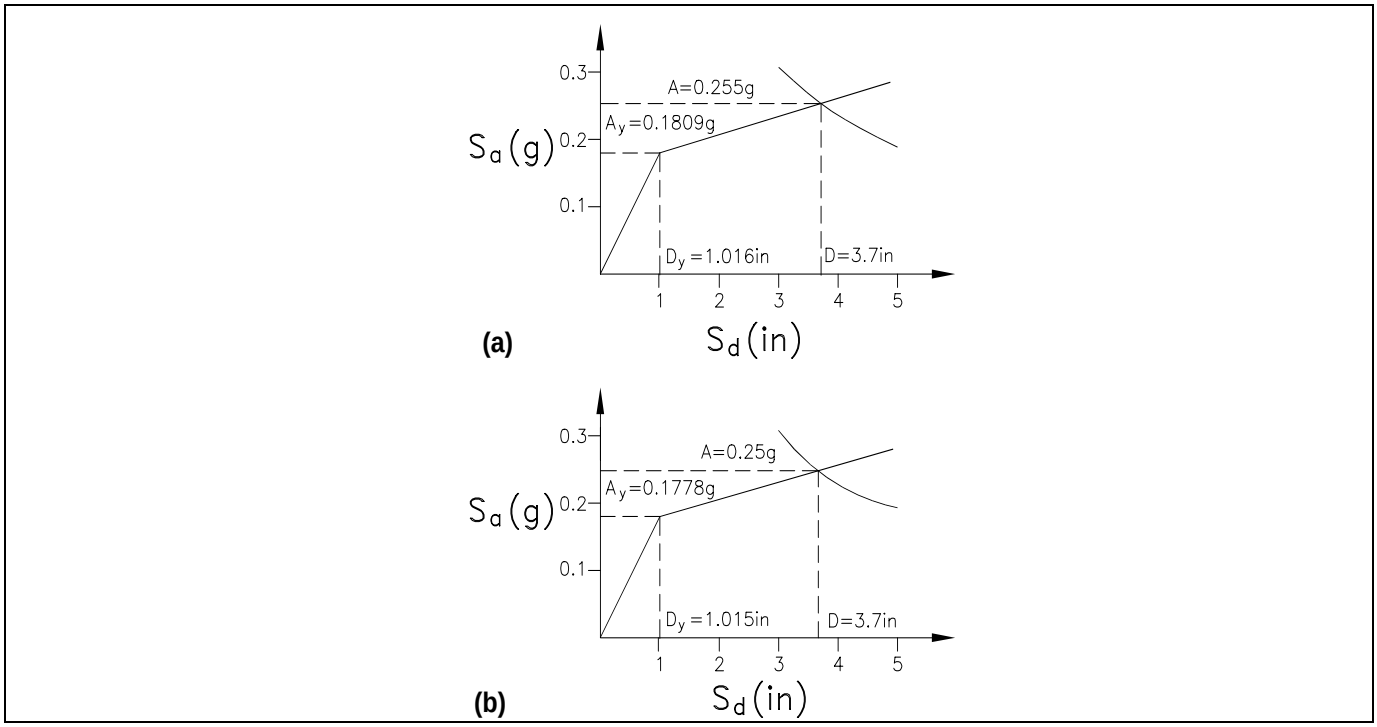

Figure C9-33 NSP Response Estimates, Method 2, Modal Pattern (a) Target Roof Displacement of 4.2 inches (b) Target Roof Displacement of 5.1 inches

5.1 inches. See Table C9-10 for details. Axial displacements and forces in the energy dissipation devices are also presented in this table. These data were calculated using the first modal frequency calculated at the roof displacement of 5.1 inches (= 5.00 radians/sec from Table C9-8).

C. Higher Mode Response Estimates, Method 2, Modal Pattern

Higher mode responses are evaluated using the Response Spectrum Method. The modal properties corresponding to a roof displacement of 5.1 inches are used. The effective modal damping is calculated using Equation 9-33 and estimates of the modal frequencies and modal displacements (see also Equation 9-30). The calculated effective modal damping ratios are 1.21 and 0.97 in the second and third modes, respectively. Near-critical damping presents a complication because conventional modal analysis can no longer be applied. However, given the upper limit on the value of B_s or B_1 (equal to 3.0 below the transition point in the spectrum), and recognizing that the stated spectrum reduction method generally produces conservative estimates of displacement and velocity (Constantinou et al., 1996), the procedure outlined above is acceptable for highly-damped systems. Note that the maximum acceleration in the short-period range for highly-damped systems will be approximately equal to the peak ground acceleration.

Table C9-10 Summary of Results of the NSP, Method 2, Modal Pattern

Response Quantity	Floor/Story	Mode 1	Mode 2	Mode 3	SRSS
Lateral Loads (kips)	3	20.9	9.6	1.4	
	2	20.4	–13.1	–7.8	
	1	9.3	–7.8	16.0	
Floor Displacement (inches)	3	5.11	0.47	0.03	5.13
	2	3.14	–0.42	–0.10	3.17
	1	1.11	–0.25	0.21	1.16
Story Drift (inches)	3	1.97	0.90	0.13	2.17
	2	2.02	0.17	0.32	2.05
	1	1.11	0.25	0.21	1.16
Damper Axial Displacement (inches)	3	1.64	0.75	0.11	1.81
	2	1.68	0.14	0.26	1.71
	1	0.93	0.21	0.18	0.97
Damper Axial Force (kips)	3	35.1	35.0	8.1	50.2
	2	36.0	6.7	19.1	41.3
	1	19.8	9.7	12.8	25.5
Actions in First Story Column 3 (P: kips, M: k-ft)	Maximum Drift	P = 13.6 M = 76.0	P = 0 M = 17.0	P = 0 M = 14.3	P = 13.6 M = 79.2
	Maximum Velocity	P = 50.4 M = 0.0	P = 10.3 M = 0.0	P = 1.0 M = 0.0	P = 51.5 M = 0.0
	Maximum Acceleration	P = 43.6 M = 56.9	P = 10.3 M = 17.0	P = 1.0 M = 14.3	P = 44.8 M = 61.1

Higher mode responses are calculated using a damping modification factor of 3.0 and with combination factors CF_1 and CF_2 both equal to 1.0. The latter assumption is conservative but likely appropriate for highly-damped modes. Higher mode response data are presented in columns 4 and 5 of Table C9-10. Total responses calculated using the SRSS modal combination rule are presented in column 6 of the table.

Consider the data presented in this table. It is evident that mode 1 displacement response is dominant; for design purposes, higher mode displacements can generally be ignored. However, the same argument cannot be made when considering the maximum forces in the dampers. Of particular interest is the damper axial force in the first story. The mode 3 damper force is more than 60% of the mode 1 damper force. Clearly, higher mode effects must be evaluated when designing

viscous dampers, damper support framing, and columns to which viscous forces can be delivered.

D. Response Estimates, Method 2, Uniform Pattern

The procedure used to evaluate the response of the sample building is identical to that outlined above except that the modal properties are established using a uniform load pattern (see Table C9-9). Starting with an assumed roof displacement of 5.1 inches, the first iteration produces a calculated roof displacement of 4.84 inches (within 5% of the assumed value). Given that modal properties are not significantly affected by displacement (see Table C9-9), no further iterations are required. Modal actions and deformations are calculated using the same procedure as that outlined above. Responses are summarized in Table C9-11.

C9.4 Other Response Control Systems

Base isolation (Section 9.2) and passive energy dissipation (Section 9.3) systems are seismic response control systems. When included in a rehabilitated building, these systems generally reduce inertia forces and drifts during earthquake shaking, thereby reducing or eliminating damage. These systems achieve this objective by either deflecting a portion of the seismic energy (base isolation) or converting kinetic energy in the framing system to heat (energy dissipation).

Other response control systems, designed and implemented for nonseismic applications, are being further developed for seismic applications. Two such classes of control systems are dynamic vibration absorbers and active control systems.

Table C9-11 Summary of Results of the NSP, Method 2, Uniform Pattern

Response Quantity	Floor/Story	Mode 1	Mode 2	Mode 3	SRSS
Lateral Loads (kips)	3	15.7	9.1	2.4	
	2	24.2	–7.3	–6.8	
	1	24.2	–10.5	8.0	
Floor Displacement (inches)	3	4.84	0.38	0.05	4.85
	2	3.90	–0.20	–0.10	3.91
	1	2.02	–0.29	0.12	2.04
Story Drift (inches)	3	0.94	0.58	0.15	1.11
	2	1.88	0.09	0.22	1.90
	1	2.02	0.29	0.12	2.04
Damper Axial Displacement (inches)	3	0.78	0.48	0.13	0.92
	2	1.57	0.07	0.18	1.58
	1	1.68	0.24	0.10	1.70
Damper Axial Force (kips)	3	16.0	24.6	8.9	30.7
	2	32.3	3.6	12.5	34.8
	1	34.7	12.1	6.7	37.4
Actions in First Story Column 3 (P: kips, M: k-ft)	Maximum Drift	P = 13.5 M = 96.2	P = 1 M = 13.1	P = 0 M = 5.4	P = 13.6 M = 97.2
	Maximum Velocity	P = 46.1 M = 0.0	P = 8.9 M = 0.0	P = 1.7 M = 0.0	P = 47.0 M = 0.0
	Maximum Acceleration	P = 38.1 M = 77.7	P = 9.9 M = 13.1	P = 1.7 M = 5.4	P = 39.4 M = 79.0

C9.4.1 Dynamic Vibration Absorbers

Dynamic vibration absorbers are oscillators that, when properly tuned and attached to a framing system, transfer kinetic energy among the vibrating modes, leading to an increase in damping in the selected mode of vibration (Den Hartog, 1956). Examples of these absorbers are tuned mass dampers (TMDs) and tuned liquid dampers (TLDs). The reader is referred to International Association for Structural Control (1994), and Soong and Constantinou (1994) for additional information.

Tuned mass dampers consist of a mass, a restoring force (spring, viscoelastic material, or pendulum action), and a means of dissipating energy (viscous damper, viscoelastic material, or friction). When attached at a

point of significant vibration, and tuned to a frequency close to the fundamental frequency of the framing system, TMDs produce a combined structure-appendage system with increased damping.

Tuned liquid dampers may take one of the following forms: (1) a tuned sloshing damper in which liquid (typically water) in a large container serves as the tuned mass, with damping resulting from either fluid sloshing or fluid flow through screens; or (2) a tuned liquid column damper that utilizes the vibration of a liquid in a U-shaped container, inducing damping by restricting the flow of the fluid through an orifice (Sakai, 1989; Kareem, 1994; Soong and Constantinou, 1994). TLDs are tuned by selecting the proper dimensions of the fluid containers; however, the frequency and damping characteristics of a TLD may be motion-dependent, that is, nonlinear.

Dynamic vibration absorbers have been used to reduce the response of structures to wind excitation, occupant activity, and machine vibration. In buildings, their use has been restricted to enhancing comfort for the occupants of tall buildings. Moreover, their application has been restricted to structures that remain in the elastic range, so that tuning is maintained during dynamic excitation. The effectiveness of a dynamic vibration absorber is significantly reduced when the structural system undergoes significant inelastic action (Kaynia et al., 1981; Sladek and Klingner, 1983), although studies summarized in Villaverde (1994) indicate that with the use of massive and highly damped vibration absorbers, it is possible to control the seismically-induced response of structures.

To date, the use of dynamic vibration absorption hardware to control the seismic response of buildings in severe earthquakes has not been demonstrated. Research and studies in this field are ongoing.

C9.4.2 Active Control Systems

The subject of active seismic control is broad. The reader is referred to Soong (1990), Soong and Constantinou (1994), ATC (1993), and International Association for Structural Control (1994) for detailed information on both active control theory and active control applications.

Active control systems are based on the premise that it is possible to modify the dynamic behavior of a structural system by the use of an automated control system composed of sensors, controllers, and actuators. The sensors measure the response of the structure. The controller processes the signals from the sensors, computes the required control forces based on a control algorithm, and supplies control signals to the actuators. The actuators impose the computed forces or displacements on the building.

To understand the function of an active control system, it is worthwhile to review the function of a passive control system, the elements of which are shown in Figure C9-34. The energy dissipation system is an integral part of the structure and develops motion control forces. The power needed to generate these forces is provided by the motion of the framing system during dynamic excitation; the amplitude and direction of these forces are based entirely on the relative motion of the attachment points of the energy dissipation devices.

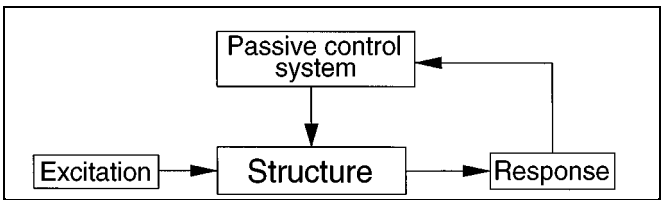

Figure C9-34 Elements of Passive Control System

An active control system also develops motion control forces, as illustrated in Figure C9-35. The sample active control system shown in Figure C9-36 is an active bracing system in which hydraulic actuators serve as the active braces (Reinhorn et al., 1992). The magnitude and direction of these forces are determined by the controller, which receives information on the response of the structure from the strategically located sensors.

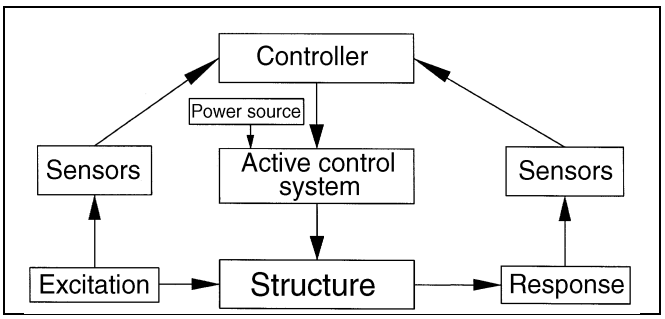

Figure C9-35 Elements of Active Control System

In principle, an active control system should provide better response control than a passive control system. However, the effective operation of active control systems is currently hampered by two significant shortcomings. First, the control forces required for mitigating the effects of strong seismic excitations are so large that the control system and its power source may assume a prohibitively large size. Second, active control systems are highly sophisticated, require continuous maintenance, and have not yet reached the level of reliability required for seismic applications. Accordingly, active control systems have not yet been used for seismic applications.

Research in active control continues at a pace that almost assures the development of practical active control systems for seismic applications in the near future. An example of new developments in this field is that of "semi-active" control systems. The term "semi-active" denotes that the operation of the control system consumes only a small amount of external power. In a semi-active control system, the mechanical properties of the system are continuously updated using sensor-based feedback from the framing system (as in active control systems), and the motion of the building is used to develop the control forces (as in passive control systems) necessary to adjust the damping and/or stiffness characteristics of the semi-active control system. Further, because the control forces in a semi-active system always oppose the motion of the building, the system is inherently more stable than an active control system. Semi-active control systems are typically considered to be fail-safe, in that the semi-active energy dissipation devices can be designed to

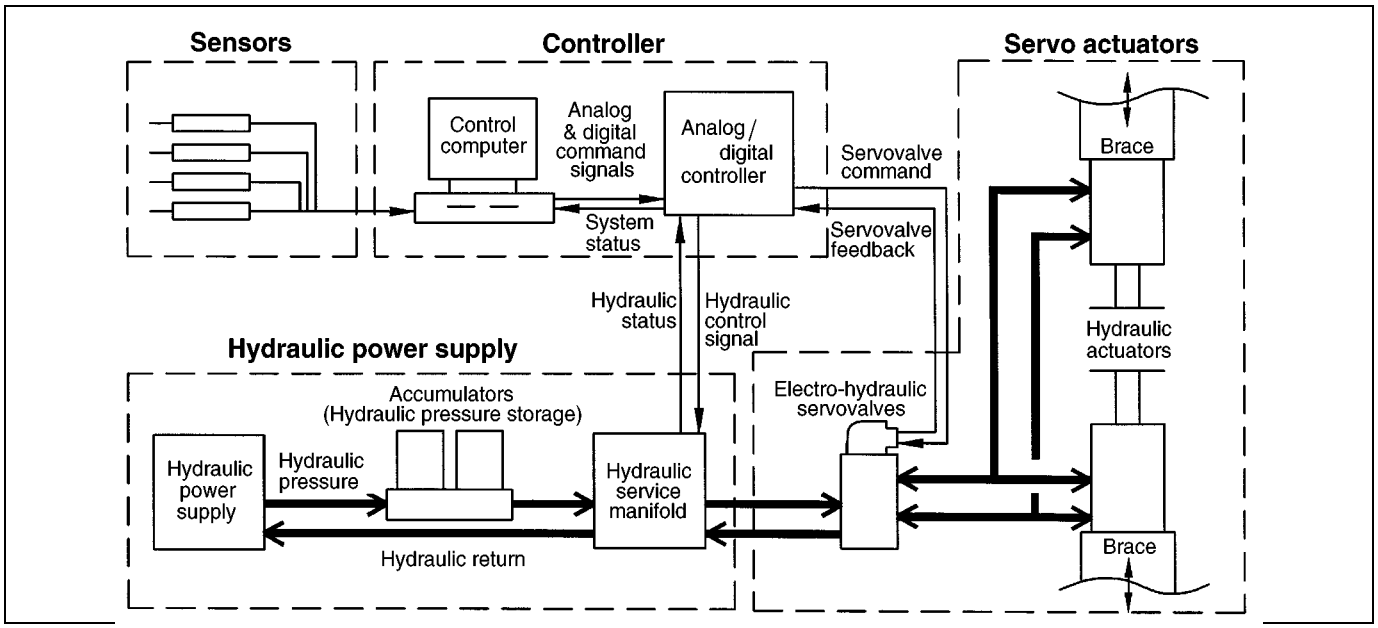

Figure C9-36 Details of Control System of Active Bracing System

exhibit prescribed damping and stiffness characteristics in the event of a complete loss of power (Patten et al., 1993; Symans et al., 1994). Figure C9-37 shows the elements of a sample semi-active energy dissipating bracing system. In this system, semi-active energy dissipators are used as bracing members. A direct-drive servovalve is used to adjust the damping coefficient of the semi-active brace. In the event of a loss of power, this servovalve is designed to close, upon which the semi-active energy dissipating braces convert to passive energy dissipating braces with a high-damping coefficient. An alternative use of semi-active devices is described in Liang et al. (1995).

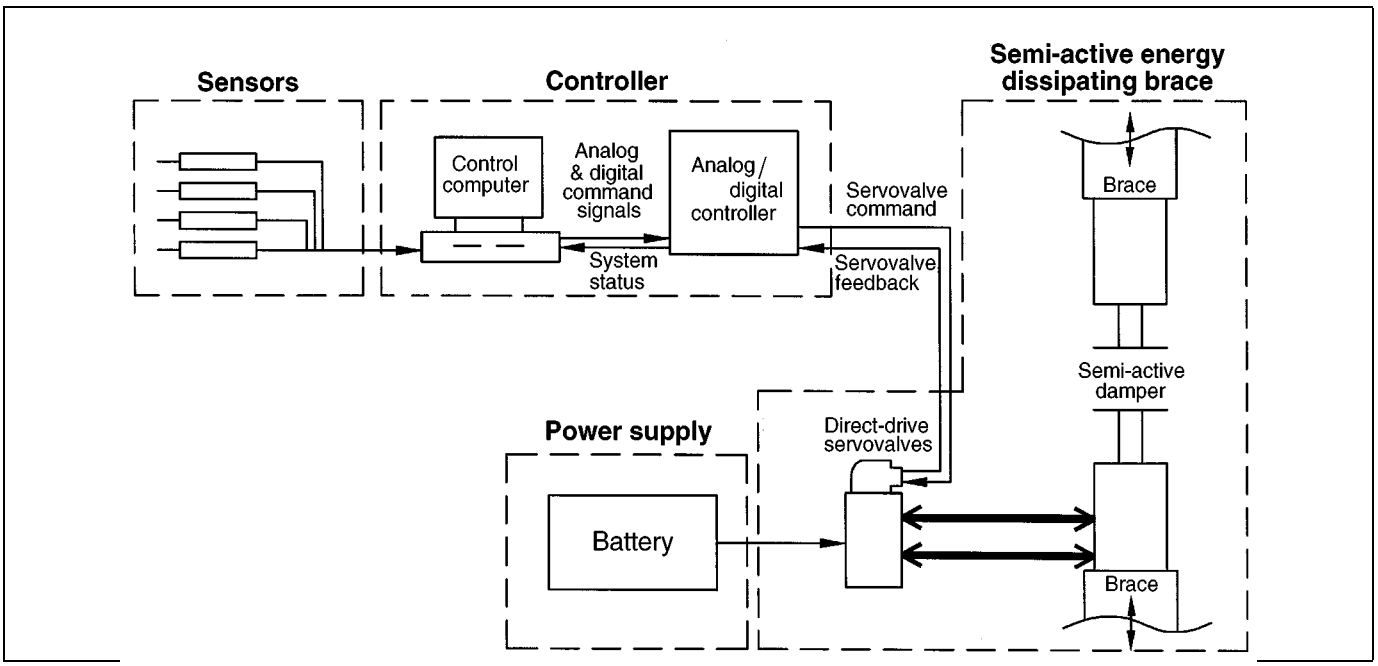

Figure C9-37 Details of Control System of Semi-Active Energy Dissipation Bracing System

C9.5 Definitions

Push-over curve: The base shear versus roof displacement relationship computed using the Nonlinear Static Procedure of Chapter 3.

Spectral capacity curve: The spectral acceleration versus spectral displacement relationship based on the capacity push-over curve as described in Section 9.3.

C9.6 Symbols

No commentary is provided for this section.

C9.7 References

Aiken, I. D., and Kelly, J. M., 1990, *Earthquake Simulator Testing and Analytical Studies of Two Energy-Absorbing Systems for Multistory Structures*, Report No. EERC-90/03, Earthquake Engineering Research Center, University of California, Berkeley, California.

Aiken, I. D., Nims, D. K., Whittaker, A. S., and Kelly, J. M., 1993, "Testing of Passive Energy Dissipation Systems," *Earthquake Spectra*, Earthquake Engineering Research Institute, Oakland, California, Vol. 9, No. 3, pp. 335–370.

Al-Hussaini, T., Zayas, V., and Constantinou, M. C., 1994, *Seismic Isolation of Multi-Story Frame Structures using Spherical Sliding Isolation Systems*, Report No. NCEER-94-0007, National Center for Earthquake Engineering Research, State University of New York at Buffalo, New York.

Amin, N., Mokha, A., and Fatehi, H., 1993, "Seismic isolation retrofit of the U.S. Court of Appeals Building," *Proceedings of Seminar on Seismic Isolation, Passive Energy Dissipation, and Active Control*, Applied Technology Council Report No. ATC-17-1, Redwood City, California.

ASTM, latest edition, Standard D4014, American Society of Testing Materials, Philadelphia, Pennsylvania.

ATC, 1993, *Proceedings of Seminar on Seismic Isolation, Passive Energy Dissipation, and Active Control*, Report No. ATC-17-1, Applied Technology Council, Redwood City, California.

Bergman, D. M., and Hanson, R. D., 1993, "Viscoelastic Mechanical Damping Devices at Real Earthquake Displacements," *Earthquake Spectra*, Earthquake Engineering Research Institute, Oakland, California, Vol. 9, No. 3, pp. 389–412.

BSSC, 1995, *NEHRP Recommended Provisions for Seismic Regulations for New Buildings, 1994 Edition, Part 1: Provisions and Part 2: Commentary*, prepared by the Building Seismic Safety Council for the Federal Emergency Management Agency (Report Nos. FEMA 222A and 223A), Washington, D.C.

Chang, K. C., Soong, T. T., Oh, S.-T., and Lai, M. L., 1991, *Seismic Response of a 2/5 Scale Steel Structure with Added Viscoelastic Dampers*, Report No. NCEER-91-0012, National Center for Earthquake Engineering Research, State University of New York at Buffalo, New York.

Cho, D. M., and Retamal, E., 1993, "The Los Angeles County Emergency Operations Center on High-Damping Rubber Bearings to Withstand an Earthquake Bigger than the Big One," *Proceedings of Seminar on Seismic Isolation, Passive Energy Dissipation, and Active Control*, Applied Technology Council Report No. ATC-17-1, Redwood City, California, pp. 209–220.

Chopra, A. K., 1995, *Dynamics of Structures*, Prentice-Hall, Englewood Cliffs, New Jersey.

CSI, 1994, *ETABS (Version 6.0): Linear and Nonlinear, Static and Dynamic Analysis and Design of Building Systems*, Computers and Structures, Inc., Berkeley, California.

Constantinou, M. C., Soong, T. T., and Dargush, G. F., 1996, *Passive Energy Dissipation Systems for Structural Design and Retrofit*, National Center for Earthquake Engineering Research, State University of New York at Buffalo, New York.

Constantinou, M. C., and Symans, M. D., 1993, "Experimental Study of Seismic Response of Buildings with Supplemental Fluid Dampers," *The Structural Design of Tall Buildings*, John Wiley & Sons, New York, New York, Vol. 2, pp. 93–132.

Constantinou, M. C., Tsopelas, P. C., Kim, Y.-S., and Okamoto, S., 1993, *NCEER-TAISEI Corporation Research Program on Sliding Seismic Isolation Systems for Bridges: Experimental and Analytical Study of Friction Pendulum System (FPS)*, Report No. NCEER-93-0020, National Center for Earthquake Engineering, State University of New York at Buffalo, New York.

Den Hartog, J. P., 1956, *Mechanical Vibrations*, Dover Publications, New York, New York.

EERI, 1993, "Theme Issue: Passive Energy Dissipation," *Earthquake Spectra*, Earthquake Engineering Research Institute, Oakland, California, Vol. 9, No. 3.

Grigorian, C. E., and Popov, E. P., 1994, *Energy Dissipation with Slotted Bolted Connections*, Report No. UCB/EERC-94/02, Earthquake Engineering Research Center, University of California, Berkeley, California.

Hart, G. G., et al., 1990, "Seismic Strengthening of a Tall Building Incorporating Base Isolation," *Proceedings: Fourth U.S. National Conference on Earthquake Engineering*, Earthquake Engineering Research Institute, Oakland, California.

Honeck, W., Walters, M., Sattary, V., and Rodler, P., 1993, "The Seismic Isolation of Oakland City Hall," *Proceedings of Seminar on Seismic Isolation, Passive Energy Dissipation, and Active Control*, Applied Technology Council Report No. ATC-17-1, Redwood City, California.

International Association for Structural Control, 1994, *Proceedings of First World Conference on Structural Control*, Los Angeles, California.

ICBO, 1991, "Division III—Earthquake Regulations for Seismic-Isolated Structures," Chapter 23, *Uniform Building Code*, 1991 Edition, International Conference of Building Officials, Whittier, California.

ICBO, 1994, "Division III—Earthquake Regulations for Seismic-Isolated Structures," Chapter 16, *Uniform Building Code*, 1991 Edition, International Conference of Building Officials, Whittier, California.

ICBO, 1995, "SEAOC Seismology Committee Code Change Proposal" for Chapter 16, Division III (Isolation Provisions) of the 1997 *UBC*, International Conference of Building Officials, Whittier, California.

Kareem, A., 1994, "The Next Generation of Tuned Liquid Dampers," *Proceedings of First World*

Conference on Structural Control, Los Angeles, CA, pp. FP5-19 to FP5-28.

Kasai, K., Munshi, J. A., Lai, M. L., and Maison, B. F., 1993, "Viscoelastic Damper Hysteretic Model: Theory, Experiment, and Application," *Proceedings: Seminar on Seismic Isolation, Passive Energy Dissipation, and Active Control*, Applied Technology Council Report No. ATC-17-1, Redwood City, California.

Kaynia, A. M., Veneziano, D., and Biggs, J. M., 1981, "Seismic Effectiveness of Tuned Mass Dampers," *Journal of the Structural Engineering Division*, American Society of Civil Engineers, New York, New York, Vol. 107, pp. 1465–1484.

Kelly, J. M., 1988, *Base Isolation in Japan, 1988*, Report No. UCB/EERC-88/20, Earthquake Engineering Research Center, University of California, Berkeley, California.

Kelly, J. M., 1993, *Earthquake-Resistant Design with Rubber*, Springer-Verlag, London, United Kingdom.

Kircher, C. A., and Bachman, R. E., 1991, "Guidelines for Design Criteria for Base Isolation Retrofit of Existing Buildings," *Proceedings, 60th Annual Convention*, Structural Engineers Association of California, Sacramento, California.

Li, C., and Reinhorn, A. M., 1995, *Experimental Study and Analytical Investigation of Seismic Retrofit of Structures with Supplemental Damping: Part II—Friction Devices*, Report No. NCEER-95-0009, National Center for Earthquake Engineering Research, State University of New York at Buffalo, New York.

Liang, Z., Tong, M., and Lee, G. C., 1995, *Real Time Structural Parameter Modification (RSPM): Development of Innervated Structures*, Report No. NCEER-95-0012, National Center for Earthquake Engineering Research, State University of New York at Buffalo, New York.

Makris, N., Constantinou, M. C., and Dargush, G. F., 1993, "Analytical Model of Viscoelastic Fluid Dampers," *Journal of the Structural Engineering Division*, American Society of Civil Engineers, New York, New York, Vol. 119, No. 11, pp. 3310–3325.

Mayes, R. M., 1988, "Analysis, Design and Testing of the Isolation System for the Salt Lake City & County Building," *International Seismic Isolation/Historic Preservation Symposium, Salt Lake City*, Salt Lake City Corporation, Salt Lake City, Utah.

Murota, N., Goda, K., Suzusi, S., Sudo, C., and Suizu, Y., 1994, "Recovery Characteristics of Dynamic Properties of High-Damping Rubber Bearings," *Proceedings of Third U.S.–Japan Workshop on Earthquake Protective Systems for Bridges, Berkeley, California, 1994*, Report No. NCEER 94-0009, National Center for Earthquake Engineering Research, State University of New York at Buffalo, New York, pp. 1-63 to 2-76.

Naaseh, Simin, 1995, "Seismic Retrofit of San Francisco City Hall - The Role of Masonry and Concrete," *Proceedings of the Third National Concrete and Masonry Engineering Conference*, San Francisco, California.

Nagarajaiah, S., Reinhorn, A., and Constantinou, M. C., 1991, *3D-BASIS: Nonlinear Dynamic Analysis of Three Dimensional Base Isolate Structures*, Report No. NCEER-91-0005, National Center for Earthquake Engineering Research, State University of New York at Buffalo, New York.

Newmark, N. M. and Hall, W. J., 1982, *Earthquake Spectra and Design*, Earthquake Engineering Research Institute, Oakland, California.

Nims, D. F., Richter, P. J., and Bachman, R. E., 1993, "The Use of the Energy Dissipation Restraint for Seismic Hazard Mitigation," *Earthquake Spectra*, Earthquake Engineering Research Institute, Oakland, California, Vol. 9, No. 3, pp. 467–498.

Patten, W. N., Sack, R. L., Yen, W., Mo, C., and Wug, H. C., 1993, "Seismic Motion Control Using Semi-active Hydraulic Force Actuators," *Proceedings of Seminar On Isolation, Passive Energy Dissipation, and Active Control*, Applied Technology Council Report No. ATC-17-1, Redwood City, California, pp. 727–736.

Pekcan, G., Mander, J., and Chen, S., 1995, "The Seismic Response of a 1:3 Scale Model RC Structure with Elastomeric Spring Dampers," *Earthquake Spectra*, Earthquake Engineering Research Institute, Oakland, California, Vol. 11, No. 2, pp. 249–267.

Pyle, S. L., Janseen, A. G., Holmes, W. T., and Kircher, C. A., 1993, "Life-Cycle Cost Study for the State of

California Justice Building," *Proceedings of Seminar on Seismic Isolation, Passive Energy Dissipation, and Active Control,* Applied Technology Council Report No. ATC-17-1, Redwood City, California.

Reinhorn, A. M., Li, C., and Constantinou, M. C., 1995, *Experimental and Analytical Investigation of Seismic Retrofit of Structures with Supplemental Damping Part I: Fluid Viscous Damping Devices*, Report No. NCEER-95-0001, National Center for Earthquake Engineering Research, State University of New York at Buffalo, New York.

Reinhorn, A. M., Nagarajaiah, S., Constantinou, M. C., Tsopelas, P., and Li, R., 1994, *3D-BASIS-TABS (Version 2.0): Computer Program for Nonlinear Dynamic Analysis of Three-Dimensional Base Isolated Structures*, Report No. NCEER-94-0018, National Center for Earthquake Engineering Research, State University of New York at Buffalo, New York.

Reinhorn, A. M., Soong, T. T., Lin, R. C., Riley, M. A., Wang, Y. P., Aizawa, S., and Higashino, M., 1992, *Active Bracing System: A Full Scale Implementation of Active Control*, Report No. NCEER-92-0020, National Center for Earthquake Engineering Research, State University of New York at Buffalo, New York.

Sakai, F., 1989, "Tuned Liquid Column Damper - New Type Device for Suppression of Building Vibrations," *Proceedings, International Conference on High Rise Buildings,* Nanjing, China.

SEAOC, 1986, *Tentative Seismic Isolation Design Requirements*, Structural Engineers Association of California, San Francisco, California.

SEAOC, 1990, *Recommended Lateral Force Requirements and Commentary*, Fifth Edition, Seismology Committee, Structural Engineers Association of California, Sacramento, California.

SEAOC, 1996, *Recommended Lateral Force Requirements and Commentary*, Sixth Edition, Seismology Committee, Structural Engineers Association of California, Sacramento, California.

Skinner, R. I., Robinson, W. H., and McVerry, G. H., 1993, *An Introduction to Seismic Isolation*, J. Wiley & Sons, New York, New York.

Sladek, J. R., and Klingner, R.E., 1983, "Effect of Tuned-Mass Dampers on Seismic Response," *Journal of the Structural Engineering Division,* American Society of Civil Engineers, New York, New York, No. 109, pp. 2004–2009.

Soong, T. T., 1990, *Active Structural Control: Theory and Practice*, Longman, London, United Kingdom.

Soong, T. T., and Constantinou, M. C., 1994, *Passive and Active Structural Vibration Control in Civil Engineering*, Springer-Verlag, Wien-New York.

Symans, M. D., Constantinou, M. C., Taylor, D. P., and Garnjost, K. D., 1994, "Semi-Active Fluid Dampers for Seismic Response Control," *Proceedings of First World Conference on Structural Control,* Los Angeles, California, pp. FA4-3 to FA4-12.

Tsopelas, P., and Constantinou, M. C., 1994, *Experimental and Analytical Study of Systems Consisting of Sliding Bearings and Fluid Restoring Force-Damping Devices*, Report No. NCEER 94-0010, National Center for Earthquake Engineering Research, State University of New York at Buffalo, New York.

Tsopelas, P. C., Constantinou, M. C., and Reinhorn, A. M., 1994, *3D-BASIS-ME Computer Program for Nonlinear Dynamic Analysis of Seismically Isolated Single and Multiple Structures and Liquid Storage Tanks*, Report No. NCEER-94-0014, National Center for Earthquake Engineering Research, State University of New York at Buffalo, New York.

Villaverde, R., 1994, "Seismic Control of Structures with Damped Resonant Appendages," *Proceedings of First World Conference on Structural Control*, Los Angeles, California, pp. WP4-113 to WP4-122.

Way, D., and Howard, J., 1990, "Seismic Rehabilitation of the Mackay School of Mines, Phase III, with Base Isolation," *Earthquake Spectra*, Earthquake Engineering Research Institute, Oakland, California, Vol. 6, No. 2.

Whittaker, A. S., Bertero, V., Alonso, J., and Thompson, C., 1989, *Earthquake Simulator Testing of Steel Plate Added Damping and Stiffness Elements*, Report No. EERC-89/02, Earthquake Engineering Research Center, University of California, Berkeley, California.

Winters, C. W., and Constantinou, M. C., 1993, *Evaluation of Static and Response Spectrum Analysis Procedures of SEAOC/UBC for Seismic Isolated Structures*, Report No. NCEER-93-0004, National Center for Earthquake Engineering Research, State University of New York at Buffalo, New York.

Yang, T.-S., and Popov, E. P., 1995, *Experimental and Analytical Studies of Steel Connections and Energy Dissipators*, Report No. UCB/EERC-95/13, Earthquake Engineering Research Center, University of California, Berkeley, California.

Zayas, V. A., Low, S. S., and Mahin, S. A., 1987, *The FPS Earthquake Resisting System: Experimental Report*, Report No. UCB/EERC-87/01, Earthquake Engineering Research Center, University of California, Berkeley, California.

Zayas, V., and Low, S. S., 1991, "Steel Seismic Isolators Applied to a Wood Frame Building," *Proceedings, 60th Annual Convention*, Structural Engineers Association of California, Sacramento, California.